

**Landslide Hazard and Climate Change in the
Mountain Glacial Environment of Northwest North
America**

**by
Madison Reid**

A thesis
presented to the University of Waterloo
in fulfilment of the
thesis requirement for the degree of
Master of Science
in
Earth Science

Waterloo, Ontario, Canada, 2017

© Madison Reid 2017

Author's Declaration

I hereby declare that I am the sole author of this thesis. This is a true copy of the thesis, including any required final revisions, as accepted by my examiners. I understand that my thesis may be made electronically available to the public.

Abstract

The aim of this thesis was to improve the understanding of the complex interactions between climate change and landslide behavior in the periglacial mountain environment of northwest North America. In particular, this thesis quantified the relationship between climate change (temperature, precipitation, and glacier change) and landslide behavior (magnitude, frequency, and distribution). To achieve this larger aim, four specific research objectives were established: (a) Determine changes in the frequency and distribution of landslides in glacial regions of northwest North America by developing a landslide inventory; (b) Quantify climate change factors, specifically trends in temperature and precipitation; (c) Assess changes in glacier ice area and volume in northwest North America; and (d) Establish a quantitative relationship between climate change, glacier ice loss, and change in landslide hazard. Changes in the frequency and distribution of large ($>1\text{Mm}^3$) catastrophic landslides in the mountain glacial environment were determined by developing a regional landslide inventory (Evans and Delaney, Unpublished). The landslide inventory was explored using a magnitude-frequency plot, and results showed that seismically triggered landslides had proportionally fewer large events than non-seismically triggered landslides, highlighting the importance of climate related triggers in large events. Also, the frequency of landslides was determined to be increasing over time, especially at high latitudes (>57 degrees N). Climate change analysis was completed using meteorological station data and trend testing (i.e., Mann-Kendall, Sen's slope) to develop indices showing temperature and precipitation change. Results show ubiquitous warming (particularly in winter and summer), as well as increasingly dry conditions in Alaska, Yukon, and northern British Columbia, with wetter conditions in central and southern British Columbia. Index results were correlated with landslide mass hypsometrically, showing strong statistical evidence (i.e., Wilcoxon Rank Sum Test) of a connection between increasing temperature and increasing landslide hazard. Precipitation was not correlated with landslide hazard with certainty. Glacier ice loss was assessed using a case study of Mount Meager Volcanic Complex (MMVC), which showed drastic reduction of ice area and volume in response to increased temperature and precipitation. Two major landslides at MMCV (1975/2010) have been found to be triggered by the aforementioned climate factors (increased temperature and precipitation leading to ice loss).

Acknowledgements

This thesis is the results of many hours of hard work, and the support, assistance, and generosity of many people was instrumental in its completion.

I would like to take the opportunity to express my gratitude to my supervisor, Dr. Stephen Evans, for all of his help and advice throughout my degree. I am very fortunate to have been his student, and very much appreciate his guidance, encouragement, and patience, as well as all of the financial support provided by him and the department of Earth Science. His enthusiasm for science and academia inspired me every time we had a meeting.

I would also like to thank Dr. Keith Delaney for always being willing to take the time and share his knowledge and expertise. His assistance and kindness was of immeasurable value to me. Furthermore, I would like to thank my fellow students with whom I shared an office: Song Ling, Jing Luo, and Negar Ghahramany. Moreover, I would like to express my gratitude to all of the people in the Earth and Environmental Science office for all of their assistance with any questions or difficulties I had.

I am very thankful for the financial assistance provided by the Ontario Graduate Scholarship, Natural Sciences and Engineering Research Council, and the University of Waterloo. Their generous support allowed me to focus solely on my academics.

I am very grateful for the support of my family throughout my education, both emotional and financial. To my mom, Janice Reid, thank you for all of your love and our endless phone conversations which got me through every hard day. To my dad, John Reid, thank you for always supporting me and encouraging me to have an inquisitive mind. To my brother, Adam Reid, thank you for always being there when I need you and for making me laugh when I'm feeling down. I would not be where I am without my family, including those not mentioned here, so thank you all.

Dedication

This thesis is dedicated to my mom, my dad, and my brother. Thank you for your endless love and support.

Table of Contents

Author’s Declaration.....	ii
Abstract.....	iii
Acknowledgements.....	iv
Dedication.....	v
Table of Contents.....	vi
List of Figures.....	x
List of Tables.....	xiv
Chapter One: Thesis Introduction.....	1
1.1 Introduction.....	2
1.2 Aims and Objectives.....	3
1.3 Study Area.....	4
1.4 Thesis Structure.....	6
Chapter Two: A Background Review of Climate Change and Landslides in Glaciated Regions of Northwest North America.....	7
2.1 Introduction.....	8
2.2 Climate Change, Glacier Ice Loss, and Landslide Response in Northwest North America.....	9
2.2.1 Climate Change in Northwest North America.....	9

2.2.2	Glacier Extent and Volume Change in Northwest North America	11
2.2.3	Ice Loss and Slope Stability in Periglacial Environments.....	13
2.2.4	Landslide Response in a Changing Climate	14
2.3	Catastrophic Periglacial Landslide Inventory of Northwest North America	21
2.3.1	Seismically Triggered Events.....	29
2.4	Conclusion.....	32
Chapter Three: An Assessment of Climate Change in Northwestern North America:		
	Temperature and Precipitation.....	34
3.1	Introduction	35
3.2	Data Sources and Pre-Processing.....	36
3.3	Mann-Kendall Trend Testing.....	40
3.3.1	Methodology.....	40
3.3.2	Mann-Kendall Trend Testing Results.....	41
3.4	Sen’s Slope Testing.....	47
3.4.1	Sen’s Slope Methodology.....	47
3.4.2	Sen’s Slope Results	47
3.5	Regional Climate Indices Generation and Visualization	49
3.5.1	Methodology	49
3.5.2	Results	51
3.6	Statistical Exploration of Regional Climate Indices	63

3.6.2	Methodology.....	63
3.6.3	Results	65
3.7	Conclusion.....	78
Chapter Four: Quantification of Deglaciation at Mount Meager Volcanic Complex, British Columbia.....		
		80
4.1	Introduction	81
4.2	Methodology	83
4.2.1	Climate Data Review.....	83
4.2.2	Landsat Image Series.....	84
4.2.3	Manual Classification in ArcMap.....	84
4.2.4	ENVI Automatic Classification.....	85
4.2.5	Ice Volume Quantification	86
4.3	Data Sources.....	87
4.4	Results and Discussion.....	87
4.4.1	Climate Data Review.....	87
4.4.2	Glacier Surface Area and Volume.....	92
4.5	Conclusion.....	100
Chapter Five: Thesis Summary and Conclusion.....		
		101
5.1	Introduction	102

5.2	Research Objective A: Determine changes in the frequency and distribution of landslides in glacial regions of northwest North America by analysing a landslide inventory	103
5.3	Research Objective B: Quantify climate change factors, specifically trends in temperature and precipitation	103
5.4	Research Objective C: Assess changes in glacier ice area and volume in northwest North America	104
5.5	Research Objective D: Establish a quantitative relationship between climate change, glacier ice loss, and landslide activity.....	104
5.6	Implications	105
5.7	Future Work	106
	References.....	108
	Appendix A – Mann-Kendall Results.....	114
	Appendix B – Comparison of Manually Digitized and Automatically Classified Glacier Extents, Mount Meager.....	134

List of Figures

Figure	Caption	Page
1.1	The study area is situated in northwest North America, with portions of British Columbia, Yukon, and Alaska. Mountain ranges included in the study area are the Coast Mountains (blue and green outlines), the Alaska Range (red outline), and the St. Elias, Chugach, and Kenai Mountains (black outline).	5
2.1	Mt. Meager 2010 Landslide (Stephen Evans, Personal Files). This photo illustrates the massive size of the event, with a volume of 48.5 Mm ³ , as well as the extensive runout over 12 km long.	19
2.2	An ortho-image of the Mount Munday landslide of 1997, with a volume of 3.2 Mm ³ and a runout over 4 km. (Delaney and Evans, 2014)	20
2.3	The length-volume scaling relation of known volumes in the landslide inventory on glaciers, used to estimate missing volumes from the landslide inventory. Based off the method of Davies (1982), however it was found that lengths were greater for a given volume than the Davies (1982) relation, as was found by Delaney and Evans (2014)	22
2.4	A magnitude (mass) frequency plot of the landslide inventory data	23
2.5	A cumulative mass plot for the entire periglacial landslide inventory of northwest North America. An increase in frequency and magnitude is visible as an increasing slope in recent years, as well as more data points. Coseismic landslides are clearly visible as vertical lines in the plot.	24
2.6	Rock avalanches in the glacial environment of NW North America 1947-2016 (n=48). See Table 2.2 for key. Epicentres of earthquakes triggering coseismic events in 1967, 1979, and 2002 are also included	28
2.7	Seismically triggered rock avalanches in the glacial environment of NW North America 1947-2016 (n=22). See Table 2.2 for key. Epicentres of earthquakes triggering coseismic events in 1967, 1979, and 2002 are also included.	30
3.1	A map displaying the location of meteorological stations (n=19) used for climate analysis, shown as purple triangles. See Table 3.1 for key.	38
3.2	A sample of the R code used for Mann-Kendall Testing. This example is for January at Grand Forks.	40
3.3	A summary of the Mann-Kendall results for temperature variables (data from Table 3.3).	44
3.4	A summary of the Mann-Kendall results for temperature variables (data from Table 3.4).	46
3.5	A sample of the Sen's slope testing code used in R	47

3.6	Summer Temperature Index (JJA). Note significant warming to the north of 56 degrees N.	53
3.7	Fall temperature index, showing pockets of cooling.	54
3.8	Winter temperature index, showing the greatest seasonal warming	55
3.9	Spring temperature index, showing the greatest warming in Alaska	56
3.10	Annual temperature index, showing significant warming western Alaska and northern British Columbia.	57
3.11	Summer precipitation index, showing wetter conditions in the south and dryer conditions in Alaska.	58
3.12	Fall precipitation index, with wetter conditions in British Columbia and northern Alaska, with dryer conditions in southern Alaska.	59
3.13	Winter precipitation index, showing drying conditions in the north and wetter in the south	60
3.14	Spring precipitation index, showing drying to the north and wetter conditions in the south	61
3.15	Annual precipitation index, showing dry conditions in Alaska and Yukon, with wetter conditions in British Columbia	62
3.16	A sample of the R code used to compute the Wilcoxon Rank Sum test.	65
3.17	The elevation distribution of seismically triggered (blue circle) and non-seismically triggered (south – black square, north – red triangle) landslides. Horizontal lines indicate limits of relief by showing the elevation of various mountain peaks. Red and blacklines indicate mountains on which there have been non-seismically triggered failures in the north and south, respectively. Blue lines indicate mountains which have co-seismically failed.	65
3.18	Summer temperature index vs. time for non-seismically triggered events. The temperature index seems to be increasing with time for both the Southern and Northern events, supporting the hypothesis that increasing temperatures and landslide activity in the mountain glacial environment share a connection. In addition, all northern events have a higher temperature index than southern events.	68
3.19	Summer Precipitation index results vs. time for non-seismically triggered events. .Precipitation index results show no visible trend in the data, suggesting precipitation may not be correlated with landslide hazard.	69
3.20	Annual temperature index results vs time for seismically triggered landslides. The annual temperature index values associated with coseismic events subjectively seems to be increasing over time, suggesting that rising temperatures are increasing coseismic landslide hazard.	70

3.21	Annual precipitation index results vs time for seismically triggered events. There is no clear observable trend in these results, indicating precipitation change may not have an effect on coseismic landslide hazard	70
3.22	Cumulative plot for all non-seismically triggered events, comparing landslide mass, summer temperature index, and summer precipitation index. There is a strong subjective match between summer temperature change and landslide mass, supporting the hypothesis that increasing summer temperatures are contributing to increased landslide hazard. Precipitation does not have a good visual correlation with landslide mass, suggesting precipitation change may be less influential on landslide activity.	72
3.23	Cumulative plot for southern non-seismically triggered events, comparing landslide mass, summer temperature index, and summer precipitation index. There is a good subjective match between temperature increase and landslide mass, suggesting temperature is an essential component of increases in landslide hazard. There is a moderate match between precipitation and landslide mass, indicating that increases in precipitation may influence landslide hazard in the south of the study area.	73
3.24	Cumulative plot for northern non-seismically triggered events, comparing landslide mass, summer temperature index, and summer precipitation index. Visually, there is a strong correlation between landslide mass and summer temperature, supporting the hypothesis that summer temperature increases are contributing to growing landslide hazard. There is a poor match between precipitation change and landslide mass, indicating that precipitation may have less of an impact on landslide hazard in the north of the study area.	74
3.25	Cumulative plot for all seismically triggered events, comparing landslide mass, summer temperature index, and summer precipitation index. There is a strong visual correlation between both annual temperature increase and annual precipitation decrease to landslide mass. This suggests that coseismic landslide hazard is influenced by both temperature and precipitation.	75
4.1	The complete outline of the Mount Meager landslide, with a Landsat base image from October 13th, 2010, showing the initiation zone (A-B), the two major bends (C and E), the facing wall of Meager Creek (F), and the bifurcated flow that travelled up Meager Creek, and across the Lillooet River (G). The image was taken following the breach of the Meager Creek dam, and fluvial reworking and considerate incision of the dam itself and evident. (Guthrie et al., 2012)	83
4.2	Changes in minimum temperature, according to subtraction of PRISM 30-year normal (1971-2000, 1981-2010). See table 2.2 for landslide key.	89

4.3	Changes in maximum temperature, according to subtraction of PRISM 30-year normals (1971-2000, 1981-2010), see table 2.2 for landslide key	90
4.4	Changes in precipitation, according to subtraction of PRISM 30-year normals (1971-2000, 1981-2010). See table 2.2 for key	91
4.5	A 1:1 comparison of manually digitized and automatically classified glacier surface area at MMVC. Overall, the automatic classification does matches the manual classification relatively well, although does consistently underestimate by a small margin.	93
4.6	Results of late summer glacier surface area analysis at MMVC from the manual digitizing method and the unsupervised classification method. Overall, both methods show a decrease in clean glacier ice at MMVC.	94
4.7	A map showing the changing area of the glaciers on MMVC, using hollow polygons to represent extents at different times, and a true colour base image from 2014. The northern landslide source location is for the landslide in 2010 (Guthrie et al., 2012)	95
4.8	A map showing the change in glacier thickness from 1988 to 2000. This is located on the eastern edge of the overall study area	98
4.9	A hypsometric analysis of ice loss volume (from 1988 to 1998) and landslide volume, showing a strong correlation between ice loss at elevations below 1900m. These results suggest ice loss may be correlated with landslide hazard in MMVC at lower elevations, but not a higher elevations.	99

List of Tables

Table	Caption	Page
2.1	The time scale of processes related to slope stability in the mountain glacier environment, and associated climate factors. Short term events range from five minutes to months, and long term events span a year to millennia. The shaded time scales illustrate the variability of each process, but are only approximate. The spatial scale is related to the temporal scale; effects lasting millennia typically covering large areas, while effects that last minutes typically have limited spatial impact. (Adapted from Huggel et al., 2012; Noetzli and Gruber, 2009)	16
2.2	Regional landslide inventory of events great than or equal to 1 Mm ³ in volume, in glacial regions of northwest North America (Evans and Delaney, Unpublished). Estimated volumes are shown in red font. Seismically triggered landslides are shown in shaded cells..	26
3.1	A summary of meteorological stations used for climate data analysis.	37
3.2	Environment Canada (2016) variables used for climate analysis, along with their definitions. Note that all variables also exist in the NOAA (2016) datasets, with the exception of total precipitation.	39
3.3	A summary of Mann-Kendall results for temperature variables	43
3.4	A summary of Mann-Kendall results for precipitation variables	45
3.5	A summary of the Sen's slope analysis by season and by variable, indicating increased temperatures and precipitation throughout the study area.	48
3.6	A summary of the comparison between regional indices' results and PRISM data, both showing increases in temperature and precipitation throughout British Columbia.	52
3.7	DEM data sources for statistical analyses of climate indices	63
3.8	Correlation analysis of climate variables and landslide mass. The null hypothesis (H ₀) is that the distributions of both variables are the same. Upon rejection of the null hypothesis, the alternate hypothesis is accepted (that the distributions of the variables tested are not the same).	77
4.1	Information about the landslides at MMVC (including mass, year, and source elevation) and corresponding climate change information. PRISM variables show average change per 10 years, and the climate indices represent change per 100 years.	88

4.2	Glacier surface areas calculated from manually digitized polygons and automatically classified rasters.	93
-----	---	----

Chapter One: Thesis Introduction

1.1 Introduction

Landslides, defined as a movement of rock, debris, or earth down a slope under the influence of gravity (Cruden and Varnes, 1996), can be highly destructive processes. On the global scale, the loss of life from landslides is substantial. Estimates made by Petley (2012) stated that from 2004 to 2010, there were 2620 fatal landslides resulting in a minimum of 32,322 fatalities. The financial burden of landslides is also a concern. A recent study investigating flood and landslide damage in Switzerland from 1972-2007 estimated the direct costs of landslides and rockfalls to be 530 million EUR, or approximately 740 million CAD (Hilker *et al.*, 2009). Landslides continue to pose a significant threat in the global setting, as well as in the glaciated mountain environment of northwest North America.

The mountain glacial environment is particularly susceptible to large, catastrophic slope failures; this is especially the case if the cryosphere is out of equilibrium due to a changing climate (Evans and Delaney, 2014; Huggel *et al.* 2010). There is a general consensus that current changes in the earth's climate may be leading to increased landslide hazard, but the exact mechanisms and consequences of these changes are yet to be fully understood by the scientific community (e.g. Uhlmann *et al.*, 2012; Guthrie *et al.*, 2010; Huggel *et al.*, 2012). Due to the complex and interconnected nature of the atmosphere and cryosphere, and their coupled influence on slope stability, it is difficult to quantitatively assess all variables which may affect landslide hazard. Proper investigation can also be limited due to the remote nature of many of these events. Despite the complexity of the issue, there have been several attempts to assess the influence of climate change, and changes in glacier ice, of landslide in various mountainous regions throughout the world (e.g. Stoffel *et al.*, 2014; Evans and Clague, 1994; Huggel *et al.*, 2012; Gariano and Guzzetti, 2016). These investigations suggest that increasing temperatures, increasing precipitation, and decreased glacier ice are resulting in increased hazard, although these links remain difficult to quantify. Moreover, interest in the subject of climate change and landslide hazard is increasing, with notable attention drawn following the release of the first assessment report by the Intergovernmental Panel on Climate Change in 1990 which identified

increasing landslide hazard as a potential consequence of climate change. (Houghton *et al.*, 1990; Gariano and Guzzetti, 2016).

In British Columbia, Alaska, and Yukon, there have been comparatively few investigations into the effects of temperature and precipitation trends and glacier ice loss on slope instability and landslide hazard (e.g. Delaney and Evans, 2014; Holm *et al.*, 2004; Uhlmann *et al.*, 2012). As such, changes in landslide hazard, and the ways in which catastrophic failures are influenced by the unique climatic and cryospheric conditions specific to the North American northwest are poorly understood. This thesis adds to the body of literature by investigating the effects of climate change on landslide hazard in northwest North America. More specifically, this thesis hypothesizes that climate trends in temperature, precipitation, and glacier ice loss will significantly influence hazard from large and catastrophic landslides in glaciated regions of British Columbia, Yukon, and Alaska.

1.2 Aims and Objectives

The main goal of this thesis is to identify and quantify the effects of climate change on landslide hazard in mountain glacial environments of northwest North America. To accomplish this larger aim, several objectives were established:

- a. Determine changes in the frequency and distribution of landslides in glacial regions of northwest North America by developing a landslide inventory.
- b. Quantify climate change factors, specifically trends in temperature and precipitation.
- c. Assess changes in glacier ice area and volume in northwest North America.
- d. Establish a quantitative relationship between climate change, glacier ice loss, and change in landslide hazard.

1.3 Study Area

The study area examined in this thesis was British Columbia, Yukon, and Alaska. More specifically, this thesis looks at landslide activity and climate change proximate to the west coast of British Columbia and Alaska; mountain ranges included in the study are the Coast Mountains, St. Elias Mountains, Alaska Range, Chugach Mountains, and Kenai Mountains (**Figure 1.1**). Northwest North America was chosen as the study area primarily due to landslide data availability, with a complete inventory of large landslide events (Delaney and Evans, 2014; Evans and Delaney, Unpublished). Also, climate change and glacier ice loss have been well documented in this region, making it a good candidate for analysis (Schiefer *et al.*, 2007; Moore *et al.*, 2009; Ommanney, 2002).

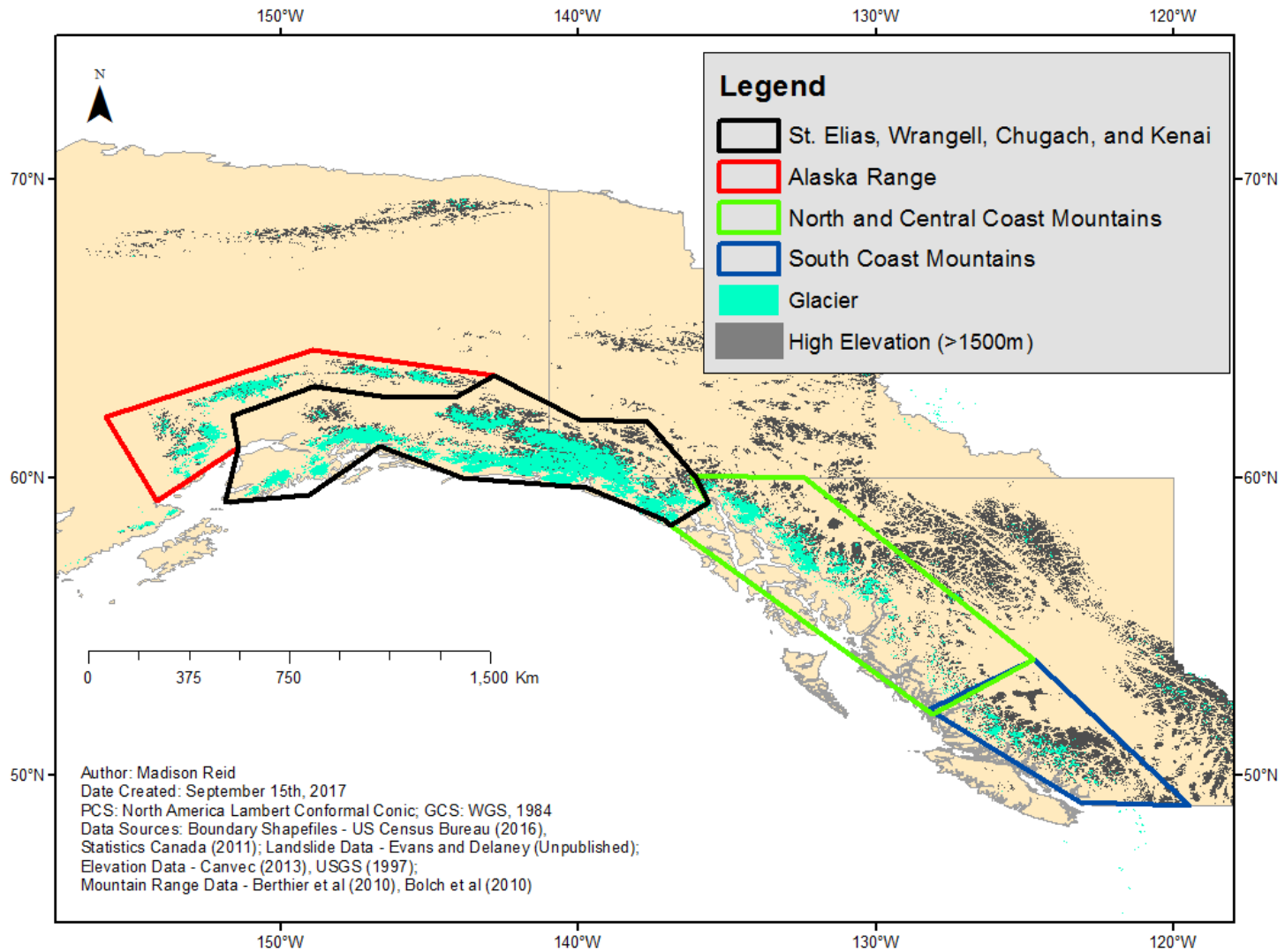


Figure 1.1: The study area is situated in northwest North America, with portions of British Columbia, Yukon, and Alaska. Mountain ranges included in the study area are the Coast Mountains (blue and green outlines), the Alaska Range (red outline), and the St. Elias, Chugach, and Kenai Mountains (black outline).

1.4 Thesis Structure

This thesis is organized into the following chapters:

1. Thesis Introduction
2. A Background Review of Climate Change and Landslides in Glaciated Regions of North West North America
3. An Assessment of Climate Change in Northwest North-America: Temperature and Precipitation
4. Quantification of Deglaciation in at Mount Meager Volcanic Complex, British Columbia
5. Thesis Summary and Conclusions

The main objective of Chapter 2 is to summarize the state of knowledge related to this thesis, and to provide an overview in a broader context. Also, Chapter 2 contains information about the landslide inventory that was used for all subsequent analysis. Chapter 3 presents an analysis of changes of temperature and precipitation based primarily on meteorological station data, and how these changes are or are not correlated with landslide hazard. Chapter 4 provides an investigation of the effects of glacier ice loss on landslide hazard by using the Mount Meager Volcanic Complex, British Columbia as a case study.

The references and appendices at the end of the thesis may also be of interest. See the table of contents for the location of all sections within the thesis.

Chapter Two: A Background Review of Climate Change and Landslides in Glaciated Regions of Northwest North America

2.1 Introduction

The mountain glacial environment is particularly sensitive to both climate change and landslide activity. As witnessed by the extensive deglaciation across northwest North America, glaciers are some of the clearest and most compelling evidences of climate change. As such, the effects of climate change on the glacial environment, as well as landslides on and around glaciers have been frequently investigated.

This chapter presents a comprehensive review of previous literature related to this thesis. The first topic addressed is the extent of recent (since the mid-1900s) climate change in northwest North America, which generally shows increased warming and precipitation. Second, changes in glacier extent and volume are discussed, with all regions showing glacier retreat and ice loss. Next, the effects of glacier ice loss on slope stability are examined, including the effects of debutressing, and permafrost degradation. Finally, several studies discussing the landslide response to climate and glacier change in the mountain environment are reviewed, looking specifically at examples from northwest North America.

A unique tool in assessing landslide hazard in a changing climate is the landslide inventory data developed by Evans and Delaney (Unpublished). It is visualized using ArcMap, and a magnitude-frequency plot. The Gutenberg-Richter relation is established for three subsets of the landslide data: seismically triggered, non-seismically triggered (north), and non-seismically triggered (south). In further exploration of the inventory, a few significant events are selected and reviewed. Moreover, the three seismic events that triggered 46% of the landslide events in the inventory are also discussed.

The results and observations in this chapter greatly influenced the hypotheses and methodologies implemented in the remainder of the thesis. Ultimately, this chapter allowed for a greater understanding of the current state of knowledge on the effects of climate change on landslide hazard in the mountain glacial environment, specifically with reference to northwest North America.

2.2 Climate Change, Glacier Ice Loss, and Landslide Response in Northwest North America

Increased potential for extreme events as a result of climate change is a concern among the general public as well as the scientific community (Stocker *et al.*, 2013). Landslides have been identified as a hazard that may be increasing in frequency and magnitude as a result of climate change (Huggel, *et al.*, 2012; Crozier, 2010, Evans and Clague, 1994; Gariano and Guzzetti, 2016). While many landslides are initiated by seismic activity (e.g. Gorum *et al.*, 2014), others have been shown to have a causal relationship with climate change, specifically changes in temperatures, precipitation, and glacier ice (e.g. Mokievsky-Zubok, 1977, Guthrie *et al.*, 2012). More frequent heavy precipitation is most strongly linked with landslide risk, however temperature can also have an effect (Huggel *et al.*, 2012). Glacier ice loss related to atmospheric warming is of particular interest, as the mountain glacial environment is especially susceptible to catastrophic mass movements.

2.2.1 Climate Change in Northwest North America

Global climate change is resulting in increases in mean, maximum, and minimum air temperatures in many regions around the world; more frequent heavy precipitation events have also been observed (Solomon *et al.*, 2007; Field *et al.*, 2014). The Intergovernmental Panel on Climate Change (IPCC) has released several emission scenarios and their resulting surface warming data which can be applied regionally to assess location specific climate change predictions.

When the IPCC A2 emission scenario is applied to temperature models in British Columbia, the predicted mean annual temperature for 2020-2029 is 1.2 degrees Celsius greater than the mean from 1961-1990, based on five locations across the province (British Columbia Ministry of Forests, Lands, and Natural Resources, 2009). By the 2080s, the average increase in mean annual temperature across the province is projected 4 degrees Celsius greater than the 1961-1990 normal (British Columbia Ministry of Forests, Lands, and Natural Resources, 2009). The predicted temperature changes would have wide ranging effects on the sensitive ecosystems of British Columbia, particularly forested and glaciated areas. The IPCC A2 scenario also anticipates precipitation changes in British Columbia, with coastal and northern British Columbia experiencing increases in precipitation, particularly in the winter (British Columbia Ministry of Forests, Lands, and Natural Resources, 2009).

Similar to British Columbia, Alaska is projected to undergo significant warming according to the IPCC A2 emission scenario (Solomon *et al.*, 2007). Warming increases are greatest in Northern Alaska, with mean annual temperature expected to increase by 5.6 to 6.7 degrees Celsius (10 to 12 degrees Fahrenheit) by the end of the century (Melillo *et al.*, 2014). Predicted warming elsewhere in the state is less severe, with projections of an increase of 4.4 to 5.6 degrees Celsius (8 to 10 degrees Fahrenheit) in the interior and 3.3 to 4.4 degrees Celsius (6 to 8 degrees Fahrenheit) throughout the remainder of the state by 2100 (Melillo *et al.*, 2014). Annual precipitation is also expected to increase in Alaska, particularly in the northwest of the state. According to the IPCC A2 emission scenario, parts of Alaska could experience 15% to 30% increases in precipitation by the end of this century (Melillo *et al.*, 2014).

Yukon is also expected to show warming and increased precipitation according to all IPCC scenarios (Solomon *et al.*, 2007). In the past 50 years, observed mean annual temperatures have already increased by 2 degrees Celsius (Streicker, 2016). Following the IPCC A2 emission scenario, mean annual temperature is expected to increase by more than 2 degrees Celsius in the next 50 years, with the greatest warming in winter (Streicker, 2016). Moreover, precipitation has already increased by 6% over the last 50 years, and is expected to increase by another 10% to 20% over the next 50 years, with the greatest increase seen in summer (Streicker, 2016).

In summary, the IPCC predicts warming and increased precipitation across northwest North America. Generally speaking, northern latitudes are expected to see the greatest increase in temperature. Warmer temperatures will result in more rain and less snow, affecting glacier ice accumulation, snowpack and spring melt. In response to the observed and anticipated climate changes in Alaska, Yukon, and British Columbia, glaciers throughout the region are expected to undergo significant change as discussed in the following section.

2.2.2 Glacier Extent and Volume Change in Northwest North America

Glaciers are sensitive indicators of climate change, and readily respond to increased temperature and precipitation across northwest North America (Moore *et al.*, 2009). More specifically, winter precipitation and summer temperature are especially impactful on glacier mass balance (Bitz and Battisti, 1999; Moore and Demuth, 2001; Moore *et al.*, 2009). In addition, glaciers in southern British Columbia are strongly affected by large scale climate factors such as the Pacific North American Pattern which shifted to its positive phase in 1976, with southerly air flow along the west coast of North America and high pressure over the Rocky Mountains, effectively reducing winter accumulation (Moore *et al.*, 2009). The glaciers of the Coast and St. Elias Mountains have experienced marked terminal retreat. In addition to area loss, many glaciers have also been thinning resulting in an overall loss of ice volume, as discussed below.

Bolch *et al.*, (2010) conducted an inventory of glaciers in British Columbia and performed a comparison of glacier surface area over a 20 year period from 1985 to 2005. In the St. Elias Mountains in 1985 glaciers covered an area of 3615.6 km². By 2005, there was a decrease in the total area to approximately 3330 km² (7.9% decrease in 20 years). This corresponds to a decrease in glacier area of approximately 15.9 +/- 6.8 km² per year. In the northern Coast Mountains, the area of glaciers in 1985 was approximately 10,863 km² which was reduced to 10,029 km² (7.7% decrease in 20 years) at a rate of -37.9 +/- 16.7 km² per year. Moving to lower latitudes in the southern Coast Mountains, Bolch *et al.* (2010) report a glacier

area of 7912 km² in 1985 which was reduced to 7097 km² by 2005 (10.3% decrease in 20 years), losing approximately 47.9 +/- 14.4 km² per year. Despite the decrease in area in each of the ranges, Bolch *et al.* (2010) reported an increasing number of glaciers; the St. Elias Mountains glaciers increased in number from 510 in 1985 to 647 in 2005, the northern Coast Mountains increased from 3131 to 3746, and the southern Coast Mountains increased from 3620 to 4507. Note that these figures do not include the glaciers in neighbouring Alaska. This observed disintegration is caused by larger glaciers being broken into several smaller glaciers in the process of retreat and downwasting, and has also been recorded in the European Alps by Paul *et al.* (2004). Ice area figures reported by Bolch *et al.* (2010) are supported by an earlier study by Schiefer *et al.* (2008). From the results of Bolch *et al.* (2010) and Schiefer *et al.* (2008), it is clear that all of northwest North America is not only experiencing rapid glacier retreat, but decrease in glacier surface area is greatest to the south. Schiefer *et al.* (2007) have completed a similar analysis, computing volume instead of area; they reported an estimated loss of 22.48 +/- 5.53 km³ per year, with thinning rates averaging 0.78 +/- 0.19 m per year. Schiefer *et al.* (2007) reported the greatest thinning in the Coast and St. Elias Mountains, and less thinning in the Rocky Mountains.

Alaska is also experiencing rapid ice loss, with some glaciers retreating at rates of up to 100 m per year (Moore *et al.*, 2009). Berthier *et al.* (2010) and Arendt *et al.* (2002) report ice loss volumes for each of the major regions in glacierized Alaska. Berthier *et al.* (2010) estimate the St. Elias Mountains to have an ice loss of 21.7 km³ per year, much higher than their reported value for the Coast Mountains of 7.88 km³ per year. In all of Alaska, Berthier *et al.* (2010) estimate the ice loss per year to be 41.9 km³. This is much lower than the estimate of Arendt *et al.* (2002), who report an annual glacier ice loss of 96 +/- 35 km³.

Despite some uncertainty surrounding the exact volume of ice disappearing in northwest North America, it is indisputable that glaciers are shrinking in both area and volume. Clarke *et al.* (2015) suggest that in comparison to 2005 glacier volumes in western Canada will be reduced

by 70% +/- 10% by the end of the 21st century. Overall, the glaciers throughout northwest North America seem to be out of equilibrium, and will likely continue to retreat (Moore et al., 2009).

2.2.3 Ice Loss and Slope Stability in Periglacial Environments

The stability of steep slopes in the high mountain glacial environment is negatively impacted by a changing cryosphere in a number of ways, namely ice instability, debutressing and ice unloading, and changes in permafrost (Deline *et al.*, 2015b). These factors, can interact in complex ways, often forming feedback loops which destabilize slopes and promote catastrophic failure.

The first and perhaps most intuitive effect of ice loss is the generation of unstable ice. A variety of factors affect ice stability, the most important being ice temperature and topography (Deline *et al.* 2015b). Less influential, but still important factors influencing ice stability are “adhesion of cold and polythermal ice on bedrock, cohesion with more stable upslope ice, supporting effects from flatter downslope glacier parts and lateral bedrock abutments, and the englacial and subglacial hydrology” (Deline *et al.* 2015b). Together the variables affecting slope stability make a complicated system, which can react in a number of ways to climate changes. Fischer *et al.* (2013) and Deline *et al.* (2015b) mention melt water infiltration and stress distribution changes, as well as subglacial and englacial temperature changes as possible consequences of ice melt leading to an unstable slope. More specifically, warmer ice temperatures lead to a decrease in viscosity, limiting cohesion to bedrock (Deline *et al.*, 2015b). Increased temperatures can also lead to greater volumes of melt water, further reducing cohesion (Faillettaz *et al.*, 2012; Deline *et al.* 2015b). With ongoing warming in northwest North America, increasing ice instability is a growing concern.

Debutressing, a process that occurs with glacier retreat or thinning, is the loss of physical slope support that was provided by the melted ice (Deline *et al.*, 2015b, McColl, 2012). Slopes which lose support from glacier ice are particularly susceptible to failure because glacial erosion has permanently weakened them, and the retreat or thinning of the glacier has shifted them out of

equilibrium (Deline *et al.*, 2015b; Blair, 1994). Unloading is a process that often occurs in tandem with debutressing, and is caused by rock slope rebound when the bedrock is no longer suppressed by glacier ice (Nichols, 1980; Deline *et al.*, 2015). This crustal rebound causes stress fractures in the rock, reducing stability and promoting slope failure.

Changes in permafrost are also known to have a significant impact on slope stability in the periglacial environment (Gruber and Haeberli, 2007). When melt water infiltrates permafrozen bedrock, it can be a source of latent heat with the potential to disrupt the system (Deline *et al.*, 2015b). Fast-freezing trapped water can also pose a hazard to slope stability by rapid expansion (Matsuoka and Murton, 2008). In addition, hydrostatic pressure due to excessive moisture in the bedrock can reduce frictional forces as well as increasing gravitational forces (Fischer *et al.*, 2010). Steep bedrock slope stability is especially sensitive to permafrost degradation and addition of meltwater to the permafrost system, both of which are seen in warm summers which is often when large catastrophic landslides occur.

The periglacial mountain environment is complex and subject to many stressors which in turn affect slope stability. In the face of a changing climate, ice retreat and thinning can lead to debutressing, unloading, and isostatic uplift, all of which greatly weaken over steepened glacier valley walls. Unstable ice and meltwater is also generated as glacier temperatures rise. Furthermore, landslide hazard is increased as permafrost is degraded either by thawing or by meltwater infiltration. All of these factors combined highlight why the mountain glacier setting is particularly prone to large catastrophic landslide events, especially in a changing climate.

2.2.4 Landslide Response in a Changing Climate

Landslide triggers are often ambiguous and a complex combination of seismic and climatic factors is common. There have been many investigations into the response of landslide hazard to changes in climate and/or changes in glacier ice (Jakob and Lambert, 2009; Evans and Clague, 1994; Huggel *et al.*, 2012; Geertsema, 2013; Geertsema *et al.*, 2007; Guthrie *et al.*, 2010; Holm *et al.*, 2004, Huggel *et al.*, 2010; Uhlmann *et al.*, 2012, Crozier, 2010, Huggel *et al.*, 2008).

In general, these methods follow one of three approaches: (1) the modelling approach which relies on downscaled climate projections, (2) the paleo approach which uses paleo-evidence to infer prehistoric climate conditions, or (3) the historical evidence approach which leverages instrumentally recorded data (Gariano and Guzzetti, 2016). While there is growing interest in landslide hazard in response to climate change, there are still relatively few integrated investigations of landslide hazard, climate change, and the mountain glacial environment.

An investigation by Holm *et al.* (2004) looked at the landslide response in southwestern British Columbia to glacier retreat and thinning. Their primary method was to recognize and catalog specific terrain characteristics which are responsible for landslide initiation, and estimate the amount of glacial influence. The results of Holm *et al.* (2004) suggest that glacier retreat has increased the frequency of failures, reflecting an increased risk of catastrophic landslides in weak rock. The findings of Holm *et al.* (2004) are agreed upon by Evans and Clague (1994), who studied the effects of climate change on catastrophic geomorphic processes in mountain environments. Ultimately, Evans and Clague (1994) hypothesize that deglaciation increases hazard from ice avalanches and landslides primarily due to debutressing. Assuming glaciers continue to retreat and more slopes experience debutressing, landslide hazard will continue to increase, with this climate driven perturbation lasting for hundreds of years or more (Evans and Clague, 1994).

Huggel *et al.* (2012) investigated the effects of climate change on landslide activity in the high mountains by analyzing a series of failures since the end of the 1990s in several mountain ranges globally. Ultimately they determined several important variables that are affected by climate change which influence slope stability (**Table 2.1**). They predict that increased warming and precipitation will result in increased frequency and magnitude of landslide events, and therefore increased hazard. More recently, a case study based in the European Alps determined that thawing mountain permafrost contributes to rock failures and periglacial debris flows; even events without historical precedents can occur due to unstable mountain permafrost (Stoffel, *et al.*, 2014).

Table 2.1: The time scale of processes related to slope stability in the mountain glacier environment, and associated climate factors. Short term events range from five minutes to months, and long term events span a year to millennia. The shaded time scales illustrate the variability of each process, but are only approximate. The spatial scale is related to the temporal scale; effects lasting millennia typically covering large areas, while effects that last minutes typically have limited spatial impact. (Adapted from Huggel *et al.*, 2012; Noetzi and Gruber, 2009)

	Short Term Effects (days)					Long Term Effects (Years)			
	10 ⁻²	10 ⁻¹	10 ⁰	10 ¹	10 ²	10 ⁰	10 ¹	10 ²	10 ³
ROCK/ICE SLOPE FAILURES									
Increasing Mean Temperature			Seasonal melt water production, snow fall elevation				Conductive heat transport to subsurface, latent heat effects, debutressing effects due to glacier retreat		
Warm Extreme Temperatures		Enhanced melt water and thawing				Conductive heat transport to subsurface			
Heavy Precipitation	Water infiltration into rock and ice								
PERIGLACIAL DEBRIS FLOWS									
Increasing Mean Temperature				Higher snow line, enhanced runoff, soil saturation		Uncovering of glacial sediments due to glacier retreat, thawing permafrost, sediment input			
Warm Extreme Temperatures			Enhanced melt water and soil saturation				Possibly alteration of sediment input systems		
Heavy Precipitation	Rapid soil saturation, enhanced surface runoff						Possibly alteration of sediment input systems		

Another study looked at a total of 123 rock avalanches in the Chugach Mountains of south-central Alaska (Uhlmann *et al.*, 2012), moving an estimated $(185 \pm 37) \times 10^6 \text{ m}^3$ of material from 1972 to 2008. They report this erosion rate to be high by global comparison, emphasizing greater rock-slope instability in the mountain glacial environment. Uhlmann *et al.* (2012) cite “strong seismic ground motion region, de-glacial slope debutressing, high rates of contemporary surface uplift driven by glacio-iso static rebound (Larsen *et al.*, 2005), and possibly permafrost degradation (Gruber and Haeberli, 2007)” as the most important contributing factors to landslide susceptibility. Debutressing due to glacier thinning is also cited

by Geertsema *et al.* (2007) as an important climate change related factor the activity of large rockslides. In contrast with some other publications assessing climate change impacts on landslide activity, Uhlmann *et al.* (2012) found that sediment flux from the landslides was uncorrelated with mean annual precipitation; they do however suggest that increasing temperature may be increasing the mean rock-slope failure size.

Several of the events included in the landslide inventory (**Table 2.2**) have been directly linked to climate factors including warmer summer temperatures, glacier ice loss, potential freeze/thaw events, and heavy precipitation (Huggel *et al.*, 2010; Evans and Delaney, 2014; Mokievsky-Zubok, 1977; Guthrie *et al.*, 2010; Delaney and Evans, 2014; Geertsema, 2012). Examples from the inventory discussed in this section include the Mount Steller events in 2005 and 2008 (Alaska), the Mount Miller event in 2008 (Alaska), the Mount Meager events of 1975 and 2010 (British Columbia), the Lituya event in 2012 (Alaska), and the Mount Munday event in 1997 (British Columbia).

Huggel *et al.* (2010) focus on the implications of rising air temperatures, as well as the associated glacier and permafrost decay, on landslide hazard. They note a few events of interest due to unusual temperature conditions in Alaska: Mount Steller, 2005; Mount Steller, 2008; and Mount Miller, 2008. In the case of the Mount Steller, 2005, Huggel *et al.* (2010) determine that warm temperatures for 10 days preceding the event allowed melt water to infiltrate the summit rock mass and destabilize it. The 2008 Mount Steller event also occurred during a very warm period with temperature above freezing, followed by a drop in temperature suggesting a possible freeze/thaw trigger mechanism. The Mount Miller landslide in 2008 also had very warm temperatures. Huggel *et al.* (2010) state “*temperature increased from -2.5 degrees Celsius on July 27th to over 11 degrees Celsius on August 2nd 2008*”. The landslide occurred four days later on August 6th, 2008. Huggel *et al.* (2010) emphasize that it is very difficult to discern climate triggers of landslides with certainty, however a repeated pattern of very warm temperatures preceding the event, followed by a rapid drop in temperature (usually below freezing) suggests that temperature does play a role in landslide hazard. The importance of freeze/thaw events is also discussed by Deline *et al.* (2015a).

There have been two major landslide events in the inventory sourced from the Mount Meager Volcanic Complex (MMVC), one in 1975 and one in 2010, as well as several smaller events (Evans and Delaney, 2015). The 1975 landslide, occurring on July 22nd near Pylon Peak, is extensively discussed by Mokievsky-Zubok (1977). It is estimated that 2.5Mm^3 of ice and 26Mm^3 of debris traveled over 6.5km, descending 1150m. The volume reported by Mokievsky-Zubok (1977) is greater than the estimate of 13Mm^3 given by Evans and Delaney (2014). The volume recorded in the landslide inventory (27Mm^3) is more aligned with the figure provided by Mokievsky-Zubok (1977). Both Evans and Delaney (2015) and Mokievsky-Zubok (1977) report that there was no seismic activity the day of the landslide. On the other hand, weather reports from Alta Lake Station (75km south-east) showed warm weather in the area on July 22nd, and several days before. As such, Mokievsky-Zubok (1977) proposes the cause of the landslide was the *“weight of glacier ice and the action of glacier meltwater”*, and *“some movement of ice in the form of a minor ice fall that triggered the collapse of a large, wet mass of supporting ground below the ice”*. Evans and Delaney (2014) also determine melt water to be the most likely trigger of the event, stating *“increased fluid pressures acting along the base of the slide and on internal shear planes, which no doubt accompanied ice melting during a period of warm summer weather, probably reduced the overall shearing resistance sufficiently to trigger the initial slide”*. Overall, it is clear that climate played a role in the 1975 landslide – with the primary factor being warm summer weather. As such, investigating temperature trends in summer months will be essential to determining the effect of climate change on landslide hazard. The second major landslide at Mount Meager was the 2010 landslide, originating above Capricorn Creek on August 6th (**Figure 2.1**). This event was comprehensively assessed by Guthrie *et al.* (2012), and is discussed by Evans and Delaney (2014). Ultimately they conclude the event was significant for several reasons, including its massive volume of 48.5Mm^3 , and its demonstration of the role of deglaciation in destabilizing slopes. They determine glacier change to be a distinct precondition to the landslide event because, similar to the 1975 event, there was no distinct seismic trigger recorded. More specifically, glacial debuitressing caused by 20th century glacier retreat is cited as a critical triggering factor (Evans and Delaney, 2014). The 2010 landslide at Mount Meager serves as an example of the importance of glacial factors in landslide hazard. While climate factors such as temperature and precipitation play a role in glacier dynamics, it is

also important to examine glacier ice trends directly. Overall, both of the Mount Meager landslide examples chosen from the inventory emphasize the potential impact of climate change on landslide hazard. The 1975 event exemplified the importance of summer temperature as a landslide trigger. In contrast, the 2010 event also occurred during summer but seemed to be more influenced by glacier ice loss. In summary, temperature and glacier ice loss have an established link to landslide hazard in the glacial regions of northwest North America, and should be investigated more thoroughly.



Figure 2.1: Mt. Meager 2010 Landslide (Stephen Evans, Personal Files). This photo illustrates the massive size of the event, with a volume of 48.5 Mm^3 , as well as the extensive runout over 12 km long.

Another example of an event that has been determined to be influenced by climate is the Mount Munday landslide that occurred sometime between July 12th and July 28th, 1997, with a volume of 3.2 Mm³ (Delaney and Evans, 2014) (**Figure 2.2**). This event was first reported by Evans and Clague (1998), and is extensively reviewed by Delaney and Evans (2014). Delaney and Evans (2014) eliminated seismic triggering as a possibility, because there were no significant earthquakes in the timeframe of the event. Following their seismic analysis, Delaney and Evans (2014) investigated possible climate factors by looking at the data from the Tatlayoko Lake data station, approximately 70km from the landslide. They identified freeze-thaw cycle between July 18th and July 28th, 1997 as well as peaks in mean, maximum, and minimum daily temperatures compared to a 30-year normal from 1971-2000. Similar to the examples from Mount Meager the 1997 event most likely had a trigger that was rooted in climate factors, either due to a freeze-thaw event, increased temperatures, or a combination of the two. Ultimately, this example reinforces the need for a more detailed analysis of climate change and the effects on landslide hazard in British Columbia, Yukon, and Alaska.



Figure 2.2: An ortho-image of the Mount Munday landslide of 1997, with a volume of 3.2 Mm³ and a runout over 4 km. (Delaney and Evans, 2014)

The 2012 landslide at Lituya Mountain, first discussed by Geertsema (2012), is another interesting example of a large event in the landslide inventory without a seismic trigger. The landslide occurred on June 11th, 2012 and was discovered by abnormal seismic signals (Geertsema, 2012). The landslide is estimated to have a volume of 18 Mm³ to 20 Mm³ (Geertsema, 2012; Evans and Delaney, 2015). The landslide was not triggered by an earthquake as there were none in the area at that time. However Geertsema (2012) presents several possible triggers: glacial debuttressing, permafrost degradation, and above average snowpack combined with rapid melt. The Lituya 2012 event is an interesting example, because it not only emphasizes the potential contribution of increasing temperature to greater landslide activity at high elevations (by citing glacial debuttressing and permafrost degradation), but also implies that an above average snowpack can also contribute to hazard. Therefore, the ambiguous trigger mechanism supports the importance of investigating both temperature and precipitation trends, which is a major objective of this thesis.

2.3 Catastrophic Periglacial Landslide Inventory of Northwest North America

One of the key datasets of this thesis is a regional landslide inventory developed by Evans and Delaney (unpublished). This dataset is an example of a regional inventory (Guzzetti *et al.*, 2012). The inventory covers northwest North America, including events in the mountains of British Columbia, Yukon, and Alaska. Events were detected using remote sensing data (primarily Landsat imagery) and a review of earlier publications (e.g., Evans and Clague, 1988). To allow for completeness of the inventory, criteria were established. First, events had a minimum volume of 1 Mm³; by including only large events, there is less risk of detection error associated with failing to include all smaller events. Second, all events had to be in close proximity to glaciers. These two criteria together help ensure the completeness and accuracy of the inventory. In total there are 48 events, with 22 of those being seismically triggered. The earliest event is in 1947 and the latest is in 2016, a period of 70 years.

The inventory is in tabular in format, including location and magnitude information (**Table 2.2**). However, not all of the landslides included in the inventory have volumes published in the literature; as such some needed to be estimated. Davies (1982) outlines a method for length-volume scaling, which was implemented to estimate landslide volume in the inventory. It is important to note however, that Davies (1982) does not consider landslides on glaciers which have notably longer runout than landslides not on glaciers (Evans and Clague, 1988, 1999; Hungr and Evans, 2004; Jiskoot, 2011). Therefore, a scaling relation unique to this dataset was produced (**Figure 2.3**). The known lengths and volumes included in the landslide inventory were plotted, and a power relation of best fit was calculated to obtain the scaling relation to estimate the unknown volumes in the inventory. Only known lengths and volumes from 1990 and after were used in **Figure 2.3** because they have greater certainty than older events. This analysis found that the volume scaling relation based on the inventory of landslides on glaciers was steeper (indicating a greater lengths for smaller volumes) than the Davies (1982) scaling relationship. This was also found by Delaney and Evans (2014). Mass was calculated from volume by multiplying by the density of gneiss, 2600 kg/m³.

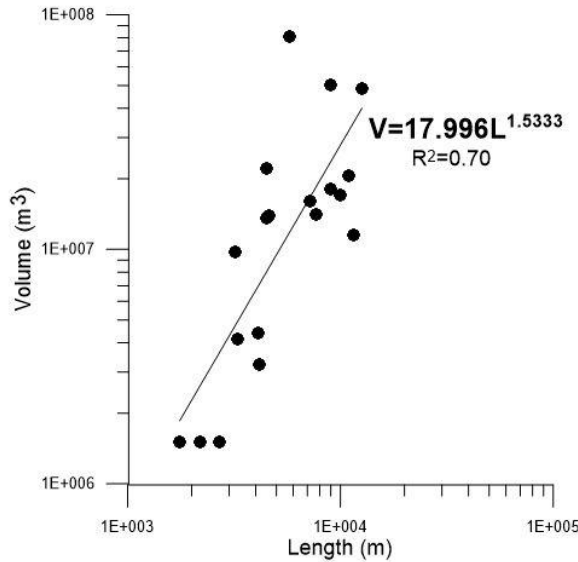


Figure 2.3: The length-volume scaling relation of known volumes in the landslide inventory on glaciers, used to estimate missing volumes from the landslide inventory. Based off the method of Davies (1982), however it was found that lengths were greater for a given volume than the Davies (1982) relation, as was found by Delaney and Evans (2014)

To visualize the inventory, data was imported into ArcMap as vector points as seen in **Figure 2.6**. To further explore the inventory data, a magnitude-frequency plot was created (**Figure 2.4**). Note that the data was divided into three categories: Non-seismic (North) – N=15, Non-seismic (South) – N=11, and Seismic – N=22. Seismic events (those triggered by earthquakes) are separated from the inventory to allow for investigation into their characteristics and how they may differ from non-seismically triggered events. North and south subsets of the non-seismic split occurs at 57 degrees north. This latitude was chosen based on a subjectively observed spatial separation in the data. Based on the analysis in **Figure 2.4** all of the data considered together had the highest b value of 1.544, followed by the coseismic data with a b value of 1.29. This means that the seismic dataset has proportionally a greater number of smaller events and less larger events than the non-seismic dataset. The southern and the northern cluster of the non-seismic data have approximately the same b-values at 0.972 and 1.088, respectively.

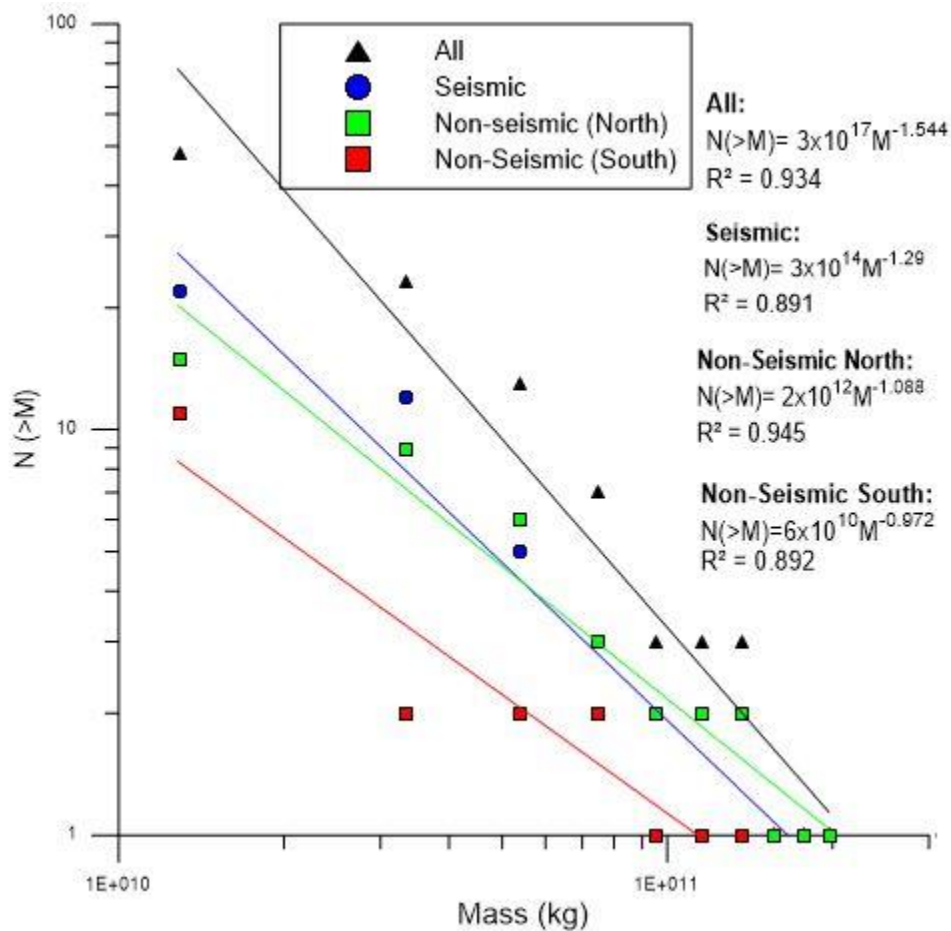


Figure 2.4: A magnitude (mass) frequency plot of the landslide inventory data.

This means that they follow approximately the same magnitude frequency distribution. Note that the northern data is located higher on the magnitude frequency plot, simply meaning there are more northern events in the inventory than southern ones. This is clearly visible in **Figure 2.6**.

The inventory was also plotted using cumulative mass versus time, generated by sorting the landslide mass data chronologically and calculating the cumulative percent of the total mass (**Figure 2.5**). From the cumulative mass plot, it is clear that landslide magnitude and frequency are both increasing with time, with a steeper slope and more data points in recent years. This increase is particularly noticeable after 2005. Seismically triggered landslides (occurring in 1964, 1979, and 2002) are also clearly visible in **Figure 2.5** as vertical lines. Overall, the cumulative plot suggests that landslide activity is increasing in the mountain glacial environment of northwest North America, and previous literature supports the hypothesis that this increase may be due to climate change.

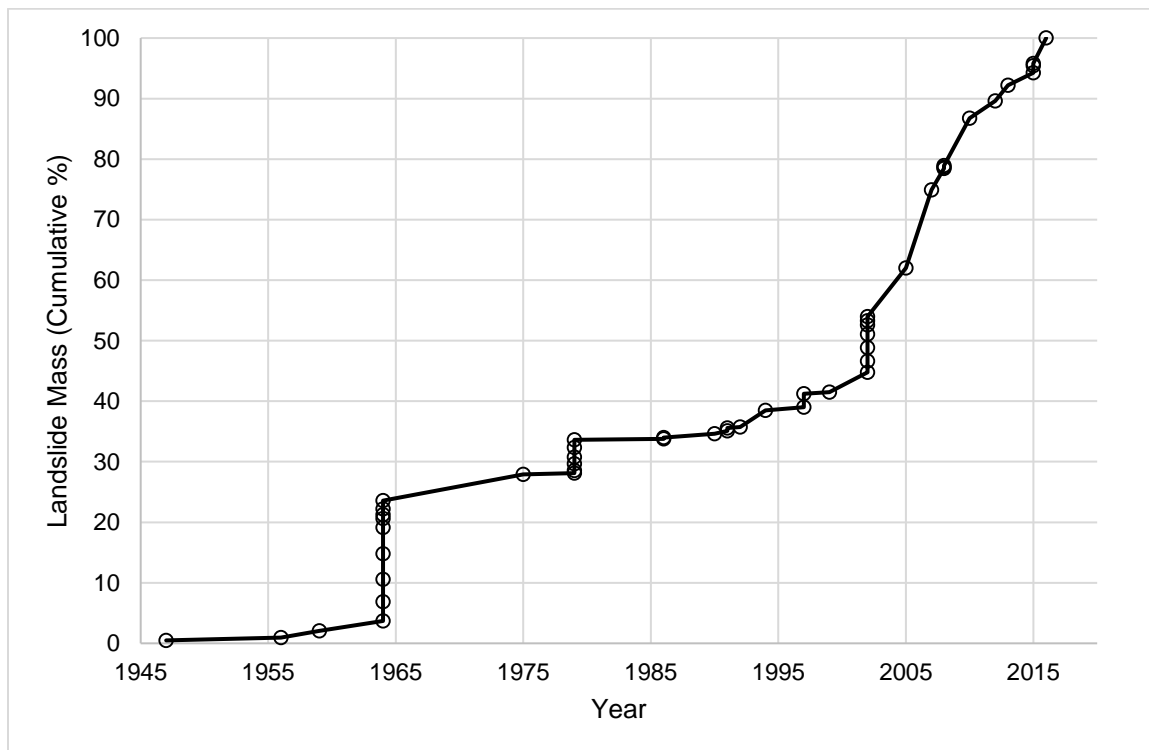


Figure 2.5: A cumulative mass plot for the entire periglacial landslide inventory of northwest North America. An increase in frequency and magnitude is visible as an increasing slope in recent years, as well as more data points. Coseismic landslides are clearly visible as vertical lines in the plot.

In summary, the inventory developed by Evans and Delaney (unpublished) is effective because it has established conditions which ensure its completeness. First, a minimum volume of 1 Mm³ is implemented. Second, all events are on or near glaciers. The completeness of the dataset is evident in the magnitude frequency plots, as there is no roll off at smaller magnitudes and all of the b-values are close to 1. The seismic dataset has a greater number of smaller events than the non-seismic datasets (proportionally). This is reflected in the data, as the majority of the largest landslides are non-seismically triggered. This result emphasizes the importance of climate factors in landslide hazard.

Table 2.2: Regional landslide inventory of events great than or equal to 1 Mm³ in volume, in glacial regions of northwest North America (Evans and Delaney, Unpublished). Estimated volumes are shown in red font. Seismically triggered landslides are shown in shaded cells.

	Location	Date	Location	Lat	Long	L (m)	Volume (Mm ³)	V=17.996 L ^{1.5333} (Mm ³)	Mass (kg)	Reference(s)
1	Devastation Glacier	1947	BC	50 36 00.24	123 32 51.00	1500	3	1.33	7.80E+09	Evans and Clague (1999)
2	Tim Williams Glacier	1956	BC	56 32 37.29	130 00 03.58	3700	3	5.32	7.80E+09	Evans and Clague (1999)
3	Pandemonium Creek	1959	BC	52 00 13.17	125 46 51.32	8600	6.7	19.41	1.74E+10	Evans and Clague (1999)
4	Sherman Glacier 1	1964	AK	60 32 40.85	145 08 20.50	6000	10.1	11.17	2.63E+10	McSaveney (1978) / Shreve (1968)
5	Steller 1	1964	AK	60 34 58.88	143 17 31.16	6700	20	13.23	5.20E+10	Nicoletti and Sorriso-Valvo (1991)
6	Allen 4	1964	AK	60 47 15.21	144 54 57.73	7700	23	16.38	5.98E+10	Nicoletti and Sorriso-Valvo (1991)
7	Fairweather	1964	AK	58 52 55.64	137 38 51.85	10000	26	24.46	6.76E+10	Nicoletti and Sorriso-Valvo (1991)
8	Schwan 1	1964	AK	60 52 43.74	145 10 46.93	6100	27	11.46	7.02E+10	Nicoletti and Sorriso-Valvo (1991)
9	Sioux Glacier 1	1964	AK	60 31 08.58	144 18 54.58	4200	9.3	6.47	2.42E+10	Reid (1969)
10	Martin River 1	1964	AK	60 36 00.37	143 39 40.17	3000	3.86	3.86	1.00E+10	
11	Martin River 2	1964	AK	60 36 03.02	143 38 51.40	4000	6.00	6.00	1.56E+10	
12	Martin River 3	1964	AK	60 38 23.98	143 35 01.20	5000	8.45	8.45	2.20E+10	
13	Devastation Glacier	1975	BC	50 36 00.24	123 32 51.00	6100	27	11.46	7.02E+10	Nicoletti and Sorriso-Valvo (1991)
14	Tweedsmuir Glacier	1979	BC	59 55 27.77	138 31 32.91	1350	1.13	1.13	2.94E+09	Evans and Clague (1999)
15	Jarvis Glacier	1979	BC	59 28 50.35	136 34 03.23	2440	2.81	2.81	7.31E+09	Evans and Clague (1999)
16	Towagh Glacier	1979	BC	59 22 29.29	137 14 21.74	4350	6.82	6.82	1.77E+10	Evans and Clague (1999)
17	Cascade 1	1979	AK	60 13 52.38	140 27 24.03	4400	6.95	6.95	1.81E+10	-
18	Cascade 2	1979	AK	60 13 47.96	140 12 43.62	5500	9.78	9.78	2.54E+10	-
19	Cascade 3	1979	AK	60 06 03.67	140 21 01.20	4750	7.81	7.81	2.03E+10	-
20	Mount Meager	1986	BC	50 38 04.37	123 30 00.15	3680	1	5.28	2.60E+09	Evans and Clague (1999)
21	North Creek	1986	BC	50 39 33.74	123 14 04.16	2850	1.5	3.57	3.90E+09	Evans and Clague (1999)
22	Frobisher Glacier 1	1990	BC	59 46 23.12	137 45 55.72	3050	3.96	3.96	1.03E+10	Evans and Clague (1999)
23	Frobisher Glacier 2	1991	BC	59 46 23.12	137 45 55.72	2380	2.71	2.71	7.05E+09	Evans and Clague (1999)

24	Kshwan Glacier	1991	BC	55 45 35.96	129 43 43.64	2250	3.1	2.48	8.06E+09	Evans and Clague (1999)
25	Salal Creek	1992	BC	50 38 25.29	123 18 59.01	1295	1.06	1.06	2.76E+09	-
26	Iliamna 94	1994	AK	60 01 31.54	153 02 20.92	9993	17	24.43	4.42E+10	Schneider et al. (2011)
27	Mount Munday	1997	BC	51 19 12.27	125 13 21.54	4163	3.2	6.38	8.32E+09	Delaney and Evans (2014)
28	Iliamna 97	1997	AK	60 01 31.54	153 02 20.92	7694	14	16.36	3.64E+10	Schneider et al. (2011)
29	Howson Range	1999	BC	54 31 24.92	127 47 17.00	2700	1.5	3.28	3.90E+09	Geertsema et al. (2006)
30	McGinnis Peak N	2002	AK	63 34 04.71	146 15 11.10	11000	20.4	28.30	5.30E+10	Jibson et al. (2006)
31	McGinnis Peak S	2002	AK	63 32 29.57	146 14 35.80	11500	11.4	30.30	2.96E+10	Jibson et al. (2006)
32	Black Rapids E	2002	AK	63 27 40.01	146 09 52.23	4600	13.9	7.44	3.61E+10	Jibson et al. (2006)
33	Black Rapids M	2002	AK	63 28 26.28	146 15 19.70	4500	13.6	7.19	3.54E+10	Jibson et al. (2006)
34	Black Rapids W	2002	AK	63 28 26.28	146 19 13.74	3200	9.7	4.26	2.52E+10	Jibson et al. (2006)
35	West Fork Glacier N	2002	AK	63 26 28.06	147 29 44.70	3300	4.1	4.47	1.07E+10	Jibson et al. (2006)
36	West Fork Glacier S	2002	AK	63 26 57.41	147 29 37.21	4100	4.4	6.23	1.14E+10	Jibson et al. (2006)
37	Mount Steller	2005	AK	60 31 13.52	143 05 27.85	9000	50	20.81	1.30E+11	Huggel et al. (2010)
38	Mount Steele 1	2007	YK	61 05 33.19	140 17 59.08	5760	80	10.50	2.08E+11	Lipovsky et al. (2008)
39	Mount Miller	2008	AK	60 28 40.45	142 14 23.94	4500	22	7.19	5.72E+10	Huggel et al. (2010)
40	Mount Steller 1	2008	AK	60 31 13.52	143 05 27.85	1767	1.5	1.71	3.90E+09	Huggel et al. (2010)
41	Mount Steller 2	2008	AK	61 31 13.52	144 05 27.85	2200	1.5	2.40	3.90E+09	Schneider et al. (2011)
42	Capricorn Creek	2010	BC	50 37 15.45	123 30 00.38	12700	48.5	35.28	1.26E+11	Guthrie et al. (2012)
43	Lituya Mountain	2012	AK	58 47 42.72	137 25 44.42	9000	18	20.81	4.68E+10	Geertsema (2012)
44	La Perouse	2013	AK	58 33 40.86	137 03 48.27	7200	16	14.78	4.16E+10	-
45	Mount Wilbur	2015	AK	58 45 25.76	137 16 59.95	6570	12.84	12.84	3.34E+10	-
46	Mt Steele 2	2015	YK	61 05 56.58	140 13 04.01	4461	7.09	7.09	1.84E+10	-
47	Icy Bay	2015	AK	60 10 26.17	141 10 21.90	2095	2.23	2.23	5.80E+09	-
48	Lamplugh	2016	AK	58 44 34.95	136 53 34.61	10475	26.26	26.26	6.83E+10	-

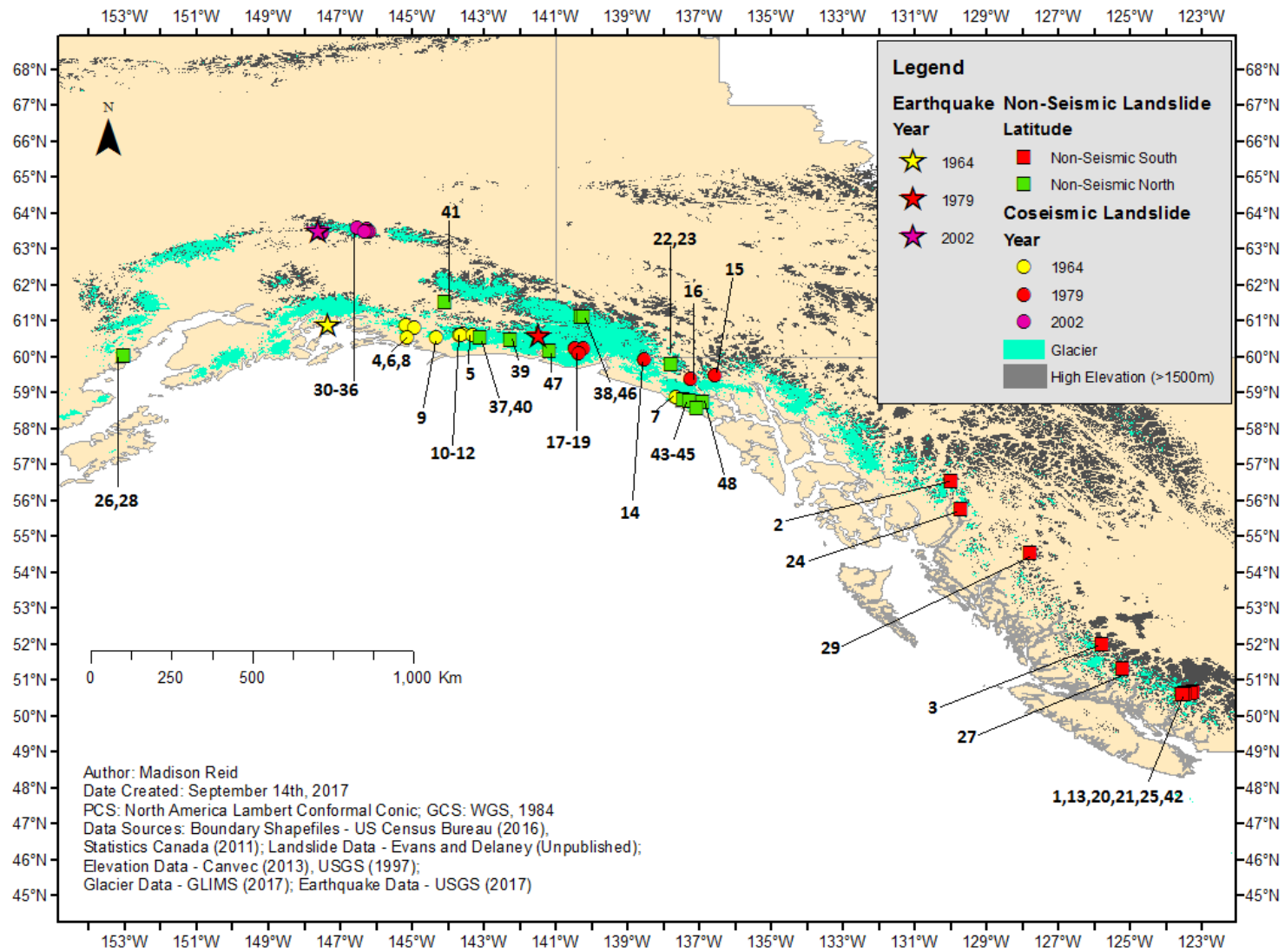


Figure 2.6: Rock avalanches in the glacial environment of NW North America 1947-2016 (n=48). See Table 2.2 for key. Epicentres of earthquakes triggering coseismic events in 1967, 1979, and 2002 are also included

2.3.1 Seismically Triggered Events

The potential importance of climate factors in seismically triggered landslides is essential to consider, as they comprise a large portion of the inventory. In the landslide inventory, 22 of the 48 events were seismically triggered (46%). In addition, seismic events make up a large portion of the total landslide mass in the inventory, an estimated 40%. Seismic events have a total mass of approximately 6.4×10^{11} kg, while non-seismically triggered events had a total mass of approximately 9.7×10^{11} kg (North – 7.1×10^{11} kg, South – 2.6×10^{11} kg). These estimates are to show that seismically triggered landslides, in addition to non-seismically (climate) triggered events, are an important component of the overall landslide hazard in Northwest North-America.

The first seismic event that triggered landslides in the inventory was the 1964 Alaska Earthquake (represented as a black star in **Figure 2.7**) which occurred on March 27th (Suleimani *et al.*, 2011; Post, 1964). The earthquake had a magnitude of **M9.2**, rupturing along 800 km of the Aleutian megathrust in South Central Alaska (Plafker, 1970; Post, 1964). It is the largest ever instrumentally recorded earthquake in North America (Wood and Peters, 2015). The 1964 megathrust event triggered 9 out of the 22 coseismic events in the inventory, including the landslide at Mount Fairweather with a volume of 26 Mm^3 and a mass of 6.76×10^{10} kg. The second earthquake (**M7.4**) occurred February 28th 1979, near the Yukon-Alaska Border (represented as a red star, see **Figure 2.7**), and generated six rock avalanches: three in Alaska and three in Yukon. The third earthquake was the Denali Earthquake which occurred on November 3rd, 2002, with a magnitude of **M7.9** (as shown by a green star in **Figure 2.7**). The Denali earthquake triggered the remaining 6 landslides in the seismic inventory, including the Mount McGinnis North event with a volume of 20.4 Mm^3 and a mass of 5.3×10^{10} kg.

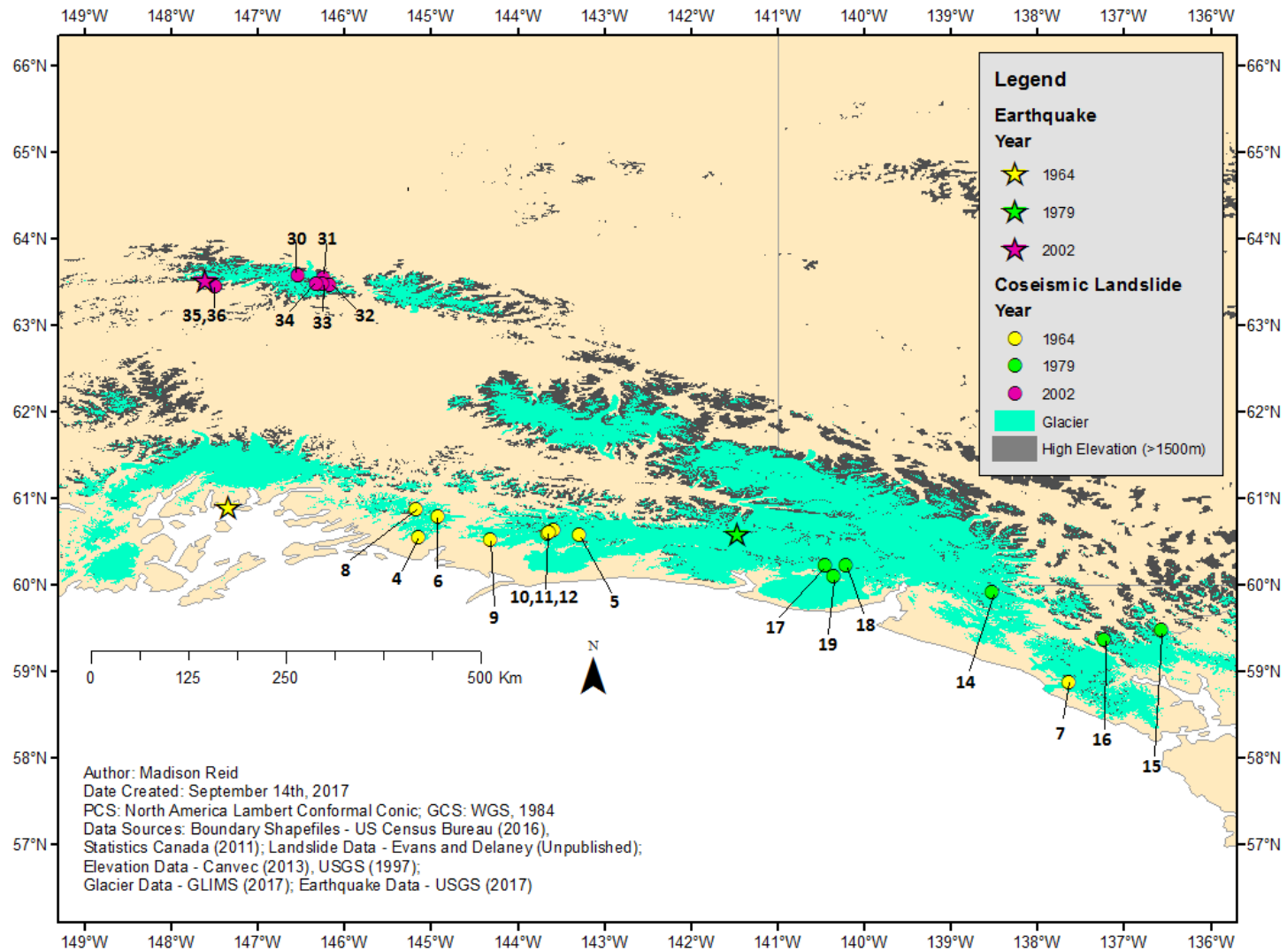


Figure 2.7: Seismically triggered rock avalanches in the glacial environment of NW North America 1947-2016 (n=22). See Table 2.2 for key. Epicentres of earthquakes triggering coseismic events in 1967, 1979, and 2002 are also included.

In general, there is insufficient research into the potential effects of climate change on seismically triggered landslides. While it seems intuitive that a changing climate could precondition slopes to a greater frequency of coseismic landslides during a given earthquake in a glacial environment, there is little evidence of this being the case, with the exception of Uhlmann *et al.* (2012), who link temperature to landslide activity. One recent study which investigated the landslides resulting specifically from the Denali Earthquake is Gorum *et al.*, (2014). Their primary goal was to provide insight on the relationships between seismology, glaciology, and geomorphology by using the Denali coseismic landslide data. McColl *et al.* (2012) indicate that glacier ice can lessen the catastrophic effects of seismicity as a landslide trigger; as loss of glacier ice increases this hazard by increasing topographic seismic amplification. The results of Gorum *et al.* (2014) also suggest that glacier ice can reduce seismic shaking in mountainous regions. Furthermore, they find that deglaciation can also lead to exposed and overstepped slopes at high elevations due to debulking, also increasing susceptibility to seismically induced landslides. Other factors that are potentially important are basal melting and high pore-water pressures, also increasing landslide susceptibility in both seismically and non-seismically triggered events (Gorum *et al.*, 2014, Clague and Evans, 1994; Schneider *et al.*, 2011; Sosio *et al.*, 2012). Ultimately, Gorum *et al.* (2014) conclude that glacial dynamics are an essential component in the triggering of coseismic landslides in the mountain glacial environment.

Overall, seismically triggered landslides are an essential component of the landslide inventory; comprising 46% of the number of events and 40% of the total mass. While the record of seismically triggered landslides is somewhat limited with only three earthquakes, it is important to further investigate the role of climate change on the hazard associated with these events. This sentiment is echoed by Gorum *et al.* (2014) who cite glacier ice as a key factor in determining the hazard of coseismic landslides in the high mountains of Alaska.

2.4 Conclusion

According to the coupled climate model simulations based on the IPCC A2 emission scenario (a higher emission scenario), northwest North America is expected to experience increasing temperature and precipitation for the remainder of the 21st century. Temperature increases are expected to be particularly strong in the winter, and precipitation increases are expected to be most severe in the summer (Solomon *et al.*, 2007; British Columbia Ministry of Forests, Lands, and Natural Resources, 2009; Field *et al.*, 2014; Melillo *et al.*, 2014; Streicker, 2016). These changes in climate are resulting in decreasing glacier ice throughout the glacierised mountains of British Columbia, Yukon, and Alaska; glaciers are experiencing both retreat and thinning resulting in a net volume loss, although the exact amount of ice volume loss remains uncertain (Moore *et al.*, 2009; Bolch *et al.*, 2010; Schiefer *et al.*, 2007; Berthier *et al.*, 2010; Clarke *et al.*, 2015; Arendt *et al.*, 2002).

The glacier changes in northwest North America have a number of consequences. First, once large and continuous glaciers are disintegrating into many smaller glaciers (Bolch *et al.*, 2010). This has also been observed in the Alps (Paul *et al.*, 2004). This ice loss creates a number of conditions which have negative effects on slope stability: debutressing, unloading, uplift, unstable ice generation, and permafrost degradation (Deline *et al.*, 2015b). There is evidence supporting the hypothesis that one or more of these processes have influenced the triggering of several landslides in the study area, including events at Mt. Steller (2005/2008, Alaska), Mt. Miller (2008, Alaska), Mt. Munday (1997, British Columbia), Mt. Meager (1975/2010, British Columbia), and Mt. Lituya (2012, Alaska) (Huggel *et al.*, 2010; Evans and Delaney, 2014; Mokievsky-Zubok, 1977; Guthrie *et al.*, 2012; Delaney and Evans 2014). The Mount Meager events emphasized the importance of warm summer temperatures and glacier ice loss (Mokievsky-Zubok, 1977; Guthrie *et al.*, 2012). Mount Munday showed similar findings, the 1997 event most likely had a trigger that was rooted in either due to a freeze-thaw event, increased temperatures, or a combination of the two (Delaney and Evans, 2014). The Lituya event illuminates the role of warming temperatures, as well as snowpack in landslide hazard, with greater snowpack increasing risk (Geertsema, 2012).

The inventory developed by Evans and Delaney (unpublished) is a unique dataset to further assess the role of climate change in landslide hazard. Preliminary visual analysis using ArcMap and a magnitude frequency plot showed that the largest events in the inventory were non-seismically triggered, emphasizing the importance of understanding climate triggers. Furthermore, there was a greater frequency of events in the north of the study area than in the south, particularly since 1990. This could be a reflection of landslide hazard increasing with warming temperatures (Huggel *et al.*, 2012; Evans and Clague, 1994; Uhlmann *et al.*, 2012; Huggel *et al.*, 2010) seeing as the greater warming being predicted in far northern latitudes (Solomon *et al.*, 2007; Field *et al.*, 2014). Despite the importance of non-seismic events, seismically triggered landslides comprise a significant portion of the inventory. The literature suggests that glacier ice loss is also important when investigating coseismic landslide events, as loss of glacier ice increases this hazard by increasing topographic seismic amplification.

The relationship between climate change and landslide events is strongly debated in the scientific community. The source of debate is the immense complexity of landslide triggers and preconditioning factors. While the exact nature of climate change consequences remains uncertain, there is strong evidence supporting the hypothesis that temperature, precipitation, and ice loss have an impact of slope stability and landslide hazard in the mountain glacial environment. Further work needs to be completed to help establish and quantify the exact relationship between each of these variables.

Chapter Three: An Assessment of Climate Change in Northwestern North America: Temperature and Precipitation

3.1 Introduction

As discussed in Chapter 2, quantifying the relationship between temperature change, precipitation change, and landslide activity is an essential component of understanding the effects of climate change on landslide hazard. From the literature review, it is hypothesized that there will be increasingly warm and wet conditions throughout the study area at least until the end of the 21st Century (Solomon *et al.*, 2007; Melillo *et al.*, 2014; Streiker 2016; British Columbia Ministry of Forests, Lands, and Natural Resources, 2009). It is also expected that these climate changes are increasing landslide hazard (e.g. Huggel *et al.*, 2012; Holm *et al.*, 2004; Evans and Clague, 1994; Uhlmann *et al.*, 2012). In this chapter, the climate change in northwest North America is quantified spatially using historical records. Significant trends in temperature and precipitation are then compared to landslide activity to explore the correlation between changing temperature, precipitation, and landslide hazard.

The primary methodology of assessing climate change was using Mann-Kendall trend testing (Mann, 1945; Helsel and Hirsch, 2002) to find significant trends in monthly station data downloaded from meteorological stations across British Columbia, Yukon, and Alaska. Once significant trends were identified, the associated climate data was assessed using a Sen's slope test to quantify the rate of climate change (Sen, 1968; Gocic and Trajkovic, 2013). These results were then used to generate climate indices, which are interpolated raster surfaces covering the entire study area. Temperature and precipitation indices were created for each season, and for the year as a whole. The climate indices were created using a novel method specifically tailored to this thesis. To assess any connection between the climate change data and the landslide inventory, the data was explored graphically, using time and elevation as independent variables. Finally, the correlation between landslide activity, temperature, and precipitation was statistically assessed using a Wilcoxon Rank Sum test and a correlation test (McGrew and Monroe, 2009).

The main objective of this chapter is to determine and quantify the relationship between climate change, specifically temperature and precipitation changes, and landslide activity,

specifically mass. This was a major component of this thesis, helping achieve the goal of better understanding how landslide hazard is effected by climate.

3.2 Data Sources and Pre-Processing

The first step in assessing climate change in northwest North America was to locate and acquire appropriate data. For British Columbia, monthly meteorological station data was downloaded from Environment Canada stations across the province (data download available from: http://climate.weather.gc.ca/historical_data/search_historic_data_e.html). The majority of the stations were along the west coast to reflect the study area or the Coast and St. Elias Mountains, however a select few were further inland to allow for a representation of climate change with varying longitude. Stations were selected based primarily on the longevity of record, but also with consideration for a variety of elevations in the dataset. For Alaska, monthly data was downloaded from National Oceanic and Atmospheric Administration's National Centers for Environmental Information (NOAA NCEI), with the same guidelines used in selecting the Canadian data (data download available from: <https://www.ncdc.noaa.gov/cdo-web/>).

To ensure consistency in data quality, each climate record was assessed for completion and currency. If the station data ended before the year 2000, the station was eliminated from consideration because recent climate trends based on current data was a priority. Any stations with greater than five consecutive years of missing data were also eliminated. For records with gaps of less than five consecutive years, linear interpolation was used based on monthly values (see **Equation 3.1**). In addition, all data was sorted and divided into separate data files for each month. A summary of the station data can be seen in **Figure 3.1** and **Table 3.1**. Changes in temperature and precipitation were of particular interest to this investigation. A brief description of each variable considered can be seen in **Table 3.2**. Note that all data was converted to metric units at a later stage in the analysis.

$$y = y_0 + (x - x_0) \times \frac{y_1 - y_0}{x_1 - x_0}$$

Equation 3.1: Linear interpolation equation used to estimate missing values in data gaps less than 5 consecutive years in length, where (x,y) is the interpolated value, (x0,y0) is the point preceding the missing value, and (x1,y1) is the point following the missing value.

Table 3.1: A summary of meteorological stations used for climate data analysis.

ID	Station Name	Region	Longitude	Latitude	Elevation (m)	Start Year	End Year
1	Agassiz CDA	BC	-121.8	49.2	15	1890	2006
2	Anchorage	AK	-150.0	61.2	36.6	1954	2016
3	Atlin	BC	-133.7	59.6	673.6	1967	2006
4	Barrow	AK	-156.8	71.3	9.4	1944	2016
5	Bella Coola	BC	-126.7	52.4	18.3	1895	2002
6	Boat Bluff	BC	-128.5	52.6	10.7	1975	2007
7	Chatham Point	BC	-125.5	50.3	22.9	1959	2007
8	Cordova	AK	-145.5	60.5	9.4	1909	2016
9	Egg Island	BC	-127.8	51.3	14	1966	2007
10	Germansen Landing	BC	-124.7	55.8	766	1952	2006
11	Graham Inlet	BC	-134.2	59.6	659.9	1974	2007
12	Grand Forks	BC	-118.5	49.0	531.9	1941	2006
13	Kitimat Townsite	BC	-128.6	54.1	98	1954	2007
14	Malibu Jarvis Inlet	BC	-123.9	50.2	18	1974	2006
15	McCarthy	AK	-143.0	61.4	381	1984	2016
16	StewartA	BC	-130.0	55.9	7.3	1975	2007
17	Tatlayoko Lake	BC	-124.4	51.7	870	1930	2005
18	Terrace A	BC	-128.6	54.5	217.3	1953	2013
19	Yakutat	AK	-139.7	59.5	10	1917	2016

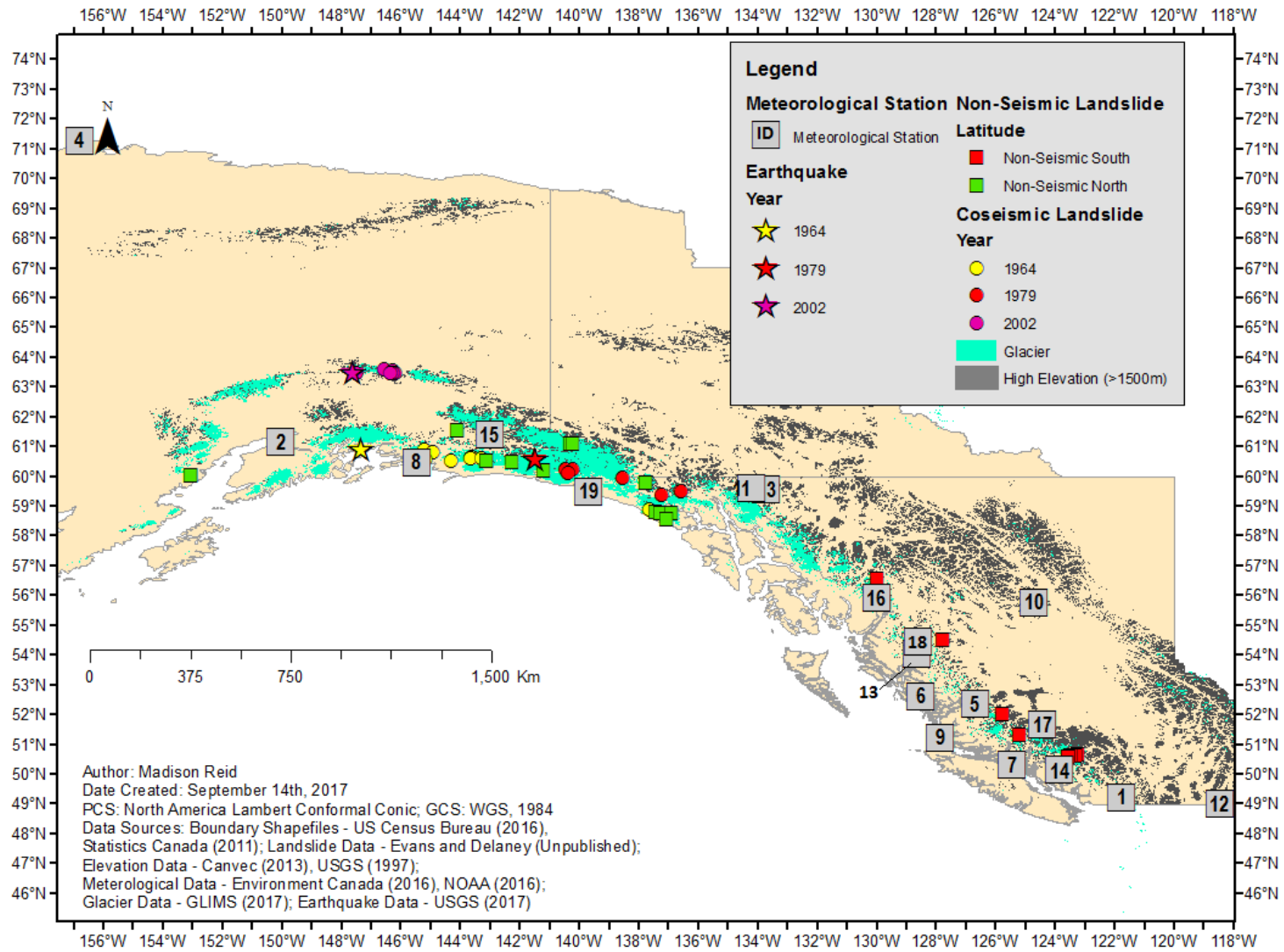


Figure 3. 1: A map displaying the location of meteorological stations (n=19) used for climate analysis, shown as purple triangles. See Table 3.1 for key.

Table 3. 2: Environment Canada (2016) variables used for climate analysis, along with their definitions.

Note that all variables also exist in the NOAA (2016) datasets, with the exception of total precipitation.

Environment Canada Variable	Definition and Units
<i>Mean Monthly Temperature</i>	The mean temperature in degrees Celsius (°C) is defined as the average of the maximum and minimum temperature at a location over the month.
<i>Mean Maximum Temperature</i>	The average of the maximum temperature in degrees Celsius (°C) observed at the location for that month.
<i>Mean Minimum Temperature</i>	The average of the minimum temperature in degrees Celsius (°C) observed at the location for that month.
<i>Extreme Maximum Temperature</i>	The highest daily maximum temperature in degrees Celsius (°C) reached at that location for that month.
<i>Extreme Minimum Temperature</i>	The lowest daily maximum temperature in degrees Celsius (°C) reached at that location for that month.
<i>Total Rain</i>	The total rainfall, or amount of all liquid precipitation in millimetres (mm) such as rain, drizzle, freezing rain, and hail, observed at the location during a specified time interval.
<i>Total Snow</i>	The total snowfall, or amount of frozen (solid) precipitation in centimetres (cm), such as snow and ice pellets, observed at the location during a specified time interval.
<i>Total Precipitation</i> <i>(note: this variable is not available in NOAA datasets)</i>	The sum of the total rainfall and the water equivalent of the total snowfall in millimetres (mm), observed at the location during a specified time interval.

3.3 Mann-Kendall Trend Testing

3.3.1 Methodology

Following the aforementioned data processing, the preliminary analysis used a Mann-Kendall trend test to determine variables of significance during each month. The Mann-Kendall trend test is a nonparametric test, meaning it does not assume the data being tested belongs to a specific distribution (i.e., normal) (Mann, 1945; Helsel and Hirsch, 2002). Using a nonparametric test is beneficial because it allows for increased flexibility, and has the capability to report existent trends in non-normalized and highly variable data. While directly analogous to regression, the Mann-Kendall test is much more forgiving of noisy data than many other approaches (Mann, 1945; Helsel and Hirsch, 2002). The test can be stated as “*a test for whether y values tend to increase or decrease with t*” (Helsel and Hirsch, 2002). In this methodology, y is the climate variable being tested and t is time.

```
> gf_jan<-read.csv(file.choose())
>
> MannKendall(gf_jan$Mean.Max.Temp)
tau = 0.126, 2-sided pvalue =0.13653
> MannKendall(gf_jan$Mean.Min.Temp)
tau = 0.292, 2-sided pvalue =0.00052059
> MannKendall(gf_jan$Mean.Temp)
tau = 0.219, 2-sided pvalue =0.0090749
> MannKendall(gf_jan$Extr.Max.Temp)
tau = -0.0834, 2-sided pvalue =0.32902
> MannKendall(gf_jan$Extr.Min.Temp)
tau = 0.143, 2-sided pvalue =0.089175
> MannKendall(gf_jan$Total.Rain)
tau = 0.111, 2-sided pvalue =0.19313
> MannKendall(gf_jan$Total.Snow)
tau = 0.0503, 2-sided pvalue =0.55159
> MannKendall(gf_jan$Total.Precip)
tau = 0.125, 2-sided pvalue =0.1367
```

Figure 3.2: A sample of the R code used for Mann-Kendall Testing. This example is for January at Grand Forks.

Mann-Kendall trend tests were performed to each month using the R package ‘Kendall’. The function ‘MannKendall’ was used instead of ‘SeasonalMannKendall’, because all data was already divided into month specific data files, thereby eliminating seasonality. A sample of the R code used can be seen in **Figure 3.2**.

3.3.2 Mann-Kendall Trend Testing Results

The results of the monthly Mann-Kendall trend tests were organized into tables for each station, and significant results (p less than or equal to 0.05) were highlighted for further assessment. All Mann-Kendall results can be seen in **Appendix A**. A summary these results can be seen in **Tables 3.3** and **3.4**, as well as **Figures 3.3** and **3.4**.

In all seasons, there are more variables that show significant warming than cooling. The annual average was that 32% of temperature-related variables showed warming, while only 3% reported cooling. The season with the most indicators of warming is summer; the cross-station average was 42% of the temperature variables considered showing statistically significant trends and only 2.8% of variables showing decreasing trends. These results emphasize the potential implications of summer warming for landslide hazard, as the majority of the landslide events considered in this thesis occur during the late summer. Overall, the results from the Mann-Kendall testing of temperature variables justifies further exploration into these trends, and their potential effects on glacier ice loss and landslide hazard.

Similar to the Mann-Kendall results from temperature variables, **Figure 3.4** demonstrates that there are more indicators reporting increasing precipitation (10% of variables considered) than decreasing precipitation (5% of variables considered). Winter shows the greatest percentage of significant trends, both increasing and decreasing. This is likely due to snowfall being able to show a trend, rather than being counted as insignificant as would be the case when there is no data for snowfall. Further analysis of the slopes of these trends, as well as their spatial

distribution is needed to assess any possible connections between precipitation and landslide hazard, as discussed further in the following sections.

Table 3.3: A summary of Mann-Kendall results for temperature variables.

JJA – June, July, August; SON – September, October, November; DJF- December, January, February; MAM – March, April, May

Station Name	JJA - % T Increase	JJA - % T Decrease	JJA - % T NonSig	SON - % T Increase	SON - % T Decrease	SON - % T NonSig	DJF - % T Increase	DJF - % T Decrease	DJF - % T NonSig	MAM - % T Increase	MAM - % T Decrease	MAM - % T NonSig	Annual Average T Increasing	Annual Average T Decreasing	Annual Average T NonSig
Agassiz CDA	53.3	20.0	26.7	46.7	6.7	46.7	80.0	0.0	20.0	46.7	6.7	46.7	56.7	8.3	35.0
Anchorage	46.7	0.0	53.3	33.3	0.0	66.7	80.0	0.0	20.0	80.0	0.0	20.0	60.0	0.0	40.0
Atlin	80.0	0.0	20.0	20.0	0.0	80.0	75.0	0.0	25.0	53.3	0.0	46.7	57.1	0.0	42.9
Barrow	86.7	0.0	13.3	73.3	0.0	26.7	73.3	0.0	26.7	73.3	0.0	26.7	76.7	0.0	23.3
Bella Coola	53.3	0.0	46.7	26.7	0.0	73.3	66.7	0.0	33.3	73.3	0.0	26.7	55.0	0.0	45.0
Boat Bluff	6.7	0.0	93.3	0.0	0.0	100.0	22.2	0.0	77.8	6.7	0.0	93.3	8.9	0.0	91.1
Chatham Point	20.0	0.0	80.0	13.3	0.0	86.7	26.7	0.0	73.3	66.7	0.0	33.3	31.7	0.0	68.3
Cordova	13.3	33.3	53.3	0.0	60.0	40.0	13.3	13.3	73.3	20.0	6.7	73.3	11.7	28.3	60.0
Egg Island	66.7	0.0	33.3	0.0	0.0	100.0	46.7	0.0	53.3	60.0	0.0	40.0	43.3	0.0	56.7
Germanse Landing	33.3	0.0	66.7	0.0	0.0	100.0	33.3	0.0	66.7	53.3	46.7	30.0	30.0	0.0	70.0
Graham Inlet	80.0	0.0	20.0	6.7	0.0	93.3	0.0	0.0	100.0	20.0	0.0	80.0	26.7	0.0	73.3
Grand Forks	46.7	0.0	53.3	13.3	0.0	86.7	26.7	6.7	66.7	53.3	0.0	46.7	35.0	1.7	63.3
Kitimat Townsite	55.6	0.0	44.4	0.0	0.0	100.0	20.0	0.0	80.0	53.3	0.0	46.7	32.2	0.0	67.8
Malibu Jervis Inlet	6.7	0.0	93.3	0.0	0.0	100.0	20.0	0.0	80.0	0.0	0.0	100.0	6.7	0.0	93.3
McCarthy	46.7	0.0	53.3	13.3	0.0	86.7	6.7	0.0	93.3	26.7	0.0	73.3	23.3	0.0	76.7
StewartA	20.0	0.0	80.0	0.0	0.0	100.0	6.7	0.0	93.3	6.7	0.0	93.3	8.3	0.0	91.7
Tatlayoko Lake	0.0	0.0	100.0	0.0	26.7	73.3	0.0	0.0	100.0	0.0	6.7	93.3	0.0	8.3	91.7
Terrace A	40.0	0.0	60.0	6.7	0.0	93.3	20.0	0.0	80.0	0.0	0.0	100.0	16.7	0.0	83.3
Yakutat	40.0	0.0	60.0	6.7	33.3	60.0	6.7	6.7	86.7	40.0	0.0	60.0	23.3	10.0	66.7
MEAN	41.9	2.8	55.3	13.7	6.7	79.6	32.8	1.4	65.8	38.6	1.1	60.4	31.7	3.0	65.3
SD	25.3	8.5	25.2	19.0	15.6	21.9	27.6	3.5	26.9	26.8	2.5	26.3	20.9	6.8	20.2
Max	86.7	33.3	100.0	73.3	60.0	100.0	80.0	13.3	100.0	80.0	6.7	100.0	76.7	28.3	93.3
Min	0.0	0.0	13.3	0.0	0.0	26.7	0.0	0.0	20.0	0.0	0.0	20.0	0.0	0.0	23.3

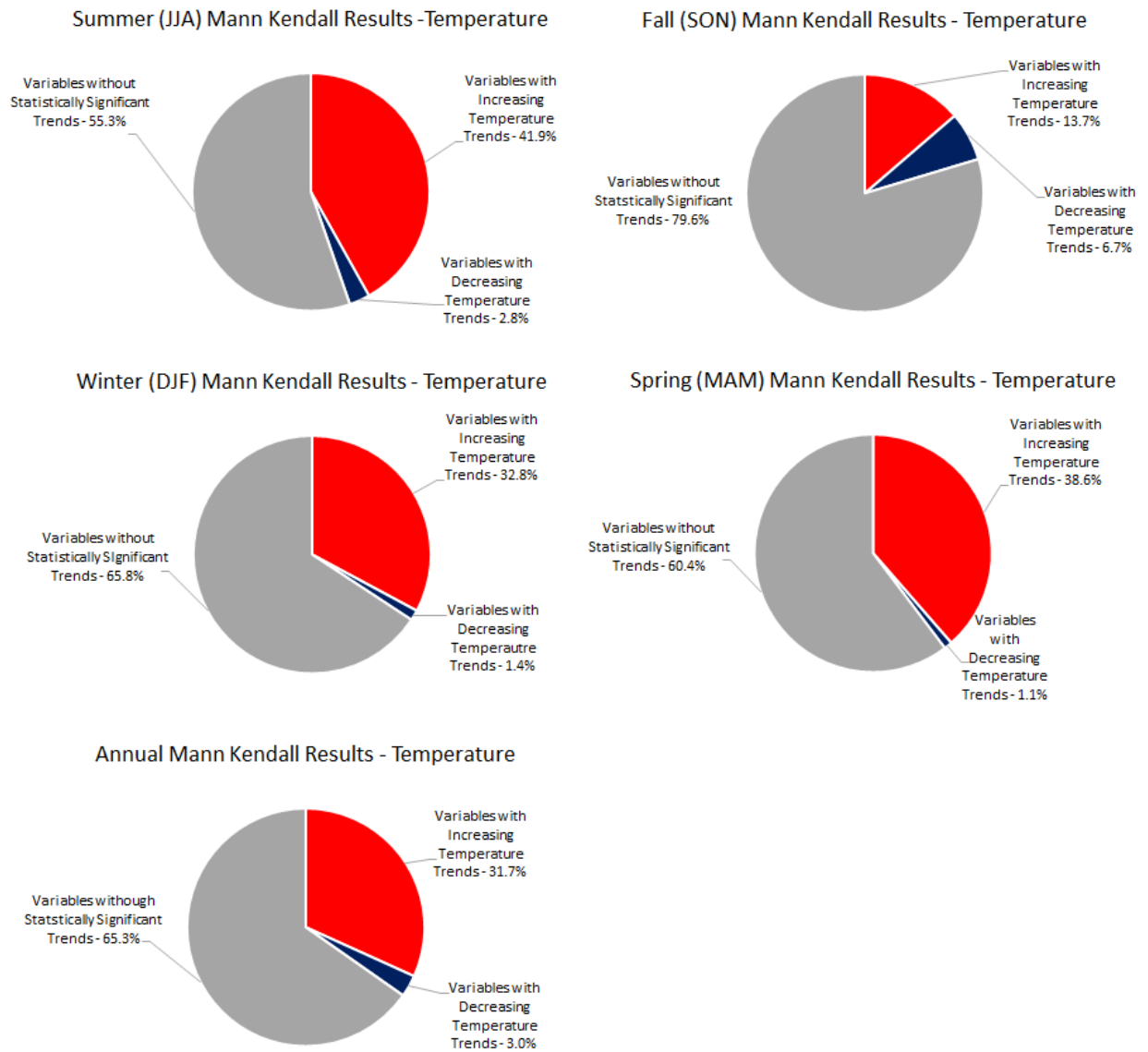


Figure 3.3: A summary of the Mann-Kendall results for temperature variables (data from **Table 3.3**).

Table 3.4: A summary of Mann-Kendall results for precipitation variables.

Station Name	JJA - % P Increase	JJA - % P Decrease	JJA - % P NonSig	SON - % P Increase	SON - % P Decrease	SON - % P NonSig	DJF - % P Increase	DJF - % P Decrease	DJF - % P NonSig	MAM - % P Increase	MAM - % P Decrease	MAM - % P NonSig	Annual P Increase	Annual P Decrease	Annual P NonSig
Agassiz CDA	0.0	0.0	100.0	0.0	0.0	100.0	33.3	0.0	66.7	0.0	0.0	100.0	8.3	0.0	91.7
Anchorage	0.0	0.0	100.0	0.0	0.0	100.0	0.0	0.0	100.0	0.0	0.0	100.0	0.0	0.0	100.0
Atlin	0.0	0.0	100.0	0.0	0.0	100.0	22.2	0.0	77.8	0.0	0.0	100.0	5.6	0.0	94.4
Barrow	0.0	0.0	100.0	33.3	0.0	66.7	50.0	0.0	50.0	50.0	0.0	50.0	33.3	0.0	66.7
Bella Coola	22.2	0.0	77.8	33.3	0.0	66.7	66.7	0.0	33.3	33.3	0.0	66.7	38.9	0.0	61.1
Boat Bluff	0.0	0.0	100.0	0.0	0.0	100.0	33.3	0.0	66.7	0.0	0.0	100.0	8.3	0.0	91.7
Chatham Point	0.0	0.0	100.0	22.2	0.0	77.8	0.0	11.1	88.9	22.2	11.1	66.7	11.1	5.6	83.3
Cordova	0.0	20.0	80.0	0.0	55.6	44.4	0.0	77.8	22.2	0.0	46.7	53.3	0.0	50.0	50.0
Egg Island	0.0	0.0	100.0	0.0	0.0	100.0	0.0	11.1	88.9	0.0	0.0	100.0	0.0	2.8	97.2
Germanse n Landing	0.0	0.0	100.0	11.1	0.0	88.9	22.2	0.0	77.8	22.2	11.1	66.7	13.9	2.8	83.3
Graham Inlet	0.0	0.0	100.0	11.1	11.1	77.8	0.0	0.0	100.0	0.0	0.0	100.0	2.8	2.8	94.4
Grand Forks	22.2	0.0	77.8	11.1	0.0	88.9	0.0	0.0	100.0	55.6	0.0	44.4	22.2	0.0	77.8
Kitimat	0.0	0.0	100.0	0.0	0.0	100.0	11.1	22.2	66.7	0.0	11.1	88.9	2.8	8.3	88.9
Malibu	0.0	0.0	100.0	0.0	0.0	100.0	22.2	11.1	66.7	0.0	0.0	100.0	5.6	2.8	91.7
Jervis Inlet	0.0	0.0	100.0	0.0	0.0	100.0	0.0	22.2	77.8	0.0	0.0	100.0	0.0	5.6	94.4
McCarthy	0.0	0.0	100.0	0.0	0.0	100.0	0.0	22.2	77.8	0.0	0.0	100.0	0.0	5.6	94.4
StewartA	22.2	0.0	77.8	0.0	0.0	100.0	11.1	0.0	88.9	0.0	0.0	100.0	8.3	0.0	91.7
Tatlayoko Lake	0.0	0.0	100.0	0.0	0.0	100.0	0.0	0.0	100.0	0.0	0.0	100.0	0.0	0.0	100.0
Terrace A	0.0	0.0	100.0	0.0	0.0	100.0	11.1	0.0	88.9	33.3	0.0	66.7	11.1	0.0	88.9
Yakutat	0.0	50.0	50.0	50.0	16.7	33.3	0.0	0.0	100.0	0.0	0.0	100.0	12.5	16.7	70.8
MEAN	3.5	3.7	92.8	9.1	4.4	86.5	14.9	8.2	76.9	11.4	4.2	84.4	9.7	5.1	85.2
SD	8.1	11.8	13.4	14.6	12.8	19.9	18.9	18.0	22.1	18.2	10.8	20.1	10.8	11.3	13.5
Max	22.2	50.0	100.0	50.0	55.6	100.0	66.7	77.8	100.0	55.6	46.7	100.0	38.9	50.0	100.0
Min	0.0	0.0	50.0	0.0	0.0	33.3	0.0	0.0	22.2	0.0	0.0	44.4	0.0	0.0	50.0

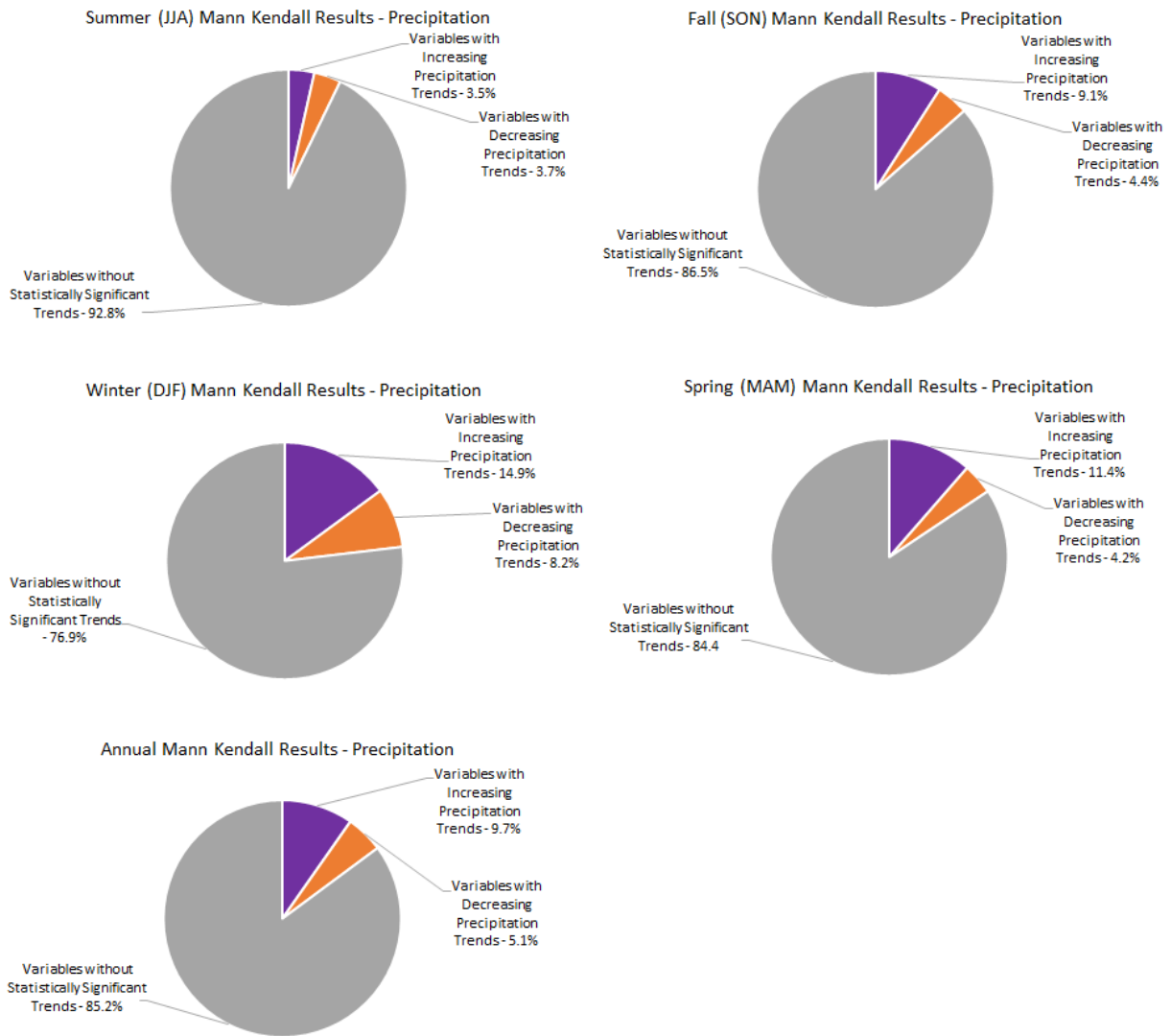


Figure 3.4: A summary of the Mann-Kendall results for temperature variables (data from **Table 3.4**).

3.4 Sen's Slope Testing

3.4.1 Sen's Slope Methodology

Once significant trends were identified from Mann-Kendall testing, Sen's slope testing was completed to quantify the slope of the established trend. The Sen's slope test is an alternative to least squares regression, and is similar to the Mann-Kendall test; it is nonparametric meaning it does not require data to be normally distributed. (Sen, 1968; Gocic and Trajkovic, 2013).

The Sen's slope analysis was complete using the 'trend' package in R. Testing was only done on variable determined to have significant trends through the Mann-Kendall analysis. A sample of the R code can be seen in **Figure 3.5**. Once testing was completed for all necessary variables, results were exported into Excel for further analysis, and the generation of climate indices

```
> gf_jan_mt<-ts(gf_jan$Mean.Temp, start=c(1941,1), end=c(2007,1), frequency=1)
> sens.slope(gf_jan_mt)

Sen's slope and intercept

slope: 0.056
95 percent confidence intervall for slope
0.1 0.0162

intercept: -7.384
nr. of observations: 67
```

Figure 3.5: A sample of the Sen's slope testing code used in R.

3.4.2 Sen's Slope Results

Sen's Slope testing was completed for all variables determined to have significant trends from Mann-Kendall analysis (Sen, 1968, Gocic and Trajkovic, 2013). The slope of the Sen's

slope results indicates the change in the input variable, with correct units. As expected from the Mann-Kendall results, the majority of the variables tested showed warming trends (89% averaged annually: 89% in summer, 71% in fall, 96% in winter, and 94% in spring) and increasing precipitation (85% averaged annually: 90% in summer, 72% in fall, 84% in winter, and 90% in spring). All summary of the Sen’s slope testing by variable can be seen in **Table 3.5**. These results, an intermediate step, were then used for the generation of climate indices, as discussed in **Section 3.5**.

Table 3.5: A summary of the Sen’s slope analysis by season and by variable, indicating increased temperatures and precipitation throughout the study area.

Variable	JJA % ↑	JJA % ↓	SON % ↑	SON % ↓	DJF % ↑	DJF % ↓	MAM % ↑	MAM % ↓	Annual % ↑	Annual % ↓
T_M	97.4	2.6	75	25.0	100.0	0.0	100.0	0.0	94.5	5.5
T_{MMx}	86.4	13.6	85.7	14.3	100.0	0.0	95.5	4.5	93.0	7.0
T_{MMn}	77.2	22.8	61.4	38.6	93.0	7.0	86.0	14.0	79.4	20.6
T_{EMx}	100.0	0.0	54.5	45.5	100.0	0.0	100.0	0.0	93.2	6.8
T_{EMn}	86.0	14.0	76.4	23.6	87.3	12.7	87.5	12.5	84.3	15.7
P_R	100.0	0.0	100.0	0.0	92.3	7.7	100.0	0.0	97.9	2.1
P_S	88.5	11.5	53.8	46.2	80.0	20.0	94.1	5.9	81.7	18.3
P_T	82.4	17.6	62.7	37.3	80.8	19.2	74.5	25.5	75.1	24.9
All Temp. Variables	89.4	10.6	70.6	29.4	96.1	3.9	93.8	6.2	88.9	11.1
All Precip Variables	90.3	9.7	72.2	27.8	84.4	15.6	89.5	10.5	84.9	15.1

3.5 Regional Climate Indices Generation and Visualization

3.5.1 Methodology

Once Sen's slope testing was completed, the magnitude of significant trends was used to generate indices to convey the type and degree of climate change at each meteorological station. Two separate indices, developed specifically for this thesis, were calculated: Temperature Index (TI) and Precipitation Index (PI) (see **Equations 3.2 to 3.5**). The temperature index is a weighted combination of the Sens's slope results for the five temperature related variables: mean maximum temperature, mean minimum temperature, mean temperature, extreme maximum temperature, and extreme minimum temperature. Mean temperature was given the greatest weight of 70%, because this variable most accurately reflects the average rate of temperature change observed. Extreme maximum and minimum temperatures were given the least weight (5% each), because while they do reflect changing temperature patterns, they do not necessarily reflect the overall change in temperature at a given location. The precipitation index expresses change in precipitation, and considers both rain and snow. Note there are some differences between the Canadian and American indices. First, the American data is input in Imperial units, so there is a conversion factor in each of the indices ($\times 5/9$ to convert between Fahrenheit and Celsius, and $\times 25.4$ to convert between inches and millimeters). Second, the American precipitation index does not have a total precipitation input because this variable was not included in the NOAA datasets. However, the equal weighting of total rain and total snow allows for direct comparability to the Canadian Index.

$$TI = (T_{MMx} \times 10) + (T_{MMn} \times 10) + (T_M \times 70) + (T_{EMx} \times 5) + (T_{EMn} \times 5) \quad (3.2)$$

$$PI = (P_T \times 80) + (P_R \times 10) + (P_S \times 10) \quad (3.3)$$

$$TIA = ((T_{MMx} \times 10) + (T_{MMn} \times 10) + (T_M \times 70) + (T_{EMx} \times 5) + (T_{EMn} \times 5)) \times \frac{5}{9} \quad (3.4)$$

$$PI_A = ((P_R \times 50) + (P_S \times 50)) \times 25.4 \quad (3.5)$$

Equations 3.2-3.5: *The regional climate change indices, generated from met station data. TI - Temperature Index; TIA - American Temperature Index; PI - Precipitation Index; PIA - American Precipitation Index; TMMx – Mean Maximum Temperature; TMMn – Mean Minimum Temperature; TM – Mean Monthly Temperature; TEMx – Extreme Maximum Temperature; TEMn – Extreme Minimum Temperature; Pt – Total Precipitation; Pr – Total Rain; Ts – Total Snow. Note that variables in the Canadian indices are to be input in degrees Celsius and millimeters; American indices use degrees Fahrenheit and inches. The output of both the Canadian and the American indices are in metric units. These indices were developed specifically for this thesis.*

Each of these weighted indices show the temperature or precipitation change at the station over 100 years. This is because the weighting process using a factor of 100, and the values of the Sen’s slope report changes per year. The value of each index was then averaged seasonally (DJF, MAM, JJA, SON), and imported into ArcMap. A raster surface for each index was then interpolated using the inverse distance weighting tool, and index values at each landslide source area were recorded.

As a secondary climate data source, PRISM (Parameter-elevation Regressions on Independent Slopes Model) climate reanalysis data was used (Pacific Climate Impacts Consortium, 2014; data download available from: < <https://www.pacificclimate.org/data/high-resolution-prism-climatology>>). PRISM data is based on thousands of temperature and precipitation observations, and was developed to accurately reflect topographic variations at a small scale, approximately 800x800m. The PRISM data is available for all of British Columbia, with two 30-year climate normals: 1971-2000 and 1981-2010. The variables included in the PRISM datasets are mean monthly minimum temperature, mean monthly maximum temperature, and mean monthly precipitation. To find the difference between the two 30-year normal datasets, they were subtracted using the ‘Raster Calculator’ tool in ArcMap. Finally, the climate change

results from the temperature and precipitation indices were compared to the PRISM climate change results, to validate the methodology used in this thesis.

3.5.2 Results

Temperature index maps are shown in **Figures 3.6-3.10**, and precipitation index maps can be seen in **Figures 3.11-3.15**.

All seasons show significant warming in most regions, with the greatest warming in winter and summer (**Figures 3.6-3.10**). Fall has the least drastic seasonal warming, with several areas actually showing cooling trends. However, on an annual scale there are only two small pockets showing cooling (around the Cordova (Alaska) and Tatlayoka lake (British Columbia) stations – see **Figure 3.1** and **Table 3.1**) and the remainder of the study area shows various levels of warming. Increasing temperatures are particularly pronounced in the north. These results are consistent with warming reported in the literature (Solomon *et al.*, 2007; Field *et al.*, 2014; Melillo *et al.*, 2014, Streiker 2016; British Columbia Ministry of Forests, Lands, and Natural Resources, 2009). The results from the precipitation indices show a consistent pattern of decreased precipitation in the North (particularly in Alaska), and increased precipitation in the south (**Figures 3.11 to 3.15**). The boundary between increasing and decreasing precipitation trends varies seasonally, between approximately 56 degrees N to 60 degrees N. These results are not entirely in agreement with the literature; based on the literature review completed in Chapter 2, increased precipitation was expected in Alaska as well as British Columbia (Solomon *et al.*, 2007; Field *et al.*, 2014; Melillo *et al.*, 2014, Streiker 2016; British Columbia Ministry of Forests, Lands, and Natural Resources, 2009)

Subjectively, it seems that more recent landslide events tend to occur in locations with more intense warming. This conclusion is based on a comparison of the years in which landslides take place (**Table 2.2**) to their associated annual climate index results (**Figure 3.10**). To investigate this observation objectively, landslide activity was plotted against climate factors,

seen in the following section. There is no clear pattern between precipitation changes and landslide activity, but any potential connections will also be investigated in **Section 3.6**.

The results from the comparison of regional index values and PRISM values shows relatively good agreement between the two datasets (see **Table 3.6**). For the landslide source areas with PRISM data available, 100% of the regional indices generated in this chapter showed increasing temperature and precipitation values. Alternatively, PRISM values reported 74% of landslide source areas to be occurring in locations with increasing temperatures, and 86% to be in locations with increasing precipitation. One reason for the lower numbers of temperature increases in the PRISM dataset, when compared to the indices results, was that the mean monthly maximum temperature data was frequently found to be decreasing, however the mean monthly minimum temperature was almost always found to be increasing. Decreasing mean monthly maximum temperatures were incorporated into the regional index values, however the index reports an increase because the other variables (i.e. mean monthly temperature, mean minimum temperature, and extreme maximum and minimum temperatures) are also included and outweigh the slight decreases in mean maximum monthly temperature. Another potential source of error when comparing the PRISM data and the regional indices is the different temporal ranges in each of the datasets, with PRISM data reflecting a much shorter period. Overall, when used as a secondary data source, the PRISM data shows relatively good agreement with the results from the regional indices, helping to increase the confidence in the results from the meteorological station analysis.

Table 3.6: A summary of the comparison between regional indices' results and PRISM data, both showing increases in temperature and precipitation throughout British Columbia.

Variable	% Regional Indices Showing Increase	% PRISM Showing Increase	% Regional Indices Showing Decrease	% PRISM Showing Decrease
Temperature	100% (21/21)	74% (31/42)	0% (0/21)	26% (11/42)
Precipitation	100% (21/21)	86% (18/21)	0% (0/21)	14% (3/21)

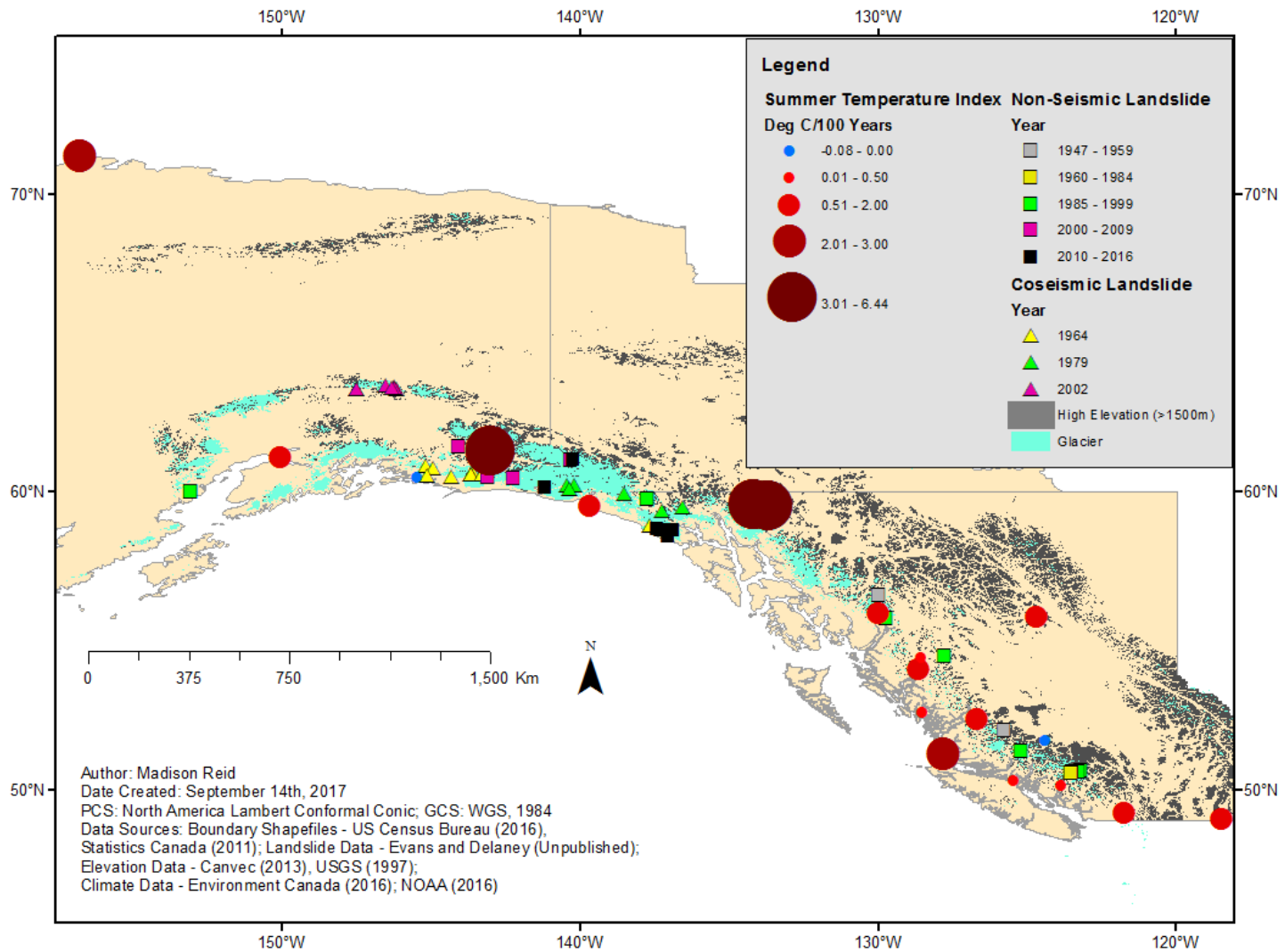


Figure 3.6: Summer Temperature Index (JJA). Note significant warming to the north of 56 degrees N..

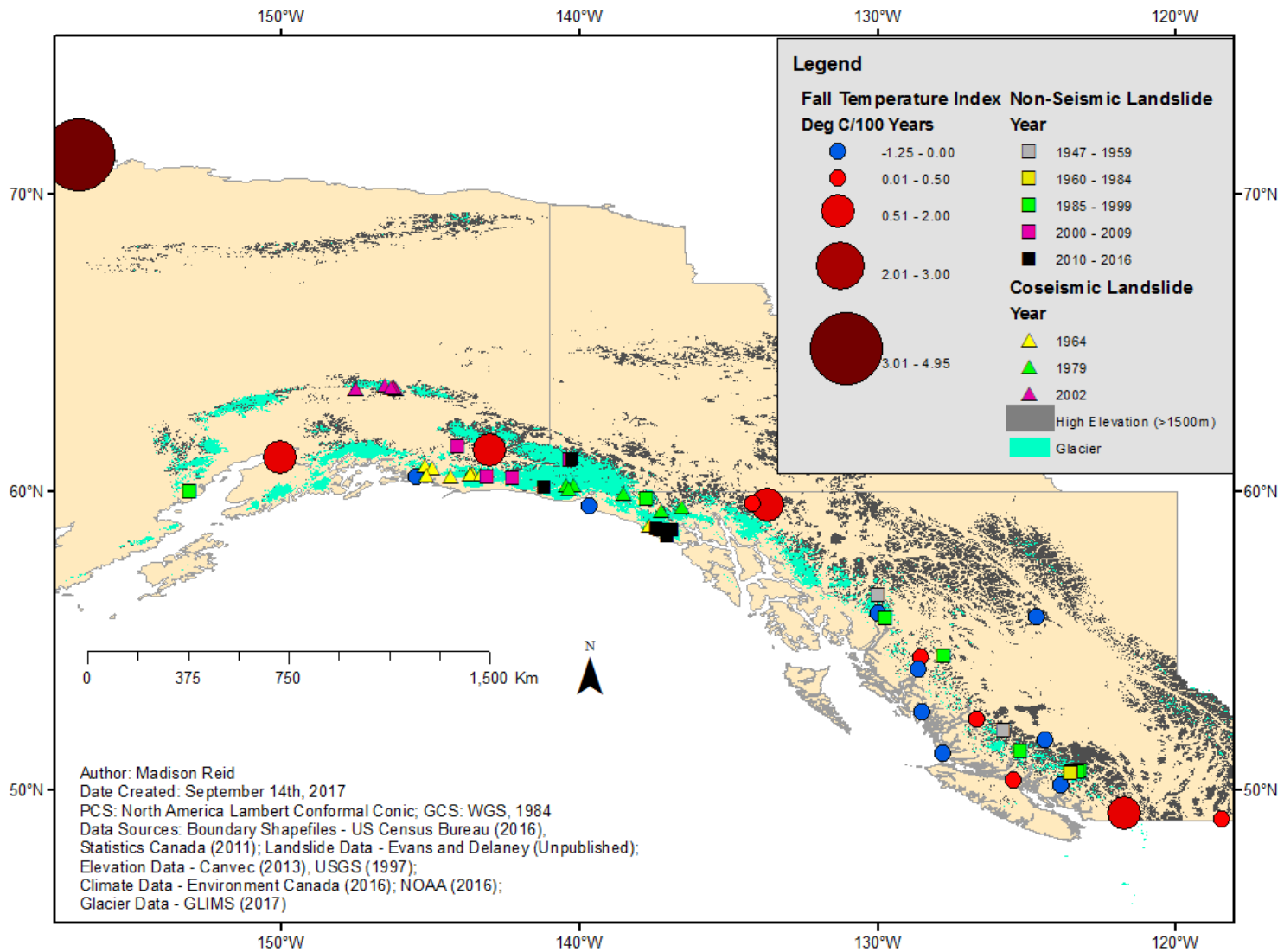


Figure 3.7: Fall temperature index, showing pockets of cooling.

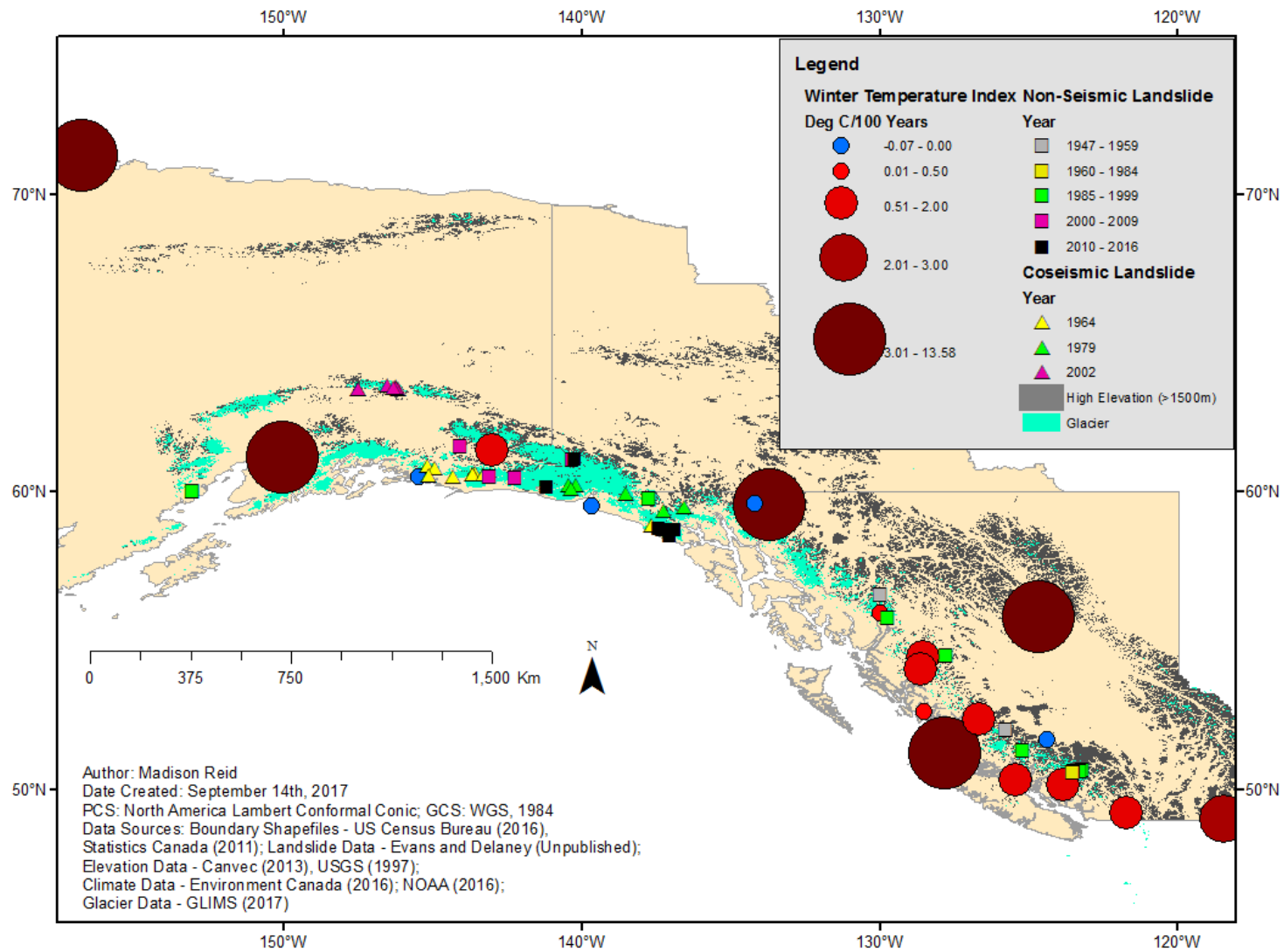


Figure 3.8: Winter temperature index, showing the greatest seasonal warming

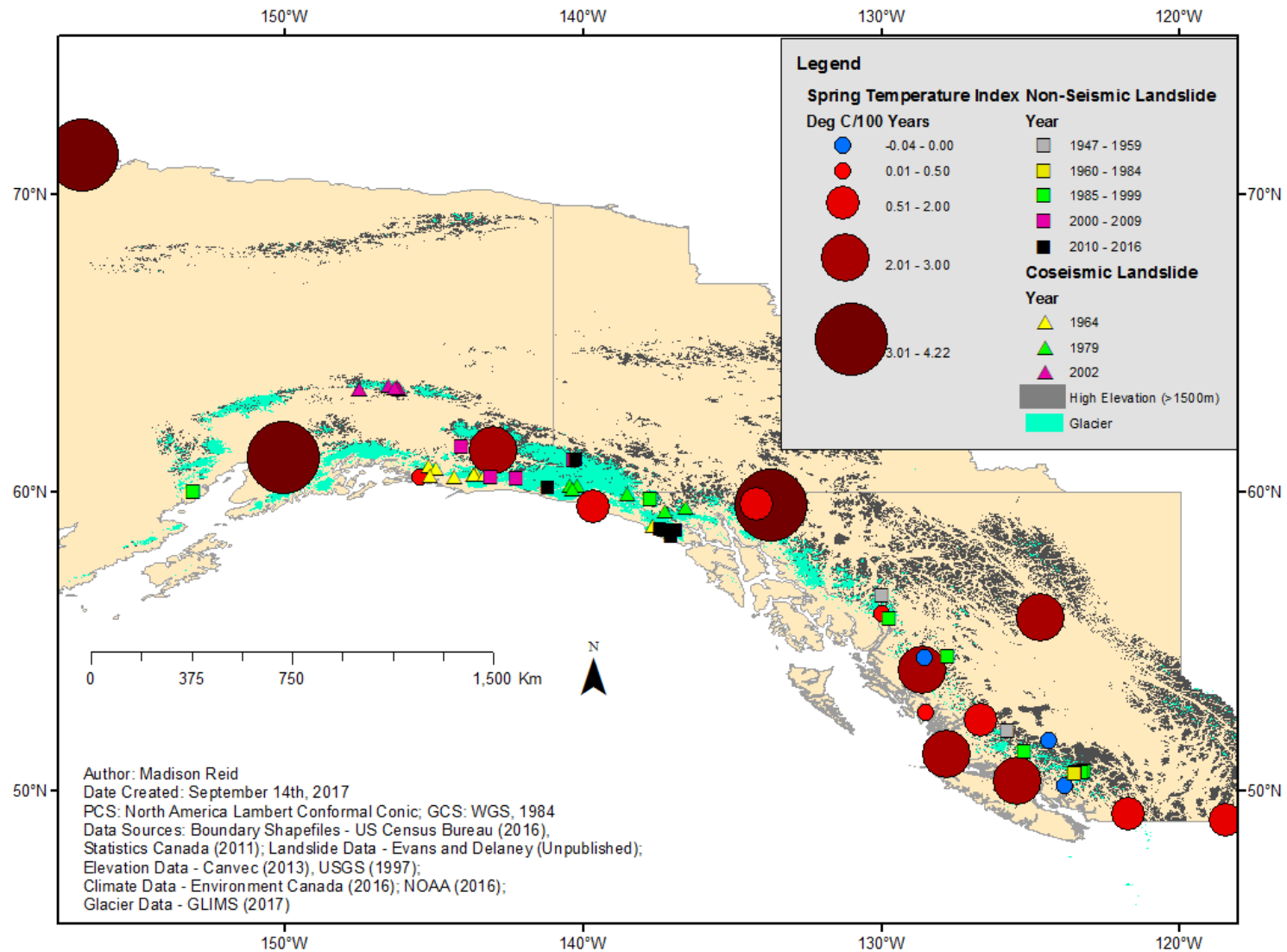


Figure 3.9: Spring temperature index, showing the greatest warming in Alaska

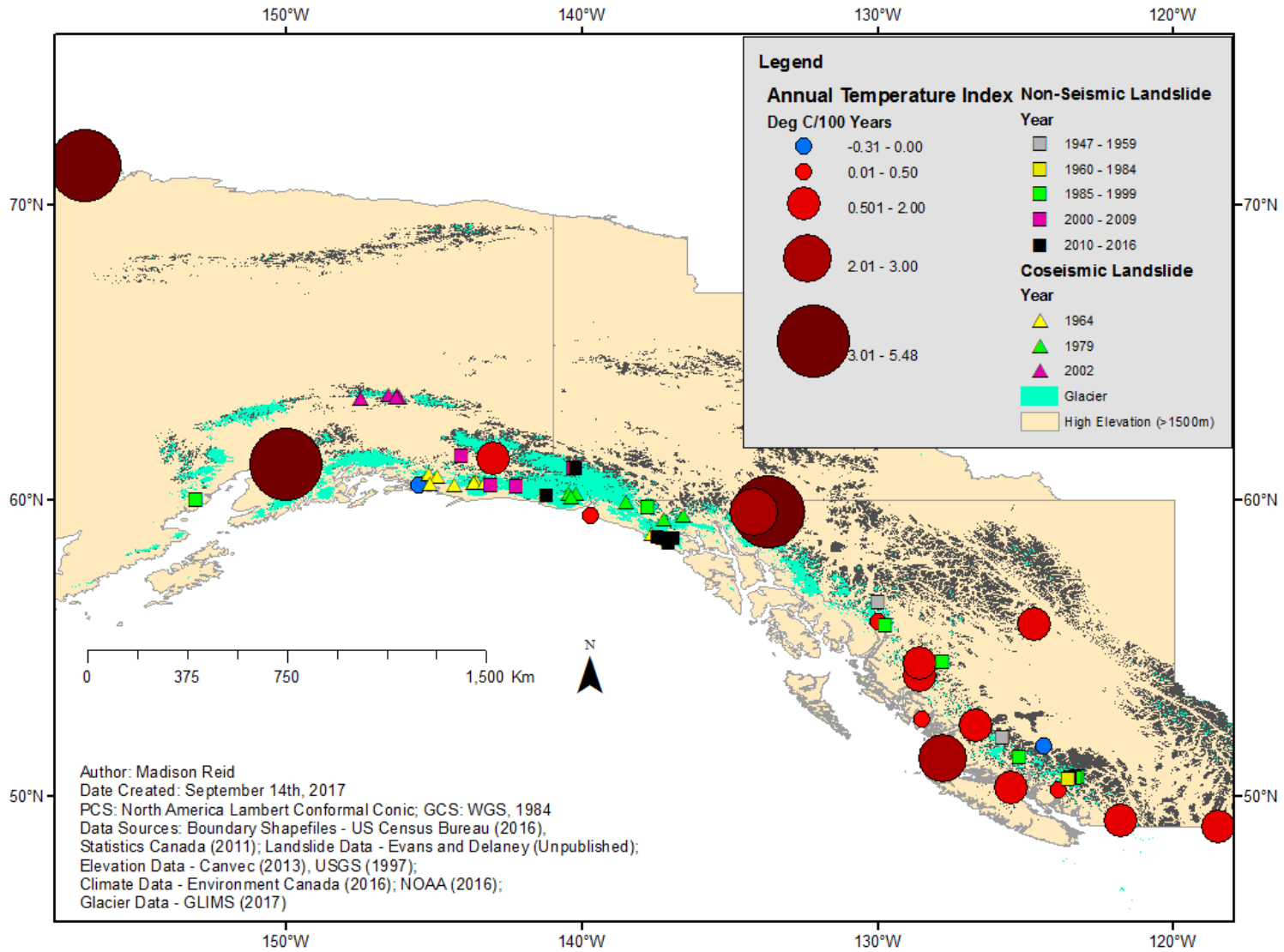


Figure 3.10: Annual temperature index, showing significant warming western Alaska and northern British Columbia.

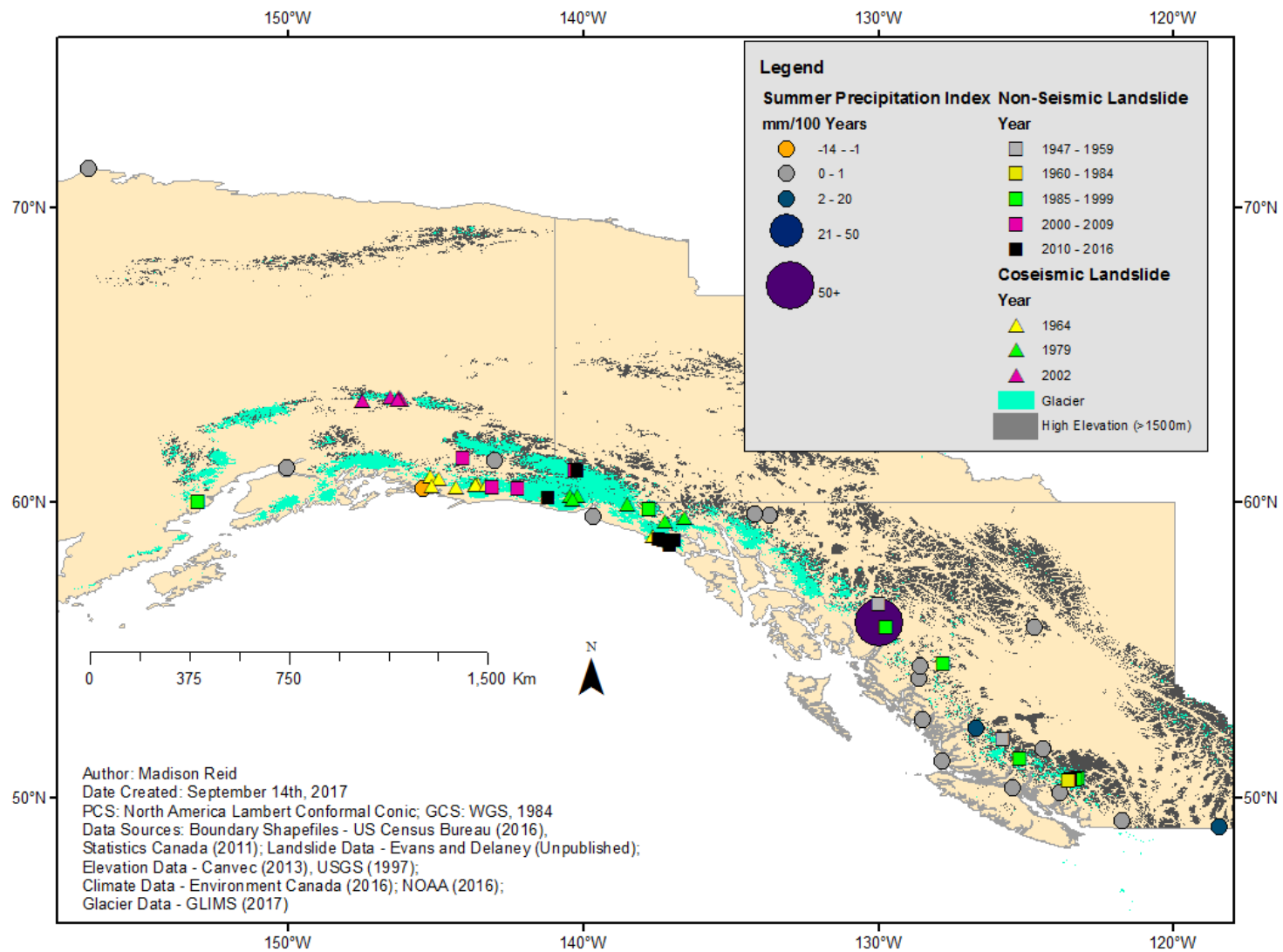


Figure 3.11: Summer precipitation index, showing wetter conditions in the south and dryer conditions in Alaska.

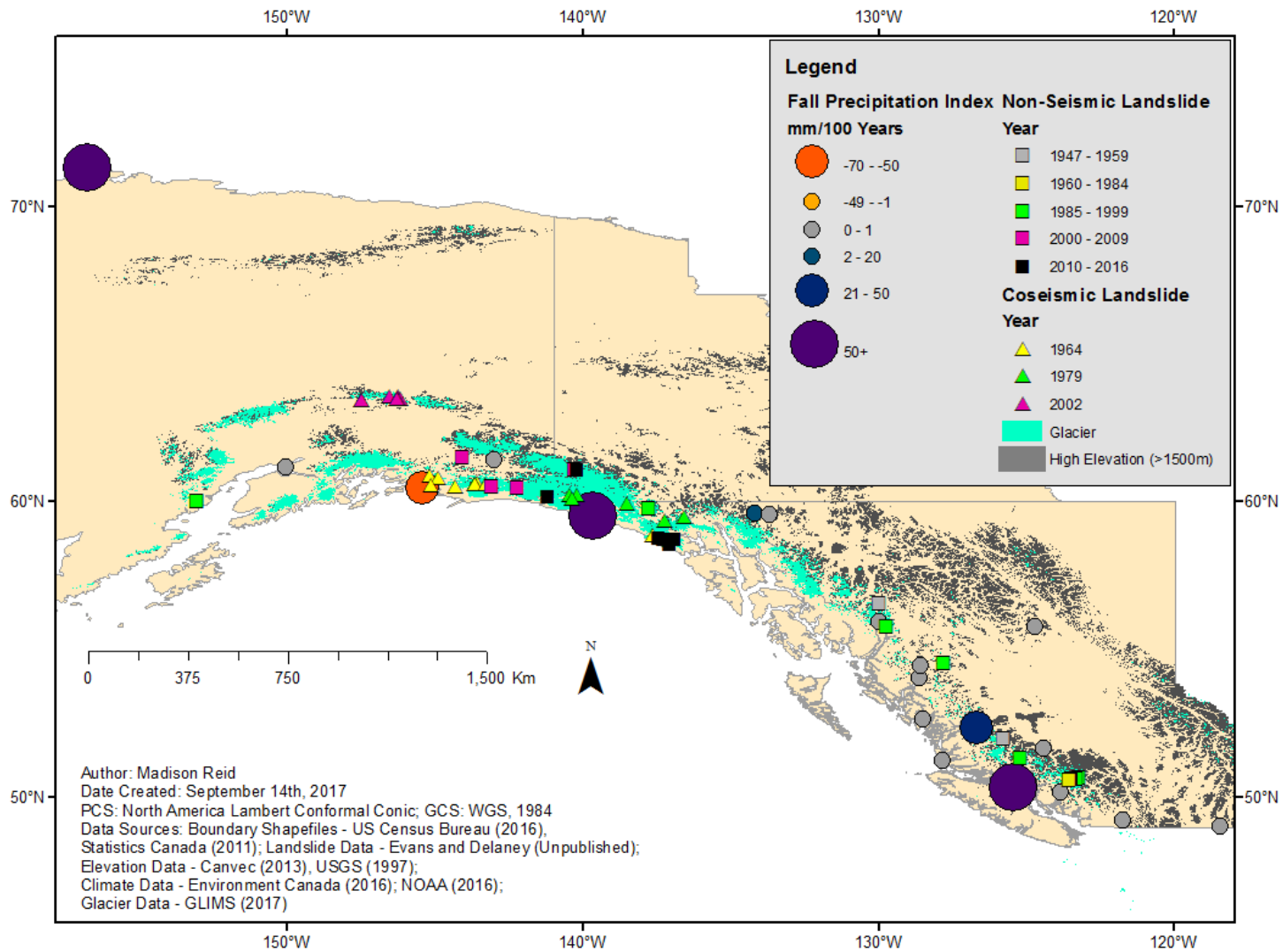


Figure 3.12: Fall precipitation index, with wetter conditions in British Columbia and northern Alaska, with dryer conditions in southern Alaska.

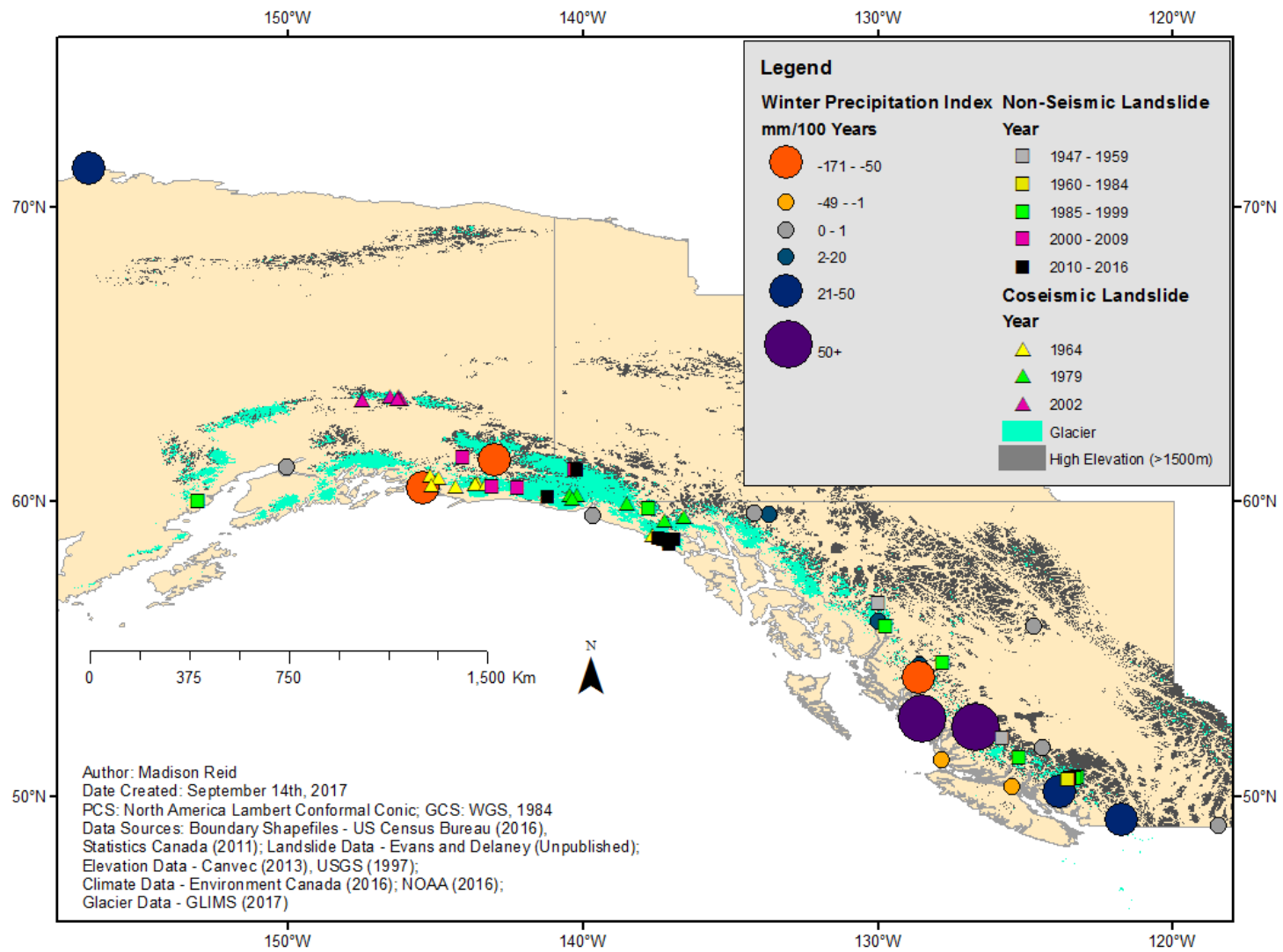


Figure 3.13: Winter precipitation index, showing wetter conditions in southern British Columbia and northern Alaska, with dryer conditions in northern British Columbia and Southern Alaska

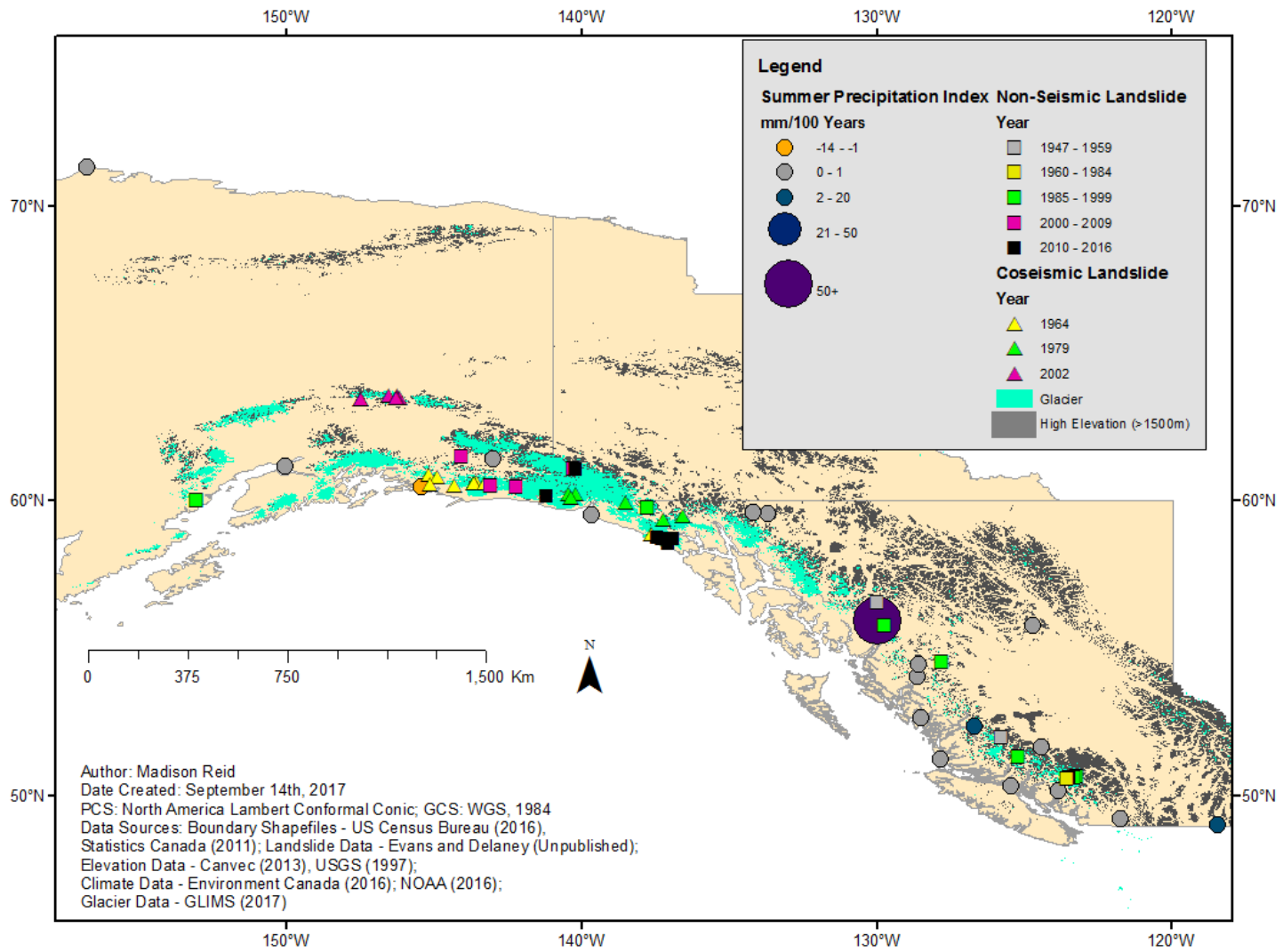


Figure 3.14: Spring precipitation index, showing drying to the north and wetter conditions in the south.

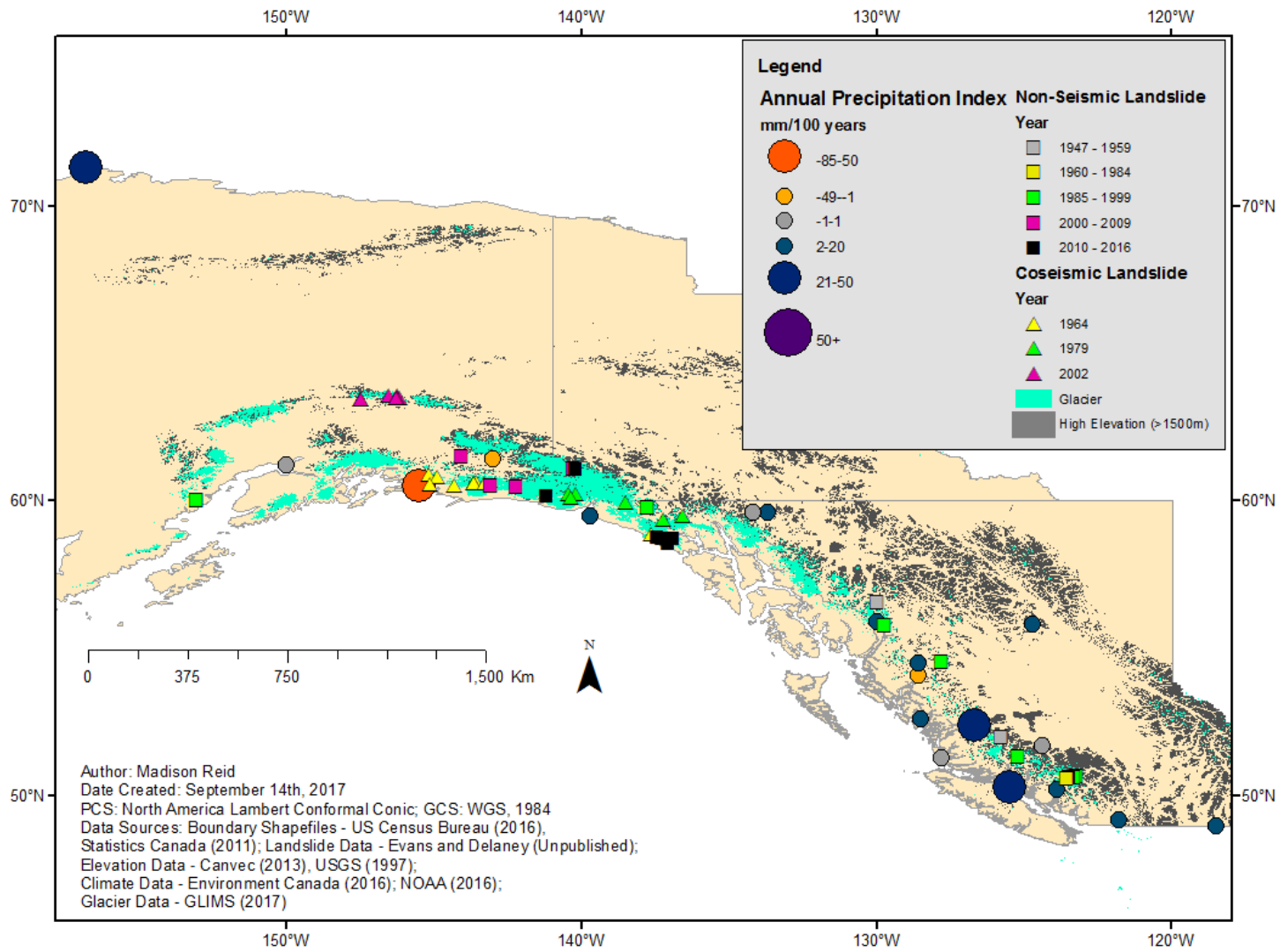


Figure 3.15: Annual precipitation index, showing dry conditions in southern Alaska and Yukon, with wetter conditions in British Columbia and northern Alaska

3.6 Statistical Exploration of Regional Climate Indices

3.6.2 Methodology

To quantitatively explore the subjectively observed relationships between landslide activity, temperature index values and precipitation index values corresponding to locations with landslide events were extracted using the ‘extract value to point’ tool in ArcMap. Using the same tool, elevation data was added to each of the landslide events. The DEMs in this process are summarized in **Table 3.7**. In addition, the landslide inventory was divided into seismic and non-seismically triggered events, creating two separate files.

Table 3.7: DEM data sources for statistical analyses of climate indices

DEM COVERAGE	DEM RESOLUTION	DEM SOURCE	NOTES
British Columbia (Province wide)	100x100m	CanVec, 2013.	This DEM was kindly provided by Marten Geertsema (BC Ministry of Forests) CanVec is a multi-source product coming mainly from the National Topographic Data Base (NTDB), the Mapping the North process conducted by the Canada Center for Mapping and Earth Observation (CCMEO), the Atlas of Canada data, the GeoBase initiative and the data update using satellite imagery coverage (e.g. Landsat 7, Spot, Radarsat, etc)
Alaska (State wide)	300x300m	U.S. Geological Survey EROS Alaska Field Office, 1997	Data download available from: < https://agdc.usgs.gov/data/usgs/erosafo/300m/300m.html > DEM is created from 1degree x 1degree blocks by the Defense Mapping Agency Topographic Center. These same data are currently available from the Earth Science Information Center.

Preliminary data visualization was completed by plotting each of the landslide events on a scatterplot comparing elevation and time. To capture some of the spatial variability of the non-seismically triggered data, events were divided into a southern and a northern cluster; the division between the two subsets was 57 degrees N based on a subjectively observed division in the data. 57 degrees N is also approximately the latitude at which precipitation trends change from wetter conditions in the south to dryer conditions to the north (**Figures 3.11-3.15**).

After assessing the basic elevation distribution of landslide events through time, a more complex assessment of the potential implications of climate factors was undertaken. The first step was to plot the temperature and precipitation index values for each of the landslide events, with time as the independent variable. The second step was to sort the dataset from lowest to highest elevation. Then, the cumulative landslide mass, temperature index, and precipitation index values were calculated and plotted. For seismic events, the annual temperature and precipitation indices were used. The reasoning for this is that seismic events occur randomly throughout the year, therefore the annual indices will be most reflective of the climate conditions. For non-seismically triggered events, the summer indices were used because almost all of the events occurred during the summer months.

Following a visual inspection, statistical analyses were used to verify the significance of observed trends. The Wilcoxon Rank Sum test (McGrew and Monroe, 2009) and correlation analysis were implemented using R. A sample of the code used to complete the Wilcoxon Rank Sum test can be seen in **Figure 3.16**. The Wilcoxon Rank Sum test is non-parametric, meaning it does not require a normal distribution, and it is designed to test for differences between two independent samples (McGrew and Monroe, 2009). The null hypothesis (H_0) is that the populations follow the same distribution, and the alternative hypothesis is that they are not the same. To reject the null hypothesis, the p-value of the Wilcoxon Rank Sum test must be less than or equal to a specified level of significance. For the Wilcoxon Rank Sum test a significance level of 0.05 was used. Finally, all results were summarized in a tabular format, and the implications were discussed.


```

> wilcox.test (NS$NSS_MCP, NS$NSS_PICP)

      Wilcoxon rank sum test with continuity correction

data:  NS$NSS_MCP and NS$NSS_PICP
W = 28.5, p-value = 0.03854
alternative hypothesis: true location shift is not equal to 0

```

Figure 3.16: A sample of the R code used to compute the Wilcoxon Rank Sum test.

3.6.3 Results

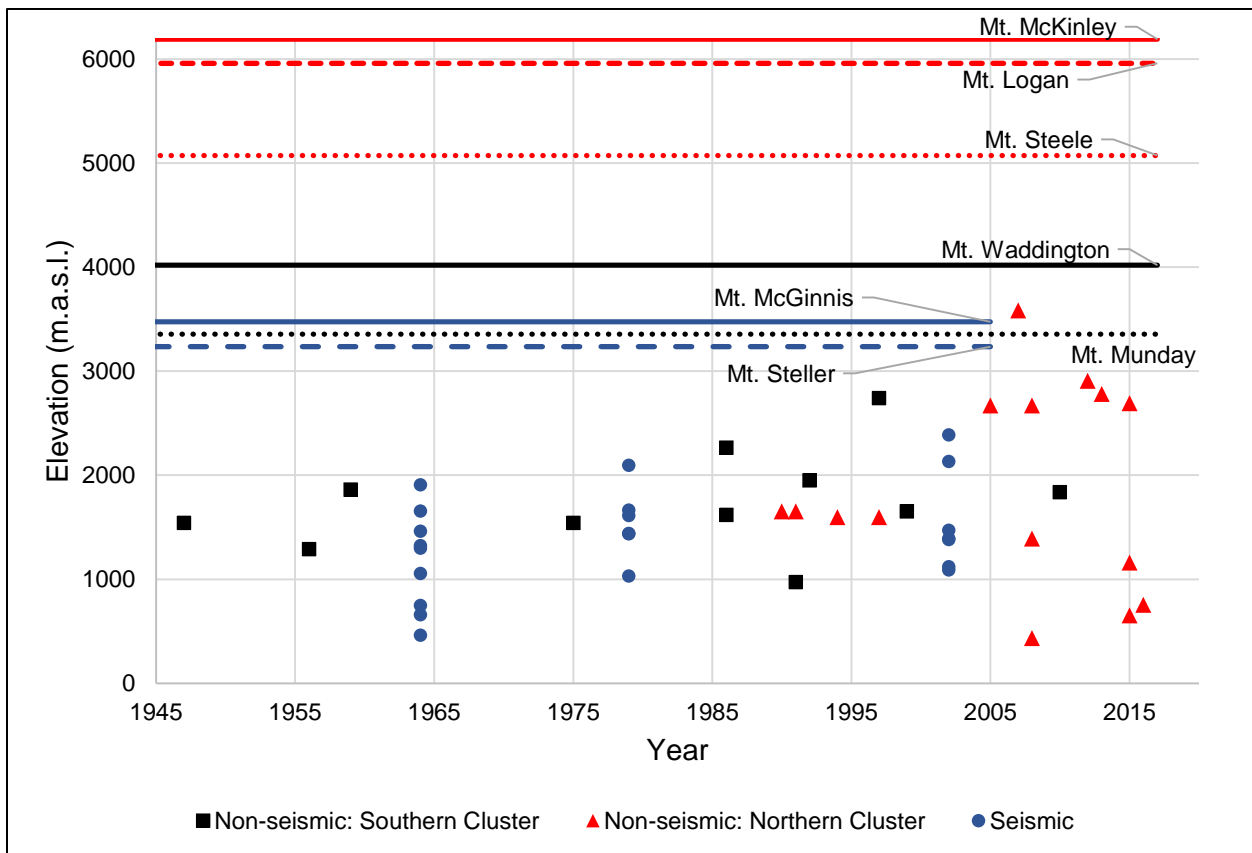


Figure 3.17: The elevation distribution of seismically triggered (blue circle) and non-seismically triggered (south – black square, north – red triangle) landslides. Horizontal lines indicate limits of relief by showing the elevation of various mountain peaks. Red and black lines indicate mountains on which there have been non-seismically triggered failures in the north and south, respectively. Blue lines indicate mountains which have co-seismically failed.

Figure 3.17 shows the source area elevation distribution of seismically triggered and non-seismically triggered events, with distinction between southern events (at a latitude less than 57 degrees N) and northern events (at a latitude greater than 57 degrees N). Also included are major peaks in the northern region (Mt. Steele, Mt. McKinley, and Mt. Logan - shown in red lines) and the southern region (Mt. Waddington and Mt. Munday - shown in a black lines). Selected mountains for seismic events are Mt. Steller and Mt. McGinnis, shown in blue lines. The inclusion of these highest peaks is helpful in illustrating the limits of relief and the maximum possible elevation range of events.

It can be seen that the source area elevation of non-seismic events is increasing over time, with more events occurring at higher elevations in recent years. Also, there is a wider range of source elevations overall after 1990. Another interesting feature of the data is the dramatic increase of events in the Northern region after 1990 with no non-seismic events in the inventory preceding that year. This indicates growing hazard in areas above 57 degrees N.

The event with the highest elevation of approximately 3587 m.a.s.l. is the Mt. Steele landslide of 2007. This particular case illustrates the potential hazard of the climbing elevation of major landslide events. The peak of Mt. Steele is 5073 m.a.s.l., leaving 1486 vertical meters of mountain that have yet to be affected by landslide activity. If landslide activity continues to increase in elevation, there could be a significant increase in hazard. A similar argument can be made for the southern events, with this highest elevation landslide being the Mt. Munday event in 1997 with an elevation of approximately 2742 m.a.s.l.. The peak of Mt. Munday is approximately 3367 m.a.s.l., therefore there is about 625m between the peak and the highest historical landslide source. Again, the increasing elevation of landslide activity reflects increasing risk of in the higher portions of peaks.

Note that the seismic dataset has not been divided into northern and southern events in this case, because there were only three earthquakes causing landslides in the inventory, and all happened to be in northern locations. Although the dataset is relatively sparse, an increase in maximum elevation with time can be seen. In 1964 the highest event was at an elevation of 1909

m.a.s.l., in 1979 the highest event was at 2097 m.a.s.l., and in 2002 the highest recorded elevation was 2388 m.a.s.l.. The event with the lowest elevation also showed an increasing trend, going from 462 m.a.s.l. in 1964 to 1092 m.a.s.l. in 2002. These results imply increasing coseismic landslide hazard to higher elevations, and potentially decreasing hazard at lower elevations. However, note that the source area elevation of seismically triggered landslides is dependent on the topography of the region affected by the triggering earthquake, meaning climate change is perhaps not the dominant factor leading to an increase in source area elevations of coseismic landslides.

To further explore the elevation distribution of seismically triggered landslides, two events were chosen to be further investigated: Mt. Steller in 1964 at an elevation of 1462 m.a.s.l., and the McGinnis Peak event in 2002 at an elevation of 2134 m.a.s.l.. The Mt. Steller event was in the bottom portion of the mountain, with the peak of Mt. Steller being 3236 m.a.s.l.. If landslide activity is moving to higher elevations, there is a significant portion of historically stable slope on the mountain that could be at increasing risk of failure. Interestingly, there was a subsequent event at Mt. Steller in 2008 which was not seismically triggered. The 2008 event occurred at a lower elevation than the 1964 event, highlighting the uncertainty of these results. Another example of potentially increasingly unstable high elevations was the 2002 event at McGinnis Peak, which occurred at 2134 m.a.s.l.. While closer to the apex than the Mt. Steller example, there is still a significant amount of vertical distance to McGinnis Peak (3475 m.a.s.l.) that could be subject to increasing landslide hazard. Overall, it cannot be conclusively determined from these results that the elevation of seismically triggered landslides is increasing due to climate change.

Figures 3.18 and **3.19** show the temperature and precipitation indices corresponding to each of the non-seismic landslides, with time on the x-axis (southern events in black square markers and northern events in red triangle markers). It is clear that the recent non-seismic landslides are in areas with high corresponding temperature index results, supporting the hypothesis that increasing temperatures and landslide activity in the mountain glacial environment share a connection. The annual temperature index values of seismic events also

seem to be increasing (**Figure 3.20**). These results reflect the increased landslide activity and warming in the northwest relative to the south, and the response of the glaciers throughout the regions starting after 1990. On the other hand, the precipitation index does not show an obvious trend in either the seismic or non-seismic plots (**Figures 3.19** and **3.21**). This suggests that precipitation has less of an impact on landslide hazard than temperature; however the following quantitative assessment will illuminate this further.

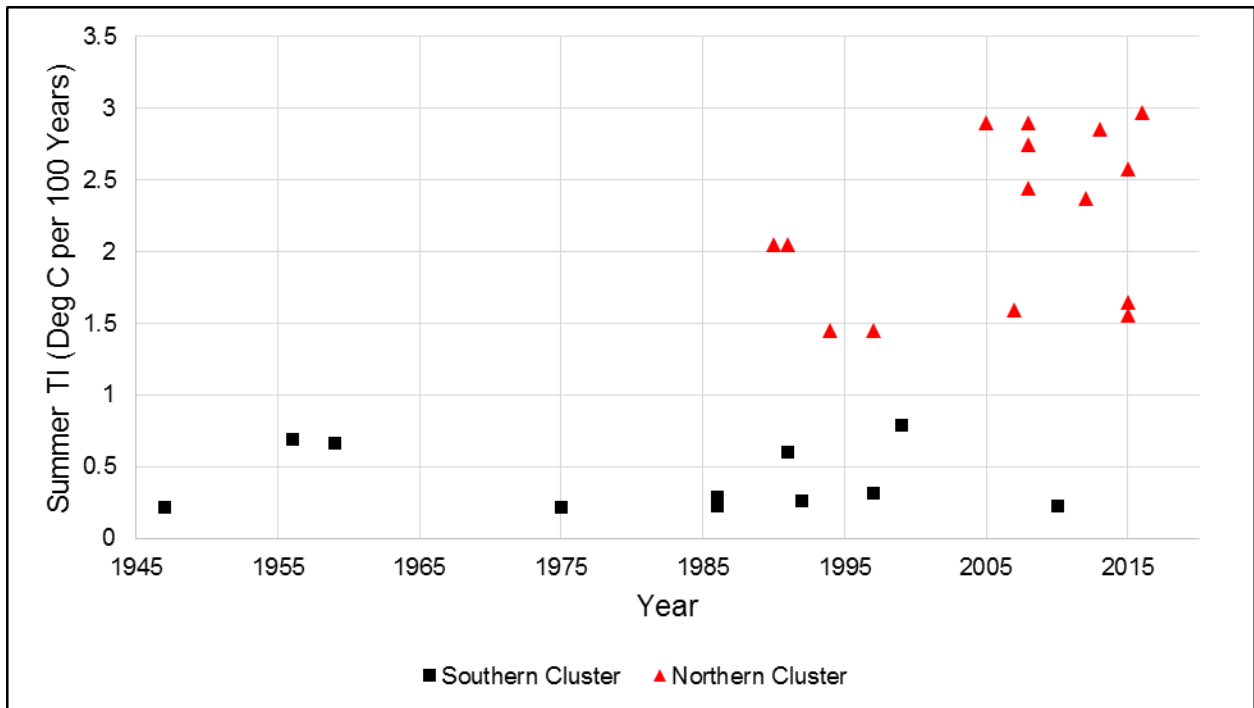


Figure 3.18: Summer temperature index vs. time for non-seismically triggered events. Landslides in recent years have been occurring in areas with greater temperature increase, supporting the hypothesis that increasing temperatures and landslide activity in the mountain glacial environment share a connection. In addition, all northern events have a higher temperature index than southern events.

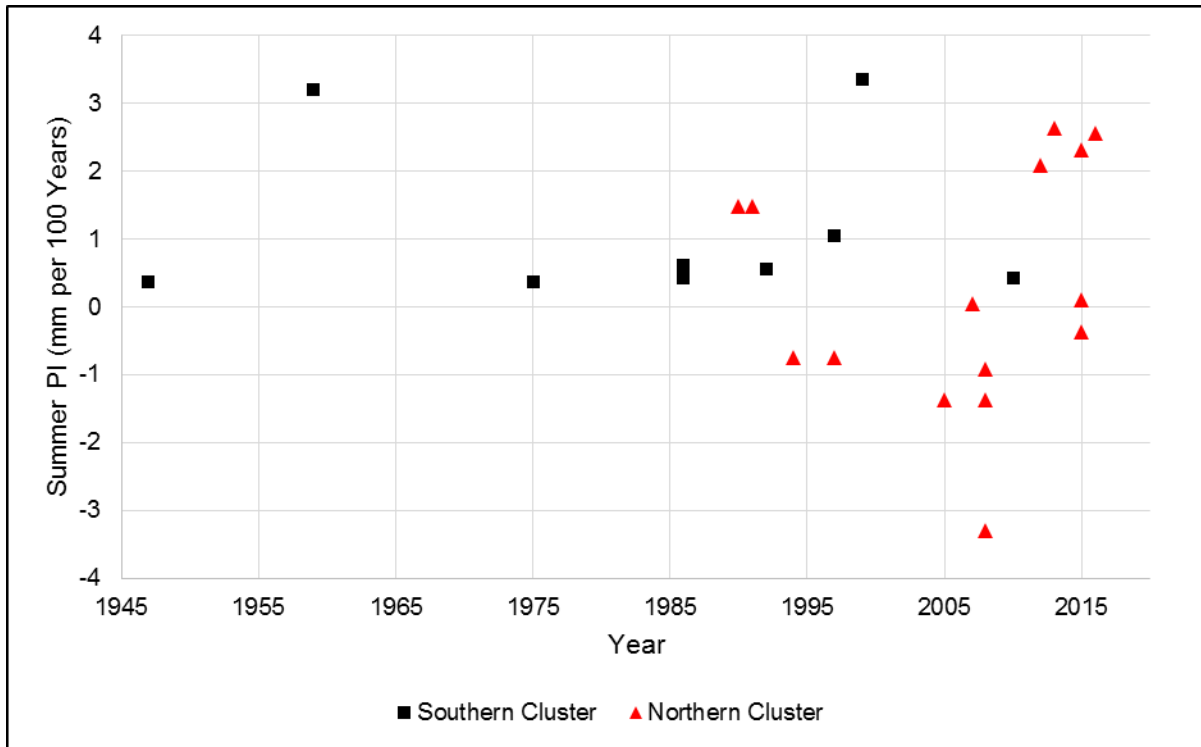


Figure 3.19: Summer Precipitation index results vs. time for non-seismically triggered events. .Precipitation index results show no visible trend in the data, suggesting precipitation may not be correlated with landslide hazard.

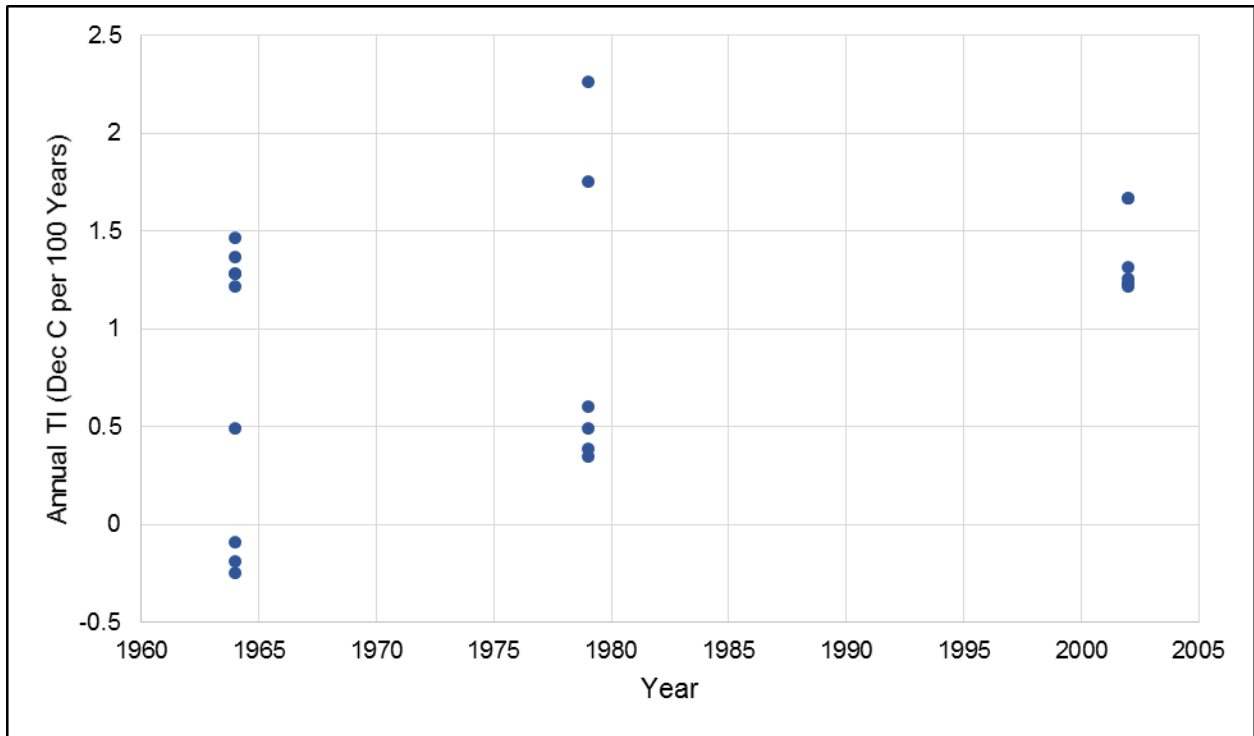


Figure 3.20: Annual temperature index results vs time for seismically triggered landslides. Recent coseismic events seem to be occurring in areas with greater annual warming (a higher annual TI), suggesting that rising temperatures are increasing coseismic landslide hazard.

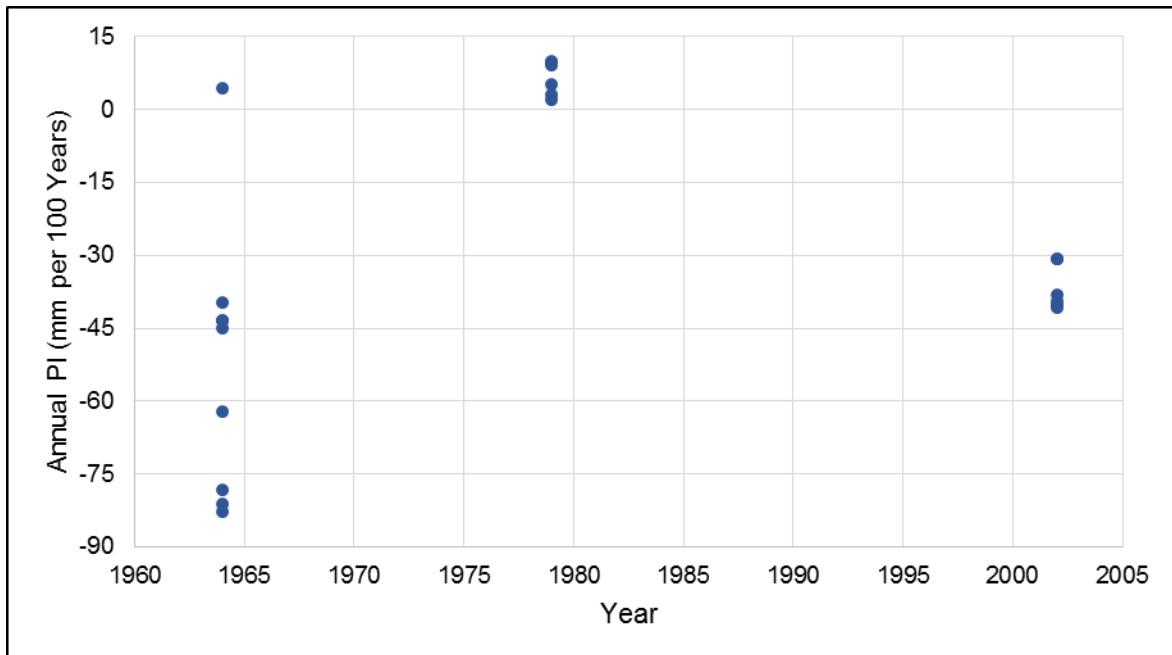


Figure 3.21: Annual precipitation index results vs time for seismically triggered events. There is no clear observable trend in these results, indicating precipitation change may not have an effect on coseismic landslide hazard.

Figure 3.22 shows the results of plotting the non-seismically triggered cumulative landslide mass, cumulative temperature index, and cumulative precipitation index against elevation; note that each of these datasets reaches a total of 100%, and each are sorted by elevation. This method is beneficial because it makes the datasets directly comparable, allowing correlations to be established. Qualitatively, there seems to be a correlation between landslide mass and the temperature index, indicated by the well matched series. This is expected from the previous results and supports the hypothesis that temperature change and landslide activity are linked. Precipitation index results are visually less correlated with landslide mass, with a greater percentage of the cumulative precipitation change occurring at lower elevations. When the non-seismic events are grouped into southern and northern sub-categories, as seen in **Figures 3.23** and **3.24**, more detail is evident than when assessed collectively. In both the northern and the southern data, there is a good match between summer temperature index and landslide mass; this is expected because it was the case in **Figure 3.22**. Interestingly, in the southern data there is also a relatively good visual match between summer precipitation values and landslide mass. This could indicate that increasing precipitation in the south is linked to landslide hazard. Conversely, the plot of northern events shows a very poor match between summer precipitation index and landslide activity. This is likely due to the fact that much of the northern landscape (particularly Alaska) have results showing less wet conditions as was previously discussed.

The same analysis for seismic events can be seen in **Figure 3.25**. Note that annual (i.e., not summer) indices for temperature and precipitation are used. This is because seismicity is assumed to occur randomly throughout the year. **Figure 3.25** shows a good subjective match to landslide mass with both the precipitation index and the temperature index. It is of note that in this case, the precipitation index reflects decreasingly wet conditions (i.e., the 100% value is negative for the precipitation index). The strong matches support the hypothesis of a link between increasing temperature and landslide activity, but also suggests some correlation to dryer conditions and seismically triggered landslides.

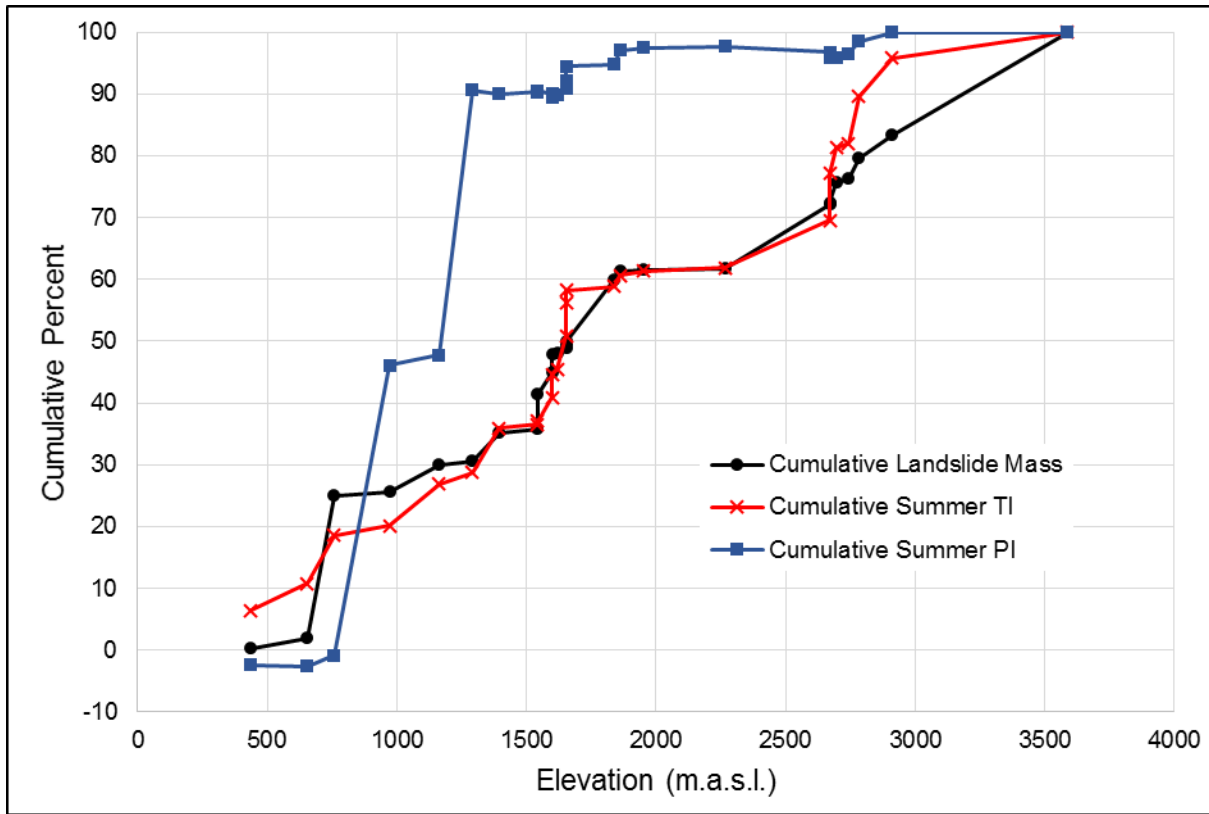


Figure 3.22: Cumulative plot for all non-seismically triggered events, comparing landslide mass, summer temperature index, and summer precipitation index. There is a strong subjective match between summer temperature change and landslide mass, supporting the hypothesis that increasing summer temperatures are contributing to increased landslide hazard. Precipitation does not have a good visual correlation with landslide mass, suggesting precipitation change may be less influential on landslide activity.

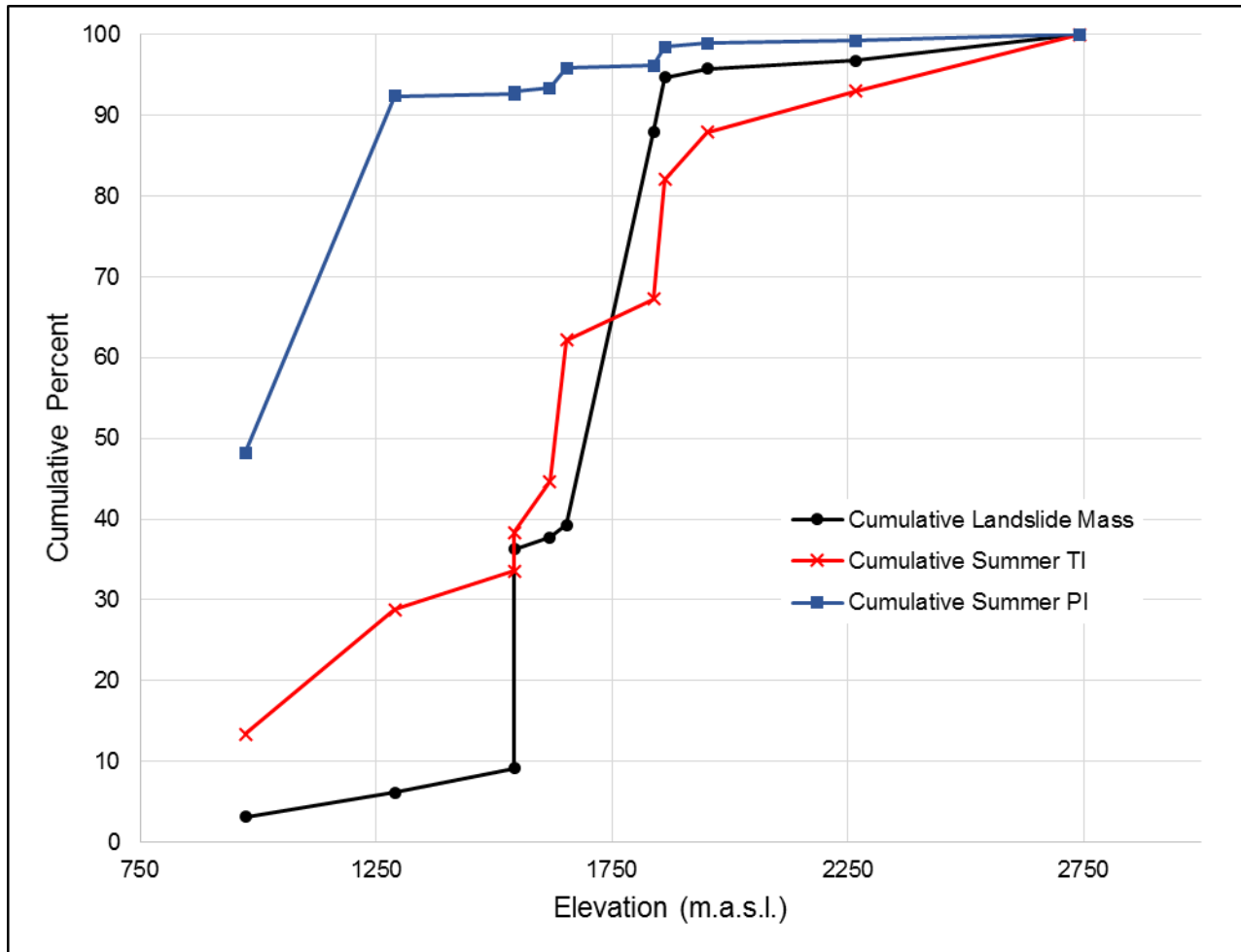


Figure 3.23: Cumulative plot for southern non-seismically triggered events, comparing landslide mass, summer temperature index, and summer precipitation index. There is a good subjective match between temperature increase and landslide mass, suggesting temperature is an essential component of increases in landslide hazard. There is a moderate match between precipitation and landslide mass, indicating that increases in precipitation may influence landslide hazard in the south of the study area.

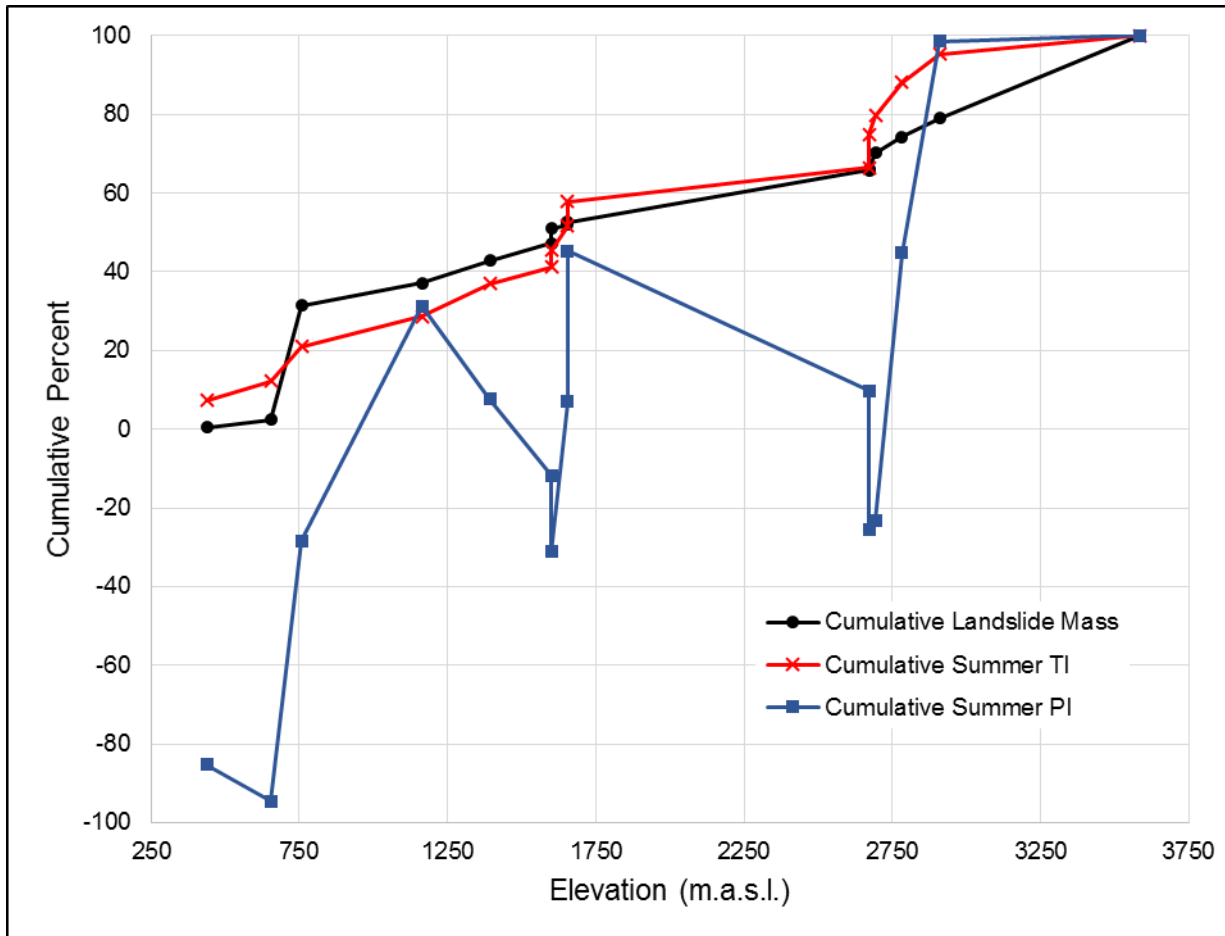


Figure 3.24: Cumulative plot for northern non-seismically triggered events, comparing landslide mass, summer temperature index, and summer precipitation index. Visually, there is a strong correlation between landslide mass and summer temperature, supporting the hypothesis that summer temperature increases are contributing to growing landslide hazard. There is a poor match between precipitation change and landslide mass, indicating that precipitation may have less of an impact on landslide hazard in the north of the study area.

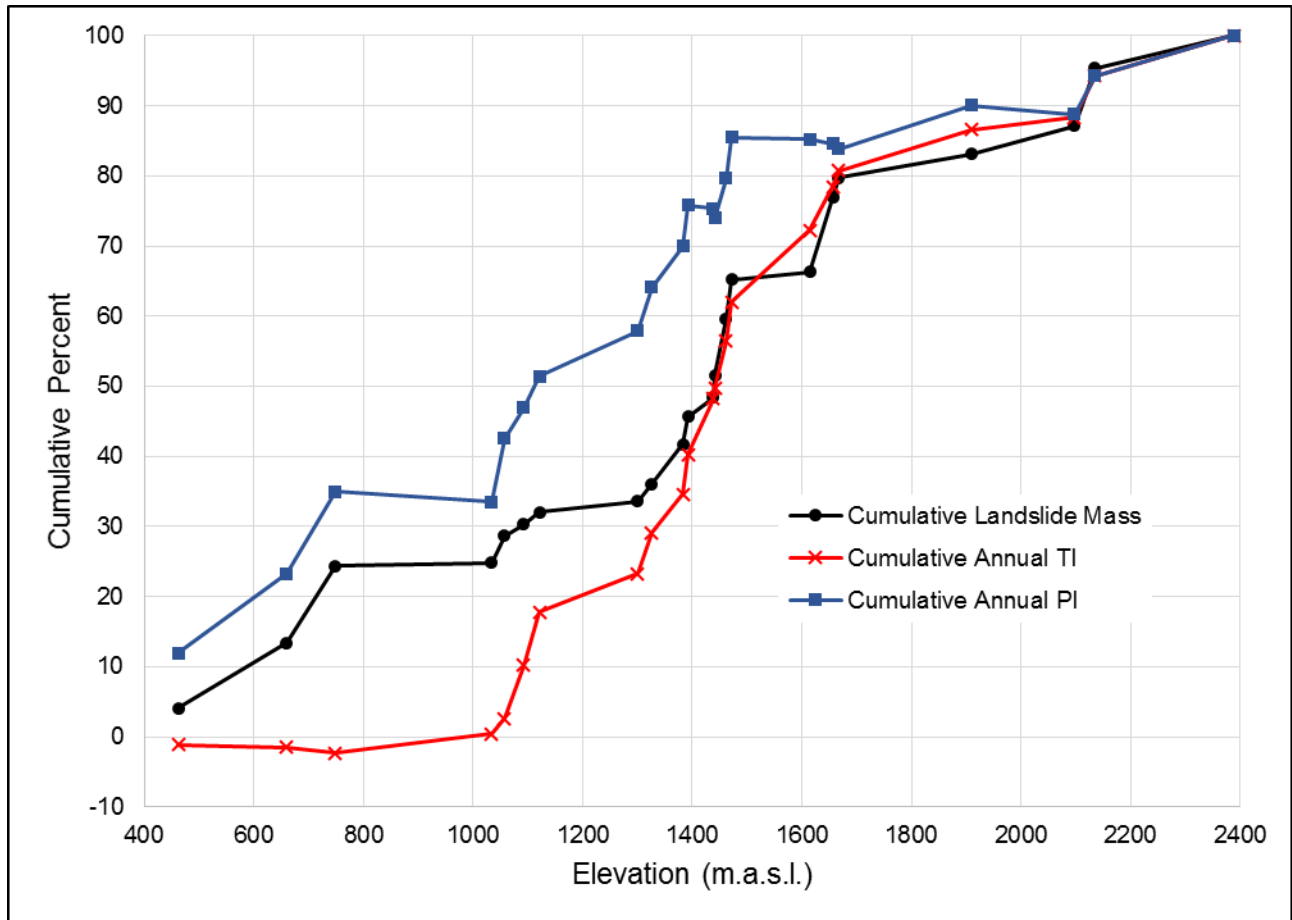


Figure 3.25: Cumulative plot for all seismically triggered events, comparing landslide mass, summer temperature index, and summer precipitation index. There is a strong visual correlation between both annual temperature increase and annual precipitation decrease to landslide mass. This suggests that coseismic landslide hazard is influenced by both temperature and precipitation.

To elaborate on qualitatively observed correlations between climate factors and landslide activity with more certainty, the results of Wilcoxon Rank Sum testing and correlation analysis are summarized in **Table 3.8**. At a significance level of 0.05, precipitation index values have significantly different distributions than all of the non-seismic cumulative landslide mass series, with the null hypothesis (H_0 is that both of the distributions are the same) being rejected. Furthermore, this finding is strengthened by lower correlation values for these pairings. The remainder of the distributions are not statistically distinguishable, with temperature index values

following the same distribution as landslide mass in every case. These results add statistical support to the implication that temperature increases are resulting in growing landslide hazard throughout northwest North America. As predicted by the aforementioned plots, temperature index results have consistently higher correlation values than precipitation index results. Overall, these results confirm the strong correlation between temperature and landslide activity.

Precipitation has less supporting evidence showing a relationship to landslide mass, however the distributions of precipitation index values and landslide mass is statistically equivalent in the case of seismically triggered events. This could indicate that decreasing precipitation is more important as a conditioning factor to seismically triggered landslides in Alaska than non-seismically triggered events.

Table 3.8: Correlation analysis of climate variables and landslide mass. The null hypothesis (H_0) is that the distributions of both variables are the same. Upon rejection of the null hypothesis, the alternate hypothesis is accepted (that the distributions of the variables tested are not the same).

Variable A	Variable B	Wilcoxon W	Wilcoxon p-value	Ho rejected?	Correlation
Non-seismic landslide mass (all)	Summer Temperature Index	332.5	0.9271	No	0.98
Non-seismic landslide mass (all)	Summer Precipitation Index	130.5	0.0001516	Yes	0.78
Non-seismic landslide mass (Southern Events)	Summer Temperature Index	59.5	0.9738	No	0.95
Non-seismic landslide mass (Southern Events)	Summer Precipitation Index	28.5	0.03854	Yes	0.59
Non-seismic landslide mass (Northern Events)	Summer Temperature Index	108.5	0.8846	No	0.96
Non-seismic landslide mass (Northern Events)	Summer Precipitation Index	178.5	0.006585	Yes	0.81
Seismic landslide mass	Annual Temperature Index	275.5	0.4386	No	0.98
Seismic landslide mass	Annual Precipitation Index	167.5	0.08238	No	0.93

3.7 Conclusion

In the preliminary visualization of the meteorological station data, all of the above results indicate significant warming across northwest North America, as expected (Solomon *et al.*, 2007; Field *et al.*, 2014; Melillo *et al.*, 2014; Streiker 2016; British Columbia Ministry of Forests, Lands, and Natural Resources, 2009). Warming is especially pronounced in winter and summer. On the other hand, precipitation data shows increasingly wet conditions in the south, and dryer conditions to the north. This finding is not in total agreement with the literature, which projects increasing precipitation in the north as well as the south (Solomon *et al.*, 2007; Field *et al.*, 2014; Melillo *et al.*, 2014; Streiker 2016; British Columbia Ministry of Forests, Lands, and Natural Resources, 2009). Subjectively, it seemed that more recent landslide events tend to occur in locations with more intense warming.

Further analysis of the landslide inventory showed that the source elevation of non-seismic events is increasing over time. Another interesting feature of the data is the dramatic increase of non-seismic events in the northern region after 1990. This indicates growing hazard in areas above 57 degrees N. The increasing elevation of landslide activity also indicates increasing risk of slope failure in the higher portions of mountain ranges, as well as potentially decreasing hazard at lower elevations. Elevation trends in the seismic data are less obvious, but landslide hazard also seems to be increasing in elevation for seismically triggered events.

Furthermore, the temperature index was visually observed to be increasing with time for both the southern and northern events, supporting the hypothesis that increasing temperatures and landslide activity in the mountain glacial environment share a connection. This is also the case for coseismic landslides. As expected, rising temperatures seem to be increasing landslide hazard, regardless of trigger mechanism. Conversely, the precipitation index does not show an obvious trend in either the seismic or non-seismic plots, suggesting precipitation has less of an impact on landslide hazard than temperature.

The cumulative plots all showed a good match between temperature index and landslide mass, further indicating that landslide hazard is increased as temperature increases regardless of trigger mechanism. This finding was supported statistically using correlation analysis and the Wilcoxon Rank Sum test. This finding is also supported by the literature review in Chapter 2. Non-seismically triggered landslides in the south also showed a correlation to precipitation qualitatively, however did not show strong statistical evidence supporting this observation. Seismically triggered landslide mass was correlation and not statistically distinguishable from both increasing temperature and decreasing precipitation, suggesting that warmer and dryer conditions (i.e. less snow – less glacial accumulation) are increasing coseismic landslide hazard in Alaska.

Overall, these results confirm the strong correlation between temperature and landslide mass, and the still significant but less strong influence of precipitation. This chapter was essential in quantifying the relationship between temperature, precipitation, and landslide hazard. These results are suggested by the literature review completed in Chapter 2, and support the hypotheses that increasing temperature and precipitation are increasing landside hazard for both seismically and non-seismically triggered events in British Columbia, Yukon and Alaska. However, this chapter did not address the role of glacier ice loss in landslide hazard. As such, glacier ice loss is the topic of Chapter 4.

Chapter Four: Quantification of Deglaciation at Mount Meager Volcanic Complex, British Columbia

4.1 Introduction

From the results discussed in Chapter 3 it is clear that there is a connection between landslide activity and temperature changes in the mountain glacial environment of NW North America. A secondary effect of climate changes is change in glacier ice volume and extent; based on the literature review in Chapter 2, ice loss could also play a significant role in slope instability through debulking, unloading (stress-relief), uplift, permafrost degradation, and generation of unstable ice. This chapter focuses on investigating and illustrating the role of glacier ice loss in landslide hazard by using a case study of the Mount Meager Volcanic Complex (MMVC), BC, Canada. MMVC was chosen due to clear delineation of glacier boundaries, a long record of mapping and air photos, as well as an extensive and well documented history of landslide activity.

The 1975 Devastation Glacier landslide, occurring on July 22nd near Pylon Peak, is extensively discussed by Mokievsky-Zubok (1977) and Evans and Delaney (2014). Mokievsky-Zubok (1977) estimated that 2.5Mm³ of ice and 26Mm³ of debris traveled over 6.5km, descending 1150m; Evans and Delaney (2014) estimate the volume of the event to be approximately 13 Mm³, dropping a vertical distance of 1220 m with a 7 km runout. There was no seismic activity the day of the landslide, and weather reports from Alta Lake Station (75km south-east) showed warm weather in the area on July 22nd, and several days before. As such, Mokievsky-Zubok (1977) proposes the cause of the landslide was the “*weight of glacier ice and the action of glacier meltwater*”, and “*some movement of ice in the form of a minor ice fall that triggered the collapse of a large, wet mass of supporting ground below the ice*”. Mokievsky-Zubok (1977) also discusses the weak geological materials of the area, formed mostly of unconsolidated Quaternary volcanic debris. Mokievsky-Zubok (1977) emphasizes the importance of glacier ice loss and warm summer temperatures in the triggering of the 1975 event. Evans and Delaney (2014) concur that the failure was a result of glacial erosion, loading and unloading, accompanied by excessive melt attributable to warm summer weather.

The 2010 landslide, originating above Capricorn Creek on August 6th, was comprehensively assessed by Guthrie *et al.* (2012) (**Figure 4.1**). The rock avalanche-debris flow, composed of pyroclastic material, rocky debris, glacier ice fragments, and water was estimated to be 48.5 Mm³ in volume, making it one of the largest recorded landslides in Canadian history (Guthrie *et al.*, 2012). The overall path height was 2183m, with a length of 12.7 km (Guthrie *et al.*, 2012). The event was significant for several reasons, including its massive volume, and the fact that it demonstrates the role of deglaciation in destabilizing slopes. Guthrie *et al.*, 2012 determined glacial change to be a distinct precondition to the landslide event. As in the 1975 event, no seismic trigger was recorded.

As previously reviewed in Chapter 2, both of the Mount Meager Volcanic Complex landslide examples illuminate the potential impact of climate change on landslide hazard. The 1975 event exemplified the importance of summer temperature as a landslide trigger, as well as glacier ice melt. In contrast, the 2010 event seemed to be more influenced by glacier ice loss; it is interesting to note that ice loss could be considered a secondary effect of changing temperature. This chapter will further investigate the relationship between ice loss and landslide activity at Mount Meager Volcanic Complex.

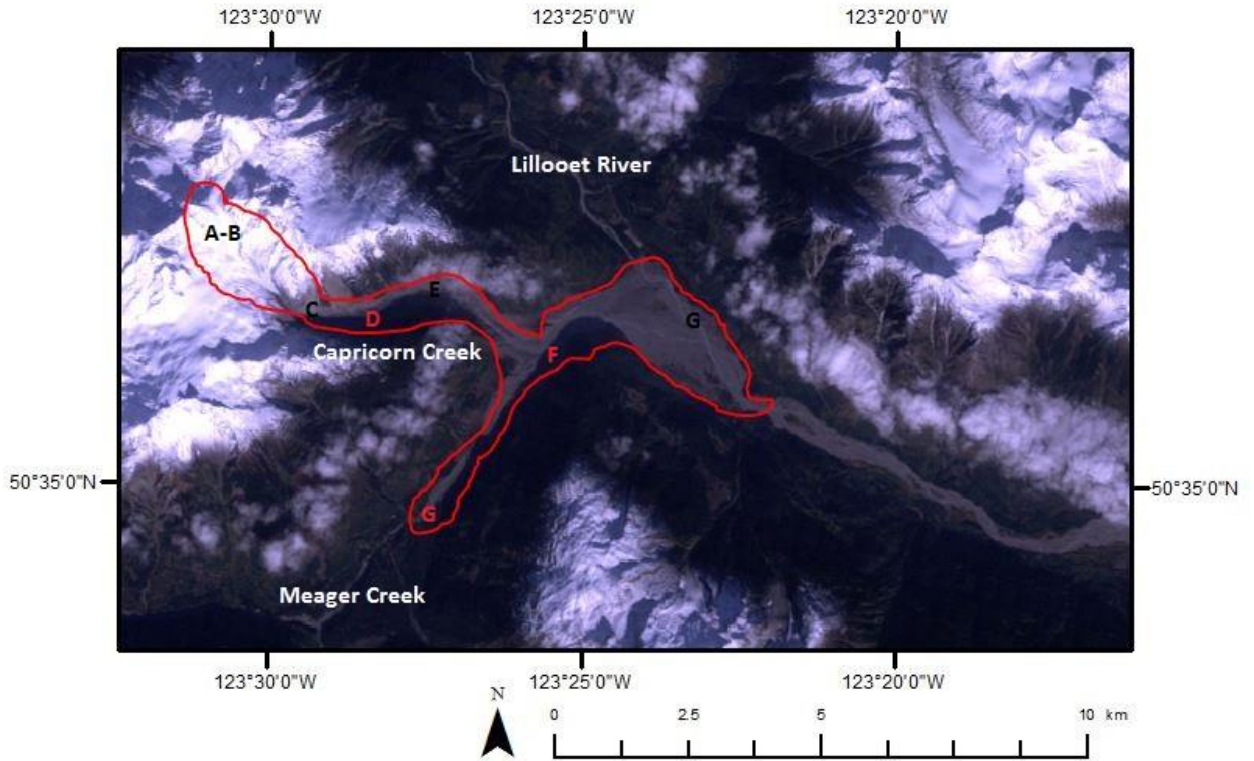


Figure 4.1: The complete outline of the Mount Meager landslide, with a Landsat base image from October 13th, 2010, showing the initiation zone (A-B), the two major bends (C and E), the facing wall of Meager Creek (F), and the bifurcated flow that travelled up Meager Creek, and across the Lillooet River (G). The image was taken following the breach of the Meager Creek dam, and fluvial reworking and considerate incision of the dam itself and evident. (Guthrie et al., 2012)

4.2 Methodology

4.2.1 Climate Data Review

To ensure a solid understanding of climate change trends at MMVC, the results from the climate indices analysis completed in the previous chapter were extracted in tabular format. Furthermore, PRISM (Parameter-elevation Regressions on Independent Slopes Model) climate reanalysis was used as an additional data source indicating climate change trends (Pacific Climate Impacts Consortium, 2014) (data download available from: <<https://www.pacificclimate.org/data/high-resolution-prism-climatology> >). PRISM

climatologies are based on thousands of temperature and precipitation observations, and designed to reflect topographic variation (Pacific Climate Impacts Consortium, 2014). PRISM data is available in two 30 year normal periods (1971-2000, 1981-2010). The spatial resolution of PRISM data is approximately 800x800m, with data available for mean maximum and minimum monthly temperature, and mean precipitation. To assess climate change, the 1971-2000 normals were subtracted from the 1981-2010 normals to find the difference in the 30 year means. This analysis was completed in ArcMap, using the 'Raster Calculator' tool.

4.2.2 Landsat Image Series

Using Earth Explorer, Landsat scenes with a maximum cloud cover of 20% taken at the end of the summer season (late August/September) were downloaded from the earliest possible date (corresponding with the launch of the Landsat 1 satellite in 1972) to present day (data download available from: <https://earthexplorer.usgs.gov/>). Any images with excessive cloud cover in the region of interest were removed. The end of the summer season was chosen because glacier extent is at a minimum, and there is minimal spectral interference from snow. Moreover, the majority of landslides occurred at the end of the summer season.

4.2.3 Manual Classification in ArcMap

To generate glacier surface area data (of clean ice), all Landsat imagery was imported into ArcGIS 10.3 using the 'composite bands' tool. Glacier extent was manually digitized for each image by creating a new polygon shapefile and tracing the edge of the glacier ice. In all cases, there were multiple features comprising the new shapefiles because the surface of the glacier was not contiguous. The area of each new polygon shapefile was then calculated in the attribute tables using 'calculate geometry' and the sum of the areas was recorded. The primary source of error associated with this method is the difficulty of ensuring all land covered with glacier ice was digitized. Smaller parcels of ice were occasionally missed resulting in an underestimate, and it is difficult to classify debris covered ice. In addition, any thin cloud cover or shadow made glacier

boundaries difficult to distinguish visually from surrounding terrain, reducing accuracy and increasing error. Also, due to the spatial resolution of 30m the ice margin was pixelated, limiting the precision of the digitized boundary. However, this error was minimized because all of the images were digitized by the same individual, therefore any subjective judgements when determining whether or not a pixel should be included was consistent between images. In addition only clean ice was measured, allowing for consistent classification without attempting to assess the area of debris covered ice.

4.2.4 ENVI Automatic Classification

In an attempt to gain more data and potentially reduce error, a secondary method of measuring glacier surface area was employed: automatic unsupervised Iso cluster classification, an iterative process which separates every pixel in the specified raster into a class. After downloading and screening images for excessive cloud cover, each Landsat scene was imported into ENVI. A region of interest shapefile (created in ArcMap) was also imported, to define the area of the glacier being measured for surface area changes. To classify the glacier surface area, the unsupervised ISO classification tool was used. No training areas were used, and the region of interest was classified into 5 classes, using 20 iterations. All Landsat bands, excluding thermal bands, were included in analysis.

Typically, results showed vegetation as one class, exposed soil or rock as two classes, and ice or snow as two classes. Classes were then merged in a binary manner using the ‘reclassify’ tool in ArcMap, with glacier surfaces being represented as a one, and non-glacier surfaces being represented as a zero. Glacier area for each Landsat image was then calculated by multiplying the number of pixels by the area of an individual pixel (30 m²), and results were recorded. In the majority of cases, automatic classification was superior to manual digitization at including small fragments of ice or snow. However, areas in shadow or covered by thin cloud cover were often excluded from the total glacier area, potentially causing an underestimate.

Occasionally, some exposed rock or soil was included as glacier in the automatic classification, artificially increasing area estimates.

4.2.5 Ice Volume Quantification

To obtain a measure of glacier volume change over time, two DEMs were used, and the difference was calculated; this generated a raster showing the change in glacier thickness over time. The first DEM was provided by the British Columbia Terrain Resource Information Management Program (TRIM), which used topographic maps from 1988 as source data. The scale of the source map was 1:20,000. The second DEM used was from the Shuttle Radar Topography Mission (SRTM), based on data collected in 2000. Both DEMs were imported into ArcMap and were projected to the same datum (WGS 84 UTM Zone 10N). The SRTM DEM was clipped to the same extent as the TRIM DEM, which only covered the most eastern portion of the overall study area (therefore all data collected from this analysis is only applicable to this area). The TRIM DEM was subtracted from the SRTM DEM to find the change in elevation from 1988 to 2000. This new raster representing change in elevation was then clipped to the extent of the 1988 glacier, using the manually digitized shapefile based on Landsat imagery. The mean change in thickness was found in the attribute table, and the total change in volume was then calculated by multiplying the mean change in elevation (m) with the total area change in area from the 1988 glacier extent to the 1998 extent (m²). Note that change in area was also based on clipped polygon shapefiles to accurately reflect the smaller study area.

Due to the uncertainty involved when comparing two products generated in using different methodologies (i.e., SRTM using RADAR, and TRIM using contour maps), it was important to assess the error included in the ice volume quantification. To do so, the area covered by the maximum glacier extent was removed from consideration (as this area is expected to undergo changes in elevation over time), and the TRIM dataset was subtracted from the SRTM DEM to find the average difference in reported elevation between the two. The results from the error

analysis were incorporated into the volume change estimations by adjusting the height of the SRTM data so the average difference recorded between the two DEMs was zero.

4.3 Data Sources

Data collected for this chapter came from multiple sources, and datasets have varying spatial and temporal ranges. The Landsat and SRTM data was from the United States Geological Survey downloaded from their online service, EarthExplorer. The TRIM data was available open access online, and was based on contour maps from 1988. Climate data was provided courtesy of Environment Canada (2016), which was used to generate the climate indices. Pacific Climate Impact Consortium's online data portal provided the PRISM datasets (Pacific Climate Impacts Consortium, 2014).

4.4 Results and Discussion

4.4.1 Climate Data Review

The climate analysis results are shown in **Table 4.1**. The results of the climate indices indicate significant summer warming, as well as annual warming. Moreover, the climate indices show that MMVC has increasingly wet conditions year round. The results from the PRISM datasets are in agreement with the climate indices, as seen in **Figures 4.2-4.4** and **Table 4.1**. Based on the PRISM results, minimum temperature is increasing more rapidly than maximum temperature, but both are rising throughout the study area. In addition, precipitation is increasing at MMVC according to PRISM data, particularly on the southern slope. The observed trends of increasing temperature and precipitation support the observed glacier ice loss at MMVC.

Table 4.1: Information about the landslides at MMVC (including mass, year, and source elevation) and corresponding climate change information. PRISM variables show average change per 10 years, and the climate indices represent change per 100 years.

LOCATION	YEAR	MASS (KG)	ELEVATION (M)	PRISM PRECIP DIFF	PRISM MAX TEMP DIFF	PRISM MIN TEMP DIFF	ANNUAL PI	ANNUAL TI	SUMMER PI	SUMMER TI
DEVASTATION GLACIER	1947	7.8E+09	1543	9.44	0.56	1.22	9.66	0.45	0.38	0.21
DEVASTATION GLACIER	1975	7.02E+10	1543	9.44	0.56	1.22	9.66	0.45	0.38	0.21
NORTH CREEK	1986	3.9E+09	1619	17.93	0.84	1.15	9.45	0.50	0.62	0.28
CAPRICORN CREEK	2010	1.26E+11	1839	7.83	0.55	1.42	9.62	0.46	0.43	0.23

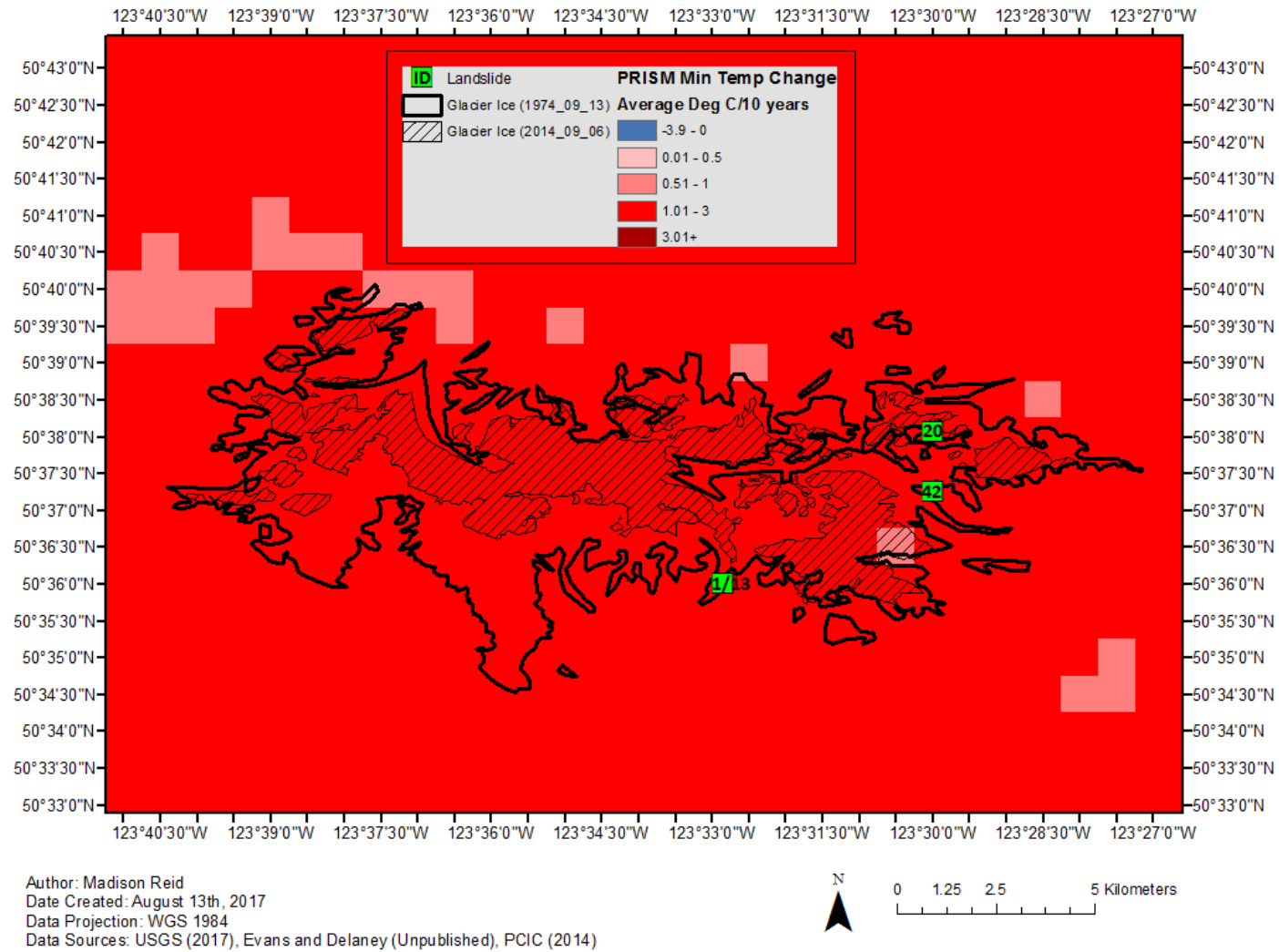


Figure 4.2: Changes in minimum temperature, according to subtraction of PRISM 30-year normal (1971-2000, 1981-2010). See table 2.2 for landslide key.

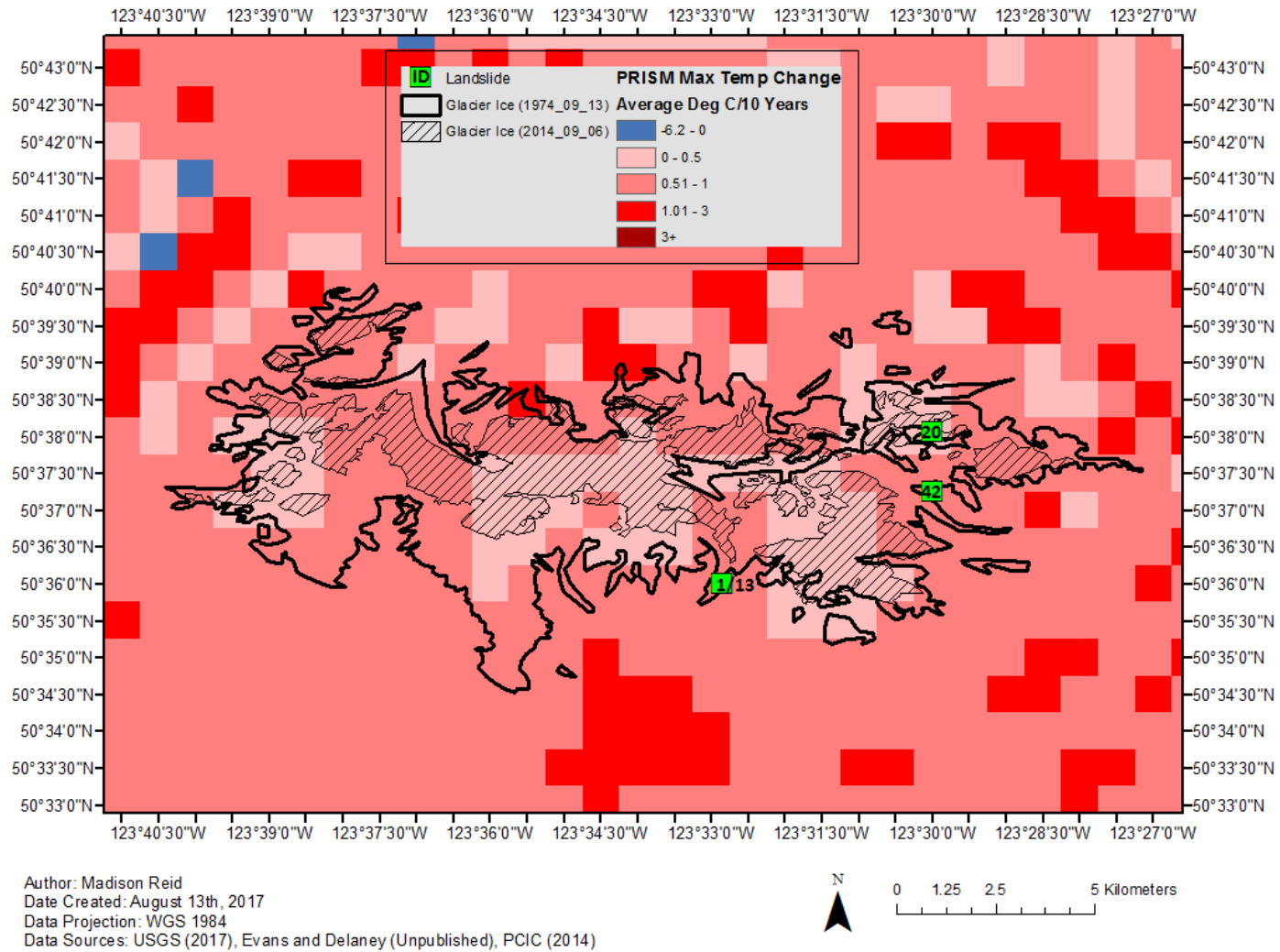


Figure 4.3: Changes in maximum temperature, according to subtraction of PRISM 30-year normals (1971-2000, 1981-2010), see table 2.2 for landslide key.

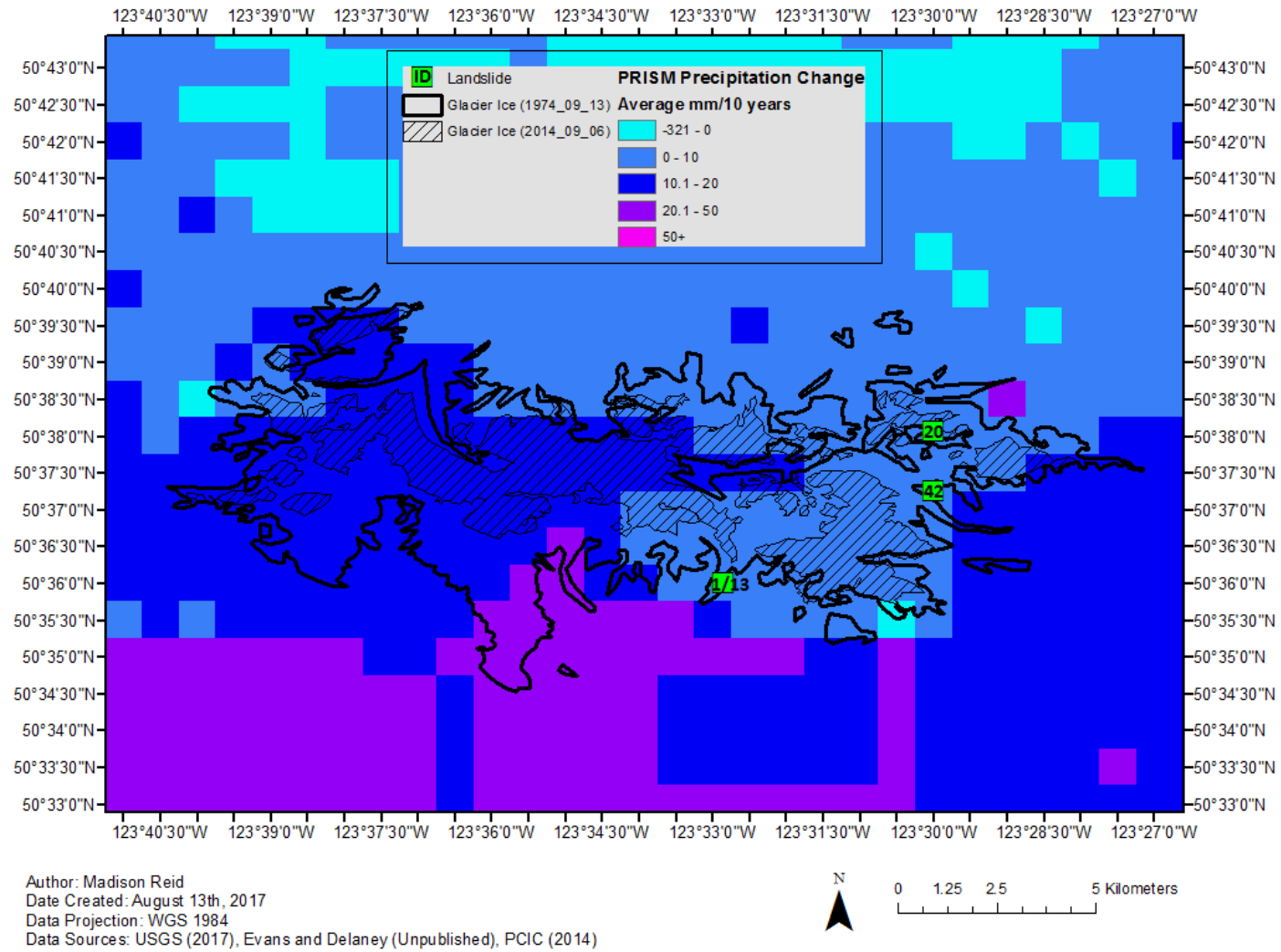


Figure 4.4: Changes in precipitation, according to subtraction of PRISM 30-year normals (1971-2000, 1981-2010). See table 2.2 for landslide key.

4.4.2 Glacier Surface Area and Volume

The results of glacier surface area analysis from the two classification methods can be seen in **Table 4.2** and **Figure 4.6**. The results of the glacier surface area analysis are also displayed for each Landsat image in **Appendix B**. Overall, the automatic classification method displayed good accuracy when determining the edge of clean glacier ice for most images, however results varied in consistency. To further quantify the error between the manual classification method and the unsupervised classification method, a 1:1 plot was generated with the manual classification area results on the x-axis and the unsupervised classification area results on the y-axis (**Figure 4.5**). It can be seen that in general, the ENVI unsupervised ISODATA classification slightly underestimated the glacier area reported by the manual classification. Due to its greater accuracy, the manual digitization results was used for the remainder of the analysis in this thesis.

The greatest glacier extent in the MMVC of the images analyzed was in 1974, with a surface area of approximately 57 km². By 2014, the total area of the glacier was reduced by 33.91 km² or almost 60 percent to 23.1 km². Over the 40 year period, the average annual loss was approximately 0.85 km² per year. As seen in **Figure 4.7** the majority of this area loss was due to retreat in glacial valleys, with the greatest retreat along the south slope of the study area. Interestingly, this area corresponds to heavy precipitation increase according to the PRISM climate reanalysis data (**Figure 4.4**), suggesting a precipitation control on glacier retreat. Retreat in glacial valleys is important when considering increased risk of landslide events due to newly exposed steep valley walls with significant slope instability (Gorum *et al.*, 2014; Evans and Clague, 1994; Deline *et al.*, 2015b). Moreover, decreased glacier ice could lead to increased topographic amplification of seismic shaking (Gorum *et al.*, 2014), therefore increasing the hazard of coseismic landslides as well as non-seismic landslides.

Table 4.2: Glacier surface areas calculated from manually digitized polygons and automatically classified rasters.

Date	Sensor	Manually Digitized Area (km ²)	Unsupervised ISO Cluster Classification (ENVI) (km ²)
1974-09-13	Landsat 1 MSS	57.01	56.29
1976-09-20	Landsat 1 MSS	55.36	47.66
1979-09-14	Landsat 2 MSS	34.39	-
1980-09-25	Landsat 2 MSS	39.01	40.91
1984-09-19	Landsat 5 TM	41.88	39.40
1985-09-22	Landsat 5 TM	35.55	31.80
1988-09-14	Landsat 5 TM	34.63	35.21
1992-08-24	Landsat 5 TM	30.10	31.53
1993-09-12	Landsat 5 TM	27.55	-
1995-09-02	Landsat 5 TM	31.37	33.79
1997-09-23	Landsat 5 TM	33.82	34.11
1998-09-26	Landsat 5 TM	26.28	-
2002-09-21	Landsat 5 TM	31.36	30.48
2009-09-24	Landsat 5 TM	24.69	19.42
2014-09-06	Landsat 8 OLI	23.10	15.44

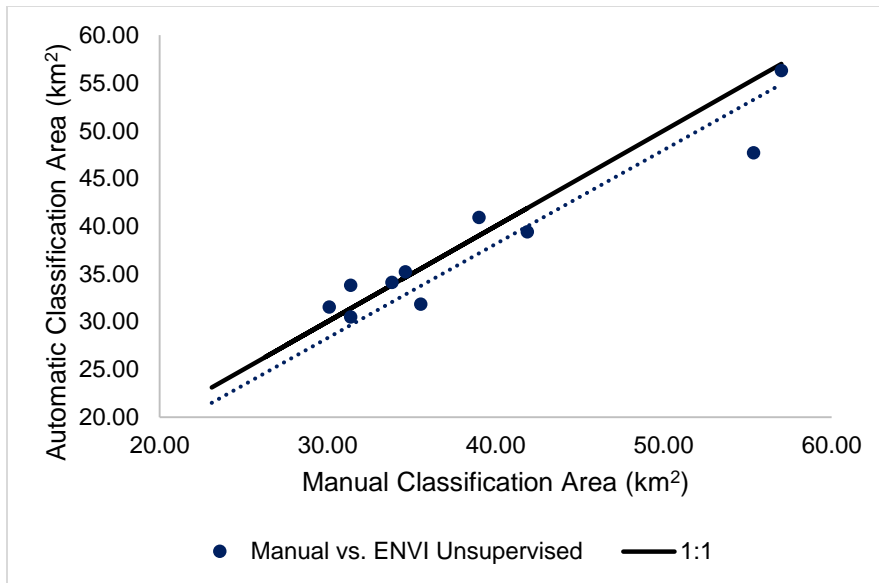


Figure 4.5: A 1:1 comparison of manually digitized and automatically classified glacier surface area at MMVC. Overall, the automatic classification does matches the manual classification relatively well, although does consistently underestimate by a small margin.

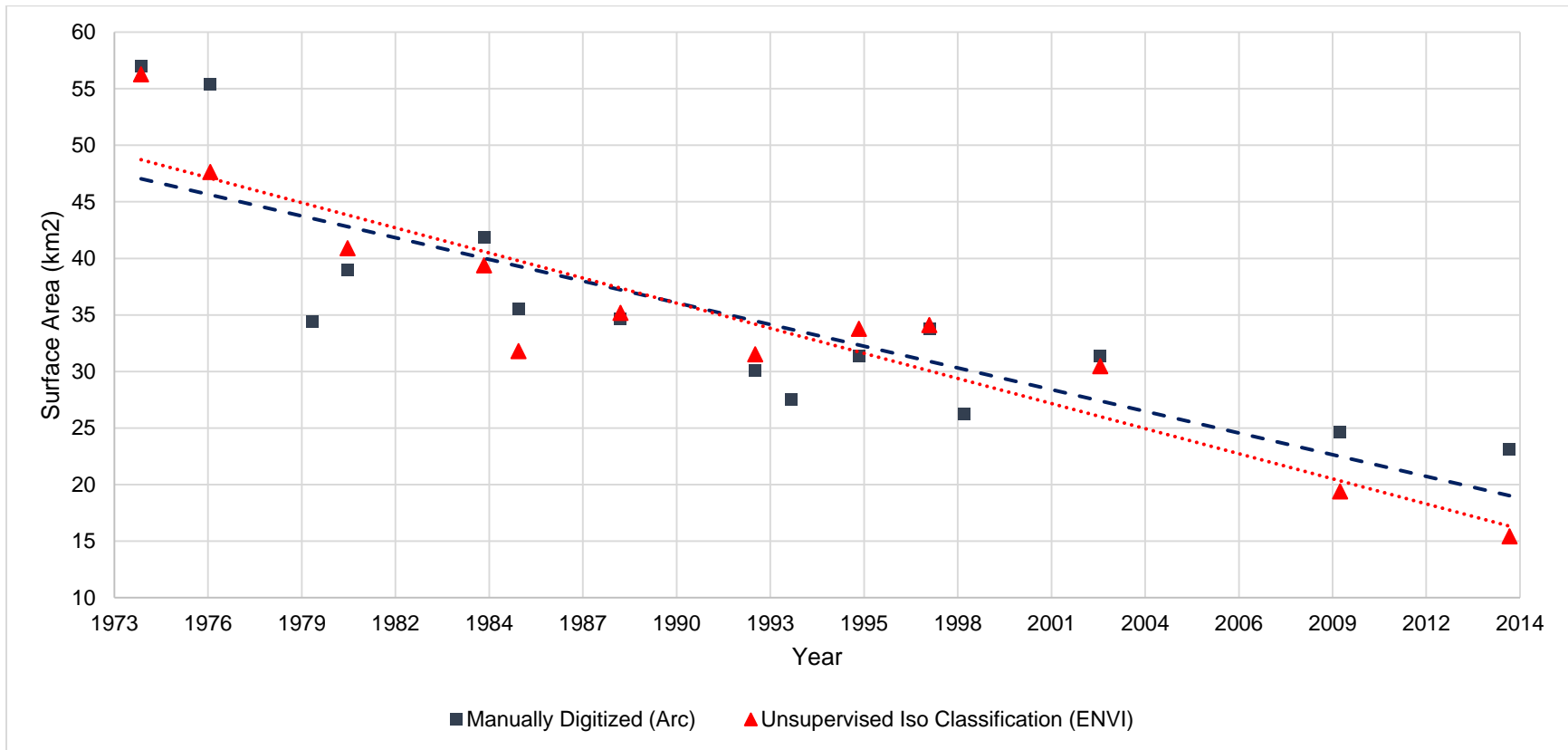


Figure 4.6: Results of late summer glacier surface area analysis at MMVC from the manual digitizing method and the unsupervised classification method. Overall, both methods show a decrease in clean glacier ice at MMVC.

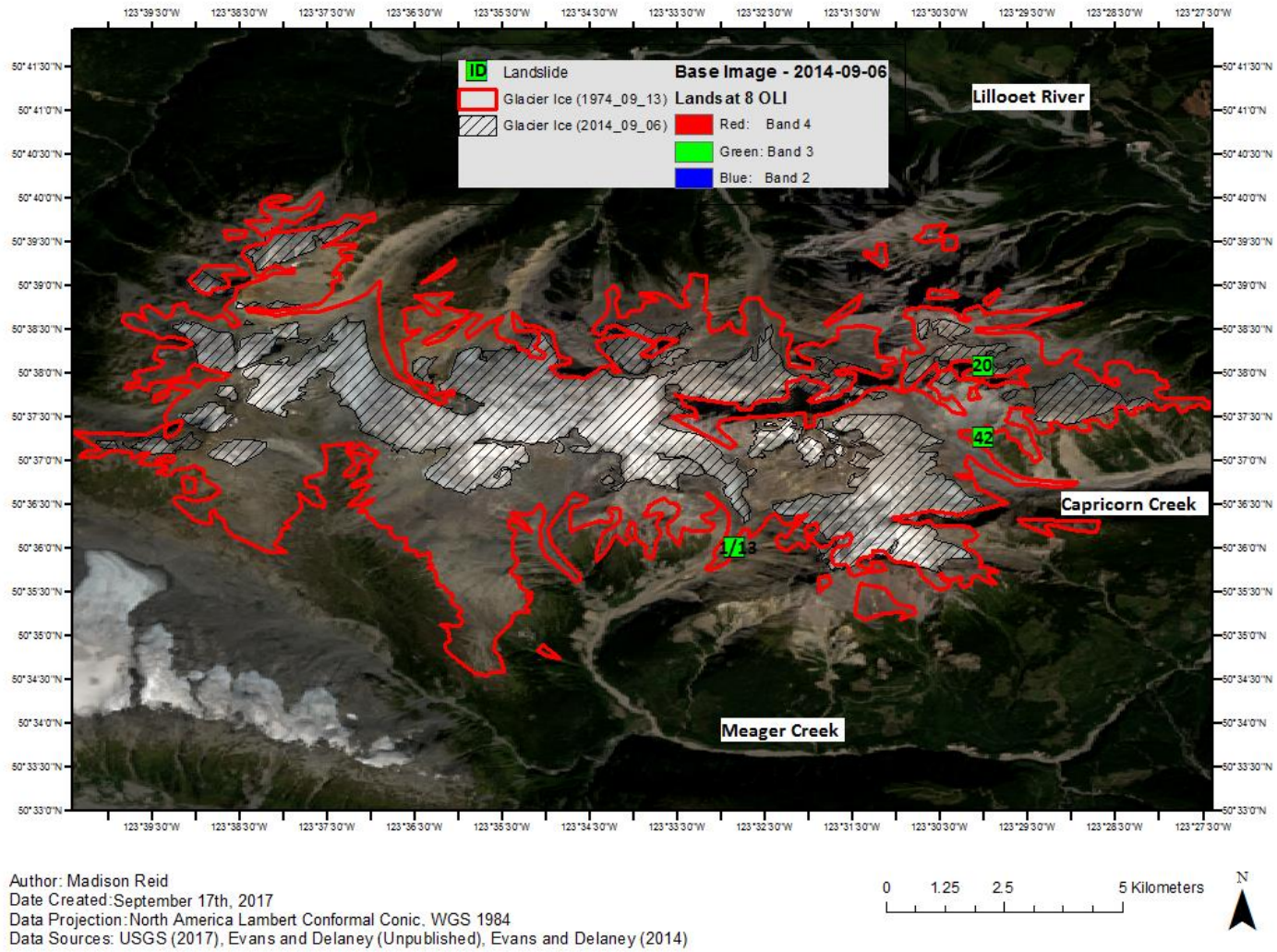


Figure 4.7: A map showing the changing area of the glaciers on MMVC, using hollow polygons to represent extents at different times, and a true colour base image from 2014. The northern landslide source location is for the landslide in 2010 (Guthrie et al., 2012)

In addition to glacier extent, temperature and precipitation also have an impact of glacier thickness and volume. The results of the DEM subtraction are shown in **Figure 4.8**. The average change in elevation was negative 8.3 m from 1988 to 2000. However, the error assessment found that the SRTM data reported elevations 3.3 m higher than the TRIM data. Therefore the corrected average thinning was 5.0 m from 1988 to 2000. This indicates that, on average, the MMVC glaciers became 5.0 m thinner over the course of 12 years. The change in area over the smaller study area was negative 2.12Mm². It is important to note that this change in area was based on Landsat imagery from 1988 and 1998. Landsat imagery in September of 2000 was not available due to cloud cover. The difference in the temporal range of the elevation dataset and the area dataset adds error to the subsequent volume calculation. However, due to the decreasing glacier extent, it can be assumed that the change in glacier volume from 1988 to 2000 was at a minimum 10.6 Mm³. To further illustrate the ice loss, a cumulative plot of ice loss and landslide mass sorted by elevation was generated (**Figure 4.9**) (Brocklehurst and Whipple, 2004). The landslide volume matches the ice loss curve well up to an elevation of approximately 1900m. This supports the hypothesis of ice loss being correlated with landslides, especially at low elevations. This relationship is less strong at higher elevations, and future work could focus on this feature. One possible explanation for the loss of the match between the datasets is a different process influencing landslides at higher elevations (i.e., not ice loss which is dominant at low elevations). Perhaps the degradation of mountain permafrost and other thermal effects are more influential at high elevations (Deline *et al.*, 2015b). It is important to note that the landslide curve is heavily influenced by the single large event which occurred in August 2010. This could be another factor leading to the curves become dissimilar. Overall, these results provide strong evidence linking climate change to glacier ice loss, and ice loss to landslide activity.

Glacier retreat as a landslide trigger is particularly evident for the 1975 landslide (ID – 13, in **Figure 4.7**). Mokievsky-Zubok (1977) proposes the rapid loss of ice volume in the source area was caused by several factors: “(a) a southern exposure; (b) highly positive summer thermal balance within a narrow valley that was wind-sheltered and sun-exposed; and (c) constant undermining below the ice cover in the upper basin forcing the glacier to calve”. Ultimately, Mokievsky-Zubok (1977) posits the landslide was caused by “the weight of the glacier ice and the

action of glacier meltwater”, especially when interacting with loosely consolidated underlying sediments. The importance of glacier melt, both in its contributions to slope instability and meltwater generation, is essential to Mokievsky-Zubok’s interpretation. The results of the Landsat imagery analysis show that the source location of the landslide was just south of the toe of the glacier, in an area recently exposed. These findings are supported by Evans and Delaney (2014). According to the area analysis, the glacier was undergoing rapid retreat at the time, with massive amounts of meltwater being released. Ultimately, the results align with existing research and contribute to the body of evidence supporting climate change and ice loss as a trigger for the landslide event near Pylon Peak on July 22nd, 1975.

Glacial processes were also a factor leading to the landslide on August 6th, 2010 (ID-42, in **Figure 4.7**). Similar to the 1975 landslide, there was no seismic or meteorological trigger recorded the day of the event (Guthrie *et al.*, 2012). Rather, the landslide was due to a combination of several preconditions. First, the Mount Meager Volcanic Complex is structurally weak, with a history of glacial unloading and explosive volcanism (Guthrie *et al.*, 2012). In addition, glacier activity since the Little Ice Age has resulted in over-steeping of slopes, leading to even greater instability (Guthrie *et al.*, 2012). Despite all of these other factors, Guthrie *et al.* (2012) hypothesize excessive groundwater causing very high pore pressures was the most important condition leading to the landslide. The water supply was exacerbated by glacier melt, leading to saturation of the already weak slopes. While the source area of this landslide does not show exceptional melt in the Landsat image analysis, the reduction of glacier surface area over the entire study period firmly shows that the glacier is undergoing significant melt. Recall the discussion of **Figure 4.9**, suggesting that glacier ice may not play a dominant role to landslide hazard in the MMVC at higher elevations; due to the high source elevation of the event factors other than glacier melt, such as permafrost degradation, should also be considered.

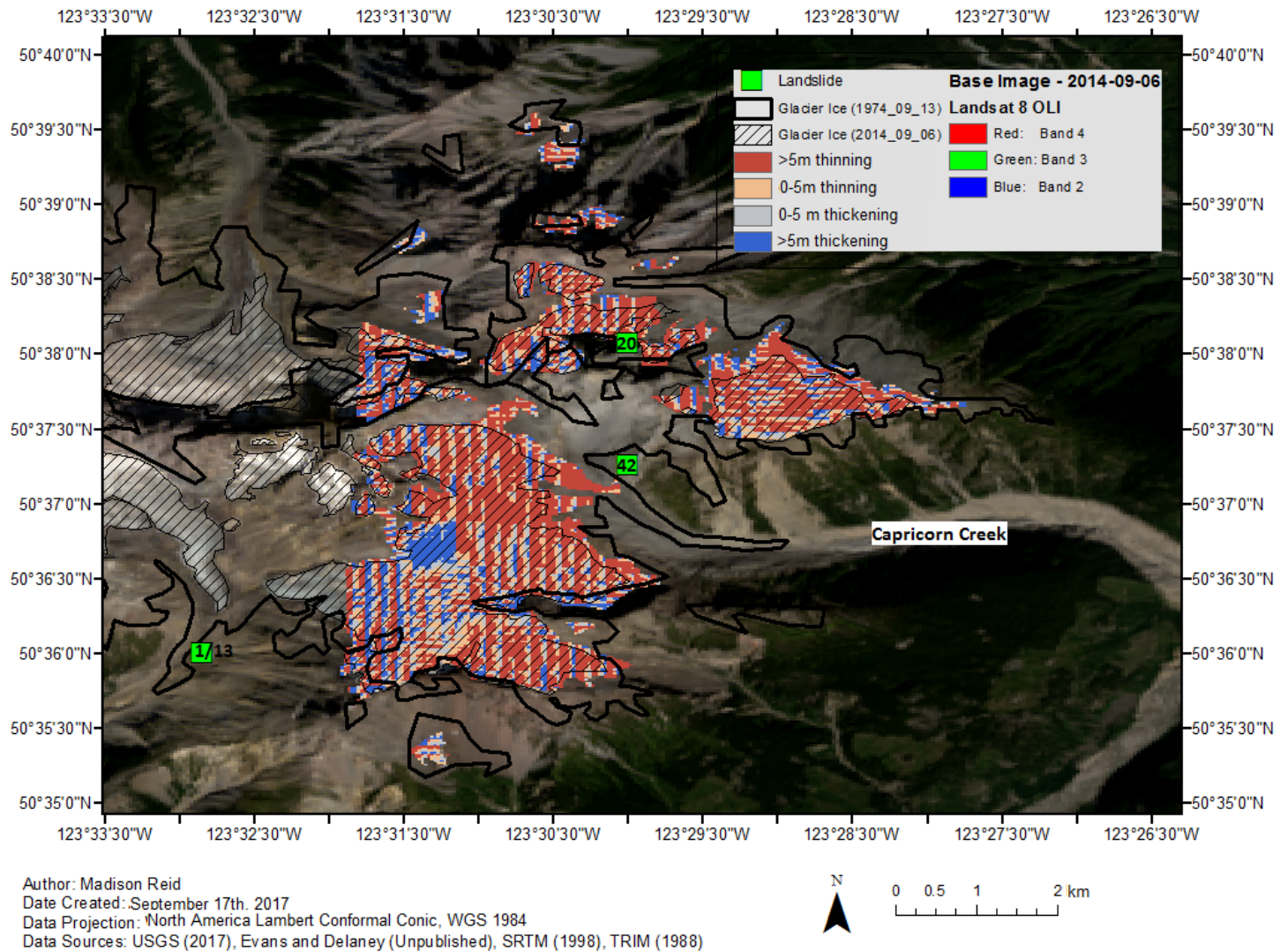


Figure 4.8: A map showing the change in glacier thickness from 1988 to 2000. This is located on the eastern edge of the overall study area.

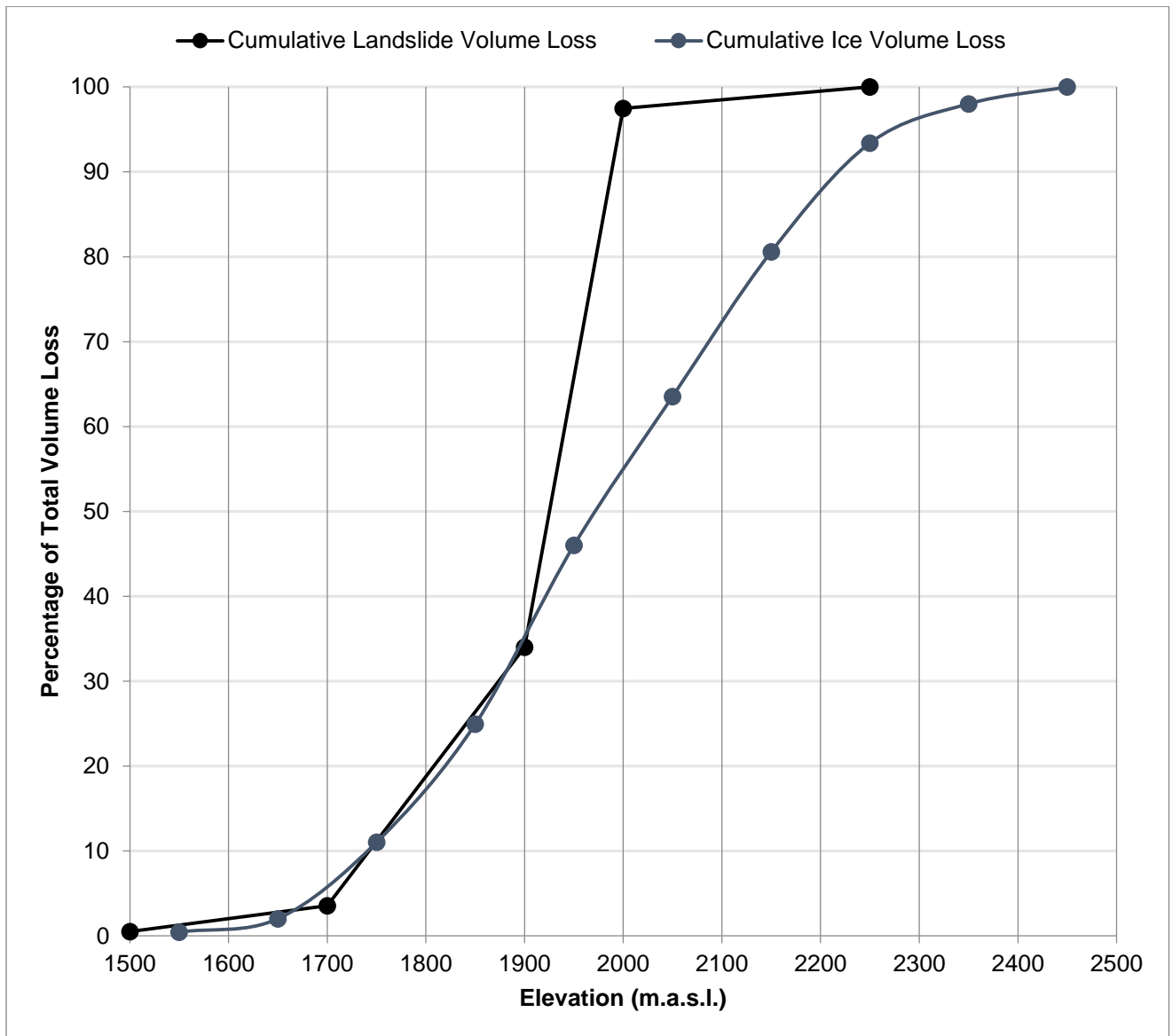


Figure 4.9: A hypsometric analysis of ice loss volume (from 1988 to 1998) and landslide volume, showing a strong correlation between ice loss at elevations below 1900m. These results suggest ice loss may be correlated with landslide hazard in MMVC at lower elevations, but not at higher elevations.

4.5 Conclusion

This chapter has successfully established a link between climate change, glacier ice loss, and landslide activity by examining Mount Meager Volcanic Complex as a site specific study. All of the climate change analysis results show warming and increasing precipitation trends at Mount Meager. Increases in temperature also shift the proportion of rain and snow, leading to great amounts of rain. The PRISM data shows the strongest trends of increasing precipitation align with the south slope of MMVC which has experienced the greatest loss of glacier extent. This observation highlights the potential importance of precipitation in glacier dynamics and consequently landslide hazard.

In response to warming temperatures and increased precipitation, the area and volume of glacier ice at MMVC has been dramatically reduced in the last 40 years. The area has been reduced by approximately 33.9 km² from 1974 to 2014. From 1988 to 2000, there was a volume decrease of at least 10.6 Mm³.

It is clear that in both major events (1975 and 2010), glacier ice loss caused by climate change contributed to the trigger mechanism of the landslides. The 1975 landslide is an excellent example of the risks associated with the shorter term effects of climate change (i.e., warm summer temperatures and increased melt water), while the 2010 landslide was more influenced by long term effects, specifically debulking (Mokievsky-Zubok, 1977; Evans and Delaney, 2014; Guthrie *et al.*, 2012). Future research should focus on providing additional quantitative analysis of glacier change, specifically focusing on meltwater effects. Hypsometric analysis would also be useful to assess any correlation between ice loss as a function of elevation, and the implications these results may have on landslide risk and probability. It is essential to quantify the mechanisms of climate change as a trigger for mass movement to generate better models and predictions, ultimately assisting in the implementation of better risk management practices.

Chapter Five: Thesis Summary and Conclusion

5.1 Introduction

This thesis was the culmination of a large amount of research and investigation into the ways in which climate change reduces slope stability in the glaciated mountains of northwest North America. The literature review presented in Chapter 2 confirmed that the majority of the scientific community concur warming temperatures and increasing precipitation increase landslide hazard (Jakob and Lambert, 2009; Evans and Clague, 1994; Huggel *et al.*, 2012; Bovis and Jones, 1992, Geertsema, 2013; Geertsema *et al.*, 2007; Guthrie *et al.*, 2010; Holm *et al.*, 2004, Huggel *et al.*, 2010; Crozier, 2010; Huggel *et al.*, 2008)), although the effects of precipitation are debated by some (Uhlmann *et al.*, 2012). Glacier ice loss is also commonly thought to destabilize slopes through one or more of the following methods: debutressing, unloading (stress-relief), uplift, mountain permafrost degradation, or generation of unstable ice (Deline *et al.*, 2015b; McColl, 2012; Fischer *et al.*, 2013; Faillettaz *et al.*, 2012; Gruber and Haeberli, 2007; Blair 1994; Setwart *et al.*, 2000; Fischer *et al.*, 2010; Matsuoka and Murton, 2008). This thesis aimed to add to the body of work assessing climate change in the alpine environment by specifically investigating temperature change, precipitation trends, and glacier ice loss in British Columbia, Yukon, and Alaska, and comparing these results to an inventory of large catastrophic landslides with source zones in the periglacial environment. To accomplish this larger goal, several smaller research objectives were met: (a) Determine changes in the frequency and distribution of landslides in glacial regions of northwest North America by analysing a landslide inventory; (b) Quantify climate change factors, specifically trends in temperature and precipitation; (c) Assess changes in glacier ice area and volume in northwest North America; and (d) Establish a quantitative relationship between climate change, glacier ice loss, and landslide activity. The main conclusions for each research objective are summarized below.

5.2 Research Objective A: Determine changes in the frequency and distribution of landslides in glacial regions of northwest North America by analysing a landslide inventory

This research objective was assessed in the second half of Chapter 2 (**Section 2.3**), and the statistical analysis portion of Chapter 3 (**Section 3.6**). After the landslide inventory was completed using a length to scaling relationship, a magnitude/frequency plot was generated based on the mass of events. The most important result from this analysis was that seismically triggering has a proportionally greater number of small events, and fewer large events, than non-seismically triggered landslides. This supposition highlights the importance of understanding climate preconditioning and triggering of large catastrophic landslides. Further exploration of the landslide inventory in Chapter 3 showed that the frequency of landslide with a volume greater than or equal to 1 Mm^3 is increasing over time, especially at high latitudes (above 57 degrees N). Also, the elevation of landslides seems to be increasing over time, potentially reflecting a systematic destabilization progressing upward toward the peaks of the mountains. This trend was observed in coseismic and non-seismic events.

5.3 Research Objective B: Quantify climate change factors, specifically trends in temperature and precipitation

The literature reports increasing temperature and precipitation throughout the study area. Assessment of temperature and precipitation changes across northwest North America based on meteorological station data was described in Chapter 3. Temperature indices developed specifically for this thesis showed wide spread warming, particularly in winter and summer. Precipitation index results show consistent decreased precipitation in Alaska, and increasingly wet conditions in British Columbia. PRISM reanalysis data was used as a secondary source, which showed warming and increased precipitation throughout British Columbia.

5.4 Research Objective C: Assess changes in glacier ice area and volume in northwest North America

The literature review presented in Chapter 2 summarized the scientific consensus that the majority of glaciers in northwest North America are retreating and thinning, resulting in a decrease in glacier area and volume. Chapter 4 presents a glacier ice loss case study of Mount Meager Volcanic Complex in southern British Columbia. The results demonstrate drastic reduction of ice area and volume in response to increased temperature and precipitation. The greatest glacier retreat is along the south slope of MMVC, which corresponds with the most significant increase in precipitation based on PRISM climate reanalysis data. In addition, there is strong evidence indicating both of the major landslide events at MMVC in the landslide inventory (1975 and 2010) were triggered by climate factors, specifically warm temperatures.

5.5 Research Objective D: Establish a quantitative relationship between climate change, glacier ice loss, and landslide activity

Chapter 3 used meteorological station data from across British Columbia and Alaska to generate temperature and precipitation change indices, representing how fast the climate is changing spatially over the entire study area. When combined with landslide magnitude information (mass) from the inventory, several correlations became apparent. First, the temperature index spatially associated with each landslide was increasing over time, suggesting that recent landslides are in areas with more rapidly increasing summer temperatures. This was the case for both seismically and non-seismically triggered events. Precipitation index results showed no obvious pattern of increasing or decreasing with time, indicating that precipitation change may have less of an influence on landslide hazard. When plotted cumulatively sorted by elevation and evaluated statistically, the correlation between landslide mass and temperature change was confirmed quantitatively for both coseismic and non-seismic failures. The correlation between precipitation and non-seismically triggered events was not significant, but it was significant for seismically triggered landslides. This could be due to decreasing precipitation trends in Alaska causing a reduction in glacial accumulation, resulting in greater hazard.

The connections between glacier ice loss, climate change, and landslide activity was further elucidated in Chapter 4. Glacier retreat at MMVC was found to be greatest in the areas with the most increase in precipitation according to PRISM climate reanalysis data. All of the climate analysis results surrounding MMVC showing increasing temperature and precipitation, which undoubtedly influenced the observed ice loss. In addition, two recent major landslide events at MMVC (1975 and 2010) have been coupled to both glacier ice loss and warm summer temperatures generating excess melt water. However, it was hypothesized that glacier ice loss has a decreasing influence on hazard at higher elevations, due to a loss of correlation at 1900 m.a.s.l. between ice volume and landslide mass in a hypsometric plot.

5.6 Implications

All of the results presented in this thesis support the hypothesis that there is warming in northwest North America, and that warming is correlated with increasing landslide hazard in the glacial environment. This is particularly the case in northern British Columbia, Yukon, and Alaska, as there has been a dramatic increase in the number of large landslides in the glacier environment since 1990. As mean temperatures continue to rise, the hazard from landslides with a minimum volume of 1 Mm³ is also expected to rise.

The hypothesis that precipitation affects landslide hazard is also supported, however it is less simple than is the case with temperature. For non-seismically triggered landslides, precipitation was not statistically correlated with landslide mass. However, decreasing precipitation in Alaska was correlated to seismically triggered landslides with significance. This could be caused by decreasing snowfall in Alaska causing a reduction in glacial accumulation, resulting in greater landslide hazard (due to glacier ice loss). The dual nature of the precipitation index results confounds the conclusions. Despite the lack of statistical support wetter conditions in the south could theoretically increase hazard in a number of ways. For example, wetter conditions would increase pore pressure, making slopes more susceptible to failure. Similarly, if precipitation is falling as snow, a heavy snowpack can increase the chance of a landslide. In the

north, dryer conditions reflect less snow. This could increase the landslide hazard by lowering the glacier mass balance promoting ice loss. Precipitation has a complex relationship with landslide hazard, and must be considered carefully in the context of landslide hazard. In conclusion, precipitation could not be conclusively linked to increasing landslide hazard in northwest North America.

Glacier ice is influenced by both temperature and precipitation, with their changes causing the majority of glaciers in North America to retreat. The results of this thesis agree with the literature, that glacier ice loss is correlated with increased landslide hazard. With glacier ice diminishing, it is expected there will be a greater frequency and/or magnitude of landslides in glacial and periglacial slopes.

With increasing temperatures and precipitation, and loss of glacier ice in northwest North America, landslide hazard from both seismically and non-seismically triggered events is expected to continue to increase in the future. Of particular concern are higher elevation slopes that have not previously failed, but are at growing risk of failure as source elevations of major rock slope failure appear to migrate upward.

5.7 Future Work

This thesis relies heavily on a very specific subset of landslide data. The only events considered are those with a large volume, in glacial regions, and after 1947. Future work could expand upon this inventory, including smaller events in different settings or regions. Different types of inventories, such as a global inventory or a synthetic inventory, could be explored. Furthermore, the approach used to identify climate trends is only one of several options. A modelling methodology, or the use of paleo-climate data could be beneficial in improving our understanding of the relationship between climate and landslide hazard.

Further investigation of the physical processes that trigger non-seismic landslides in a changing climate is warranted. The analysis in Chapter 3 relied partially on correlation analysis,

but it is important to remember that correlation does not imply causation. As such, a careful examination of the driving mechanisms behind each of the landslide events would help prevent erroneous claims based on correlative statistics.

More sophisticated methods of estimating glacier volume loss would also improve the reliability of any findings. The DEM subtraction method allows for a crude estimation, but there are hi-tech solutions available with far superior accuracy, such as interferometry. Moreover, it would be beneficial to generate a glacier ice loss estimate for the entire study area, not simply the MMVC case study.

In conclusion, while this thesis is a valuable addition to the growing body of evidence indicating that climate change has significant impacts on landslide hazard in the mountain glacial environment, there are still many uncertainties to be resolved. This will remain to be an important research subject, because climate, the cryosphere, and the mountain environment are dynamic entities in constant flux.

References

1. Arendt, A.A., Echelmeyer, K.A., Harrison, W.D., Lingle, C.S. & Valentine, V.B. Rapid wastage of Alaska glaciers and their contribution to rising sea level. *Science* 297, 382-386 (2002).
2. Berthier, E., Schiefer, E., Clarke, G.K., Menounos, B. and Rémy, F., 2010. Contribution of Alaskan glaciers to sea-level rise derived from satellite imagery. *Nature Geoscience*, 3(2), p.92.
3. Bitz, C.M. and Battisti, D.S., 1999. Interannual to decadal variability in climate and the glacier mass balance in Washington, western Canada, and Alaska. *Journal of Climate*, 12(11), pp.3181-3196.
4. Blair Jr, R.W., 1994. Moraine and valley wall collapse due to rapid deglaciation in Mount Cook National Park, New Zealand. *Mountain Research and Development*, pp.347-358.
5. Bolch, T., Menounos, B. and Wheate, R., 2010. Landsat-based inventory of glaciers in western Canada, 1985–2005. *Remote sensing of Environment*, 114(1), pp.127-137.
6. British Columbia Ministry of Forests, Lands, and Natural Resources, 2009. *Climate Change*. [online] Available at: <<https://www.for.gov.bc.ca/hre/topics/climate.htm>> [Accessed: 13 August 2017].
7. Brocklehurst, S.H. and Whipple, K.X., 2004. Hypsometry of glaciated landscapes. *Earth Surface Processes and Landforms*, 29(7), pp.907-926.
8. Clarke, G.K., Jarosch, A.H., Anslow, F.S., Radić, V. and Menounos, B., 2015. Projected deglaciation of western Canada in the twenty-first century. *Nature Geoscience*, 8(5), pp.372-377.
9. Crozier, M.J., 2010. Deciphering the effect of climate change on landslide activity: A review. *Geomorphology*, 124(3), pp.260-267.
10. Cruden, D.M. and Varnes, D.J., 1996. Landslides: investigation and mitigation. Chapter 3-Landslide types and processes. *Transportation research board special report*, (247).
11. Davies, T.R., 1982. Spreading of rock avalanche debris by mechanical fluidization. *Rock Mechanics and Rock Engineering*, 15(1), pp.9-24.
12. Delaney, K.B., 2014. Characterisation and Analysis of Catastrophic Landslides and Related Processes using Digital Topographic Data. University of Waterloo.
13. Delaney, K.B. and Evans, S.G., 2014. The 1997 Mount Munday landslide (British Columbia) and the behaviour of rock avalanches on glacier surfaces. *Landslides*, 11(6), pp.1019-1036.
14. Deline, P., Hewitt, K., Reznichenko, N. and Shugar, D., 2015a. Rock avalanches onto glaciers. *Landslide Hazards, Risks and Disasters*. Elsevier, Amsterdam, pp.263-319.
15. Deline, P., Gruber, S., Delaloye, R., Fischer, L., Geertsema, M., Giardino, M., Hasler, A., Kirkbride, M., Krautblatter, M., Magnin, F. and McColl, S., 2015b. Ice loss and slope stability in high-mountain regions. *Snow and Ice-Related Hazards, Risks, and Disasters*, edited by: Haeberli, W., Whiteman, C., and Shroder, JF, Elsevier Science, Saint Louis, pp.521-561.

16. Evans, S.G. and Clague, J.J. 1988. Catastrophic rock avalanches in glacial environments. *Proceedings, V International Symposium on Landslides*, 2: 1153-1158.
- Evans, S.G. and Clague, J.J. 1999. Rock avalanches on glaciers in the Coast and St. Elias Mountains, British Columbia. In *Slope stability and landslides*, Proceedings, 13th Annual Vancouver Geotechnical Society Symposium, p. 115-123.
17. Evans, S.G. and Clague, J.J., 1994. Recent climatic change and catastrophic geomorphic processes in mountain environments. *Geomorphology*, 10(1-4), pp.107-128.
18. Evans, S.G. and Delaney, K.B., 2014. Catastrophic mass flows in the mountain glacial environment. *Snow and ice-related hazards, risks and disasters*. Elsevier, Amsterdam, pp.563-606.
19. Faillettaz, J., Funk, M. and Sornette, D., 2012. Instabilities on Alpine temperate glaciers: new insights arising from the numerical modelling of Allalingsletscher (Valais, Switzerland). *Natural Hazards and Earth System Sciences*, 12(9), p.2977.
20. Field, C.B., V.R. Barros, K.J. Mach, M.D. Mastrandrea, M. van Aalst, W.N. Adger, D.J. Arent, J. Barnett, R. Betts, T.E. Bilir, J. Birkmann, J. Carmin, D.D. Chadee, A.J. Challinor, M. Chatterjee, W. Cramer, D.J. Davidson, Y.O. Estrada, J.-P. Gattuso, Y. Hijjoka, O. Hoegh-Guldberg, H.Q. Huang, G.E. Insarov, R.N. Jones, R.S. Kovats, P. Romero-Lankao, J.N. Larsen, I.J. Losada, J.A. Marengo, R.F. McLean, L.O. Mearns, R. Mechler, J.F. Morton, I. Niang, T. Oki, J.M. Olwoch, M. Opondo, E.S. Poloczanska, H.-O. Pörtner, M.H. Redster, A. Reisinger, A. Revi, D.N. Schmidt, M.R. Shaw, W. Solecki, D.A. Stone, J.M.R. Stone, K.M. Strzepek, A.G. Suarez, P. Tschakert, R. Valentini, S. Vicuña, A. Villamizar, K.E. Vincent, R. Warren, L.L. White, T.J. Wilbanks, P.P. Wong, and G.W. Yohe, 2014: Technical summary. In: *Climate Change 2014: Impacts, Adaptation, and Vulnerability. Part A: Global and Sectoral Aspects. Contribution of Working Group II to the Fifth Assessment Report of the Intergovernmental Panel on Climate Change* [Field, C.B., V.R. Barros, D.J. Dokken, K.J. Mach, M.D. Mastrandrea, T.E. Bilir, M. Chatterjee, K.L. Ebi, Y.O. Estrada, R.C. Genova, B. Girma, E.S. Kissel, A.N. Levy, S. MacCracken, P.R. Mastrandrea, and L.L. White (eds.)]. Cambridge University Press, Cambridge, United Kingdom and New York, NY, USA, pp. 35-94.
21. Fischer, L., Amann, F., Moore, J.R. and Huggel, C., 2010. Assessment of periglacial slope stability for the 1988 Tschierwa rock avalanche (Piz Morteratsch, Switzerland). *Engineering Geology*, 116(1), pp.32-43.
22. Fischer, L., Huggel, C., Käab, A. and Haerberli, W., 2013. Slope failures and erosion rates on a glacierized high-mountain face under climatic changes. *Earth surface processes and landforms*, 38(8), pp.836-846.
23. Gariano, S.L. and Guzzetti, F., 2016. Landslides in a changing climate. *Earth-Science Reviews*, 162, pp.227-252.
24. Geertsema, M., Clague, J.J., Schwab, J.W. and Evans, S.G., 2006. An overview of recent large catastrophic landslides in northern British Columbia, Canada. *Engineering Geology*, 83(1), pp.120-143.

25. Geertsema, M., 2012, June. Initial observations of the 11 June 2012 rock/ice avalanche, Lituya Mountain, Alaska. In *The First Meeting of International Consortium of Landslides Cold Region Landslides Network, Harbin, China* (pp. 49-54).
26. Geertsema, M., 2013. Quick clay landslides, landscape evolution, and climate change: a perspective from British Columbia. In *Landslide science and practice* (pp. 115-120). Springer Berlin Heidelberg.
27. Geertsema, M., Egginton, V.N., Schwab, J.W. and Clague, J.J., 2007, May. Landslides and historic climate in northern British Columbia. In *Landslides and climate change: Challenges and solutions, Proceedings from the International Conference on Landslides and Climate Change, Ventor, Isle of Wight, UK* (pp. 9-16).
28. Gocic, M. and Trajkovic, S., 2013. Analysis of changes in meteorological variables using Mann-Kendall and Sen's slope estimator statistical tests in Serbia. *Global and Planetary Change*, 100, pp.172-182.
29. Gorum, T., Korup, O., van Westen, C.J., van der Meijde, M., Xu, C. and van der Meer, F.D., 2014. Why so few? Landslides triggered by the 2002 Denali earthquake, Alaska. *Quaternary Science Reviews*, 95, pp.80-94.
30. Gruber, S. and Haeberli, W., 2007. Permafrost in steep bedrock slopes and its temperature-related destabilization following climate change. *Journal of Geophysical Research: Earth Surface*, 112(F2).
31. Guthrie, R.H., Mitchell, S.J., Lanquaye-Opoku, N. and Evans, S.G., 2010. Extreme weather and landslide initiation in coastal British Columbia. *Quarterly Journal of Engineering Geology and Hydrogeology*, 43(4), pp.417-428.
32. Guthrie, R.H., Friele, P., Allstadt, K., Roberts, N., Evans, S.G., Delaney, K.B., Roche, D., Clague, J.J. and Jakob, M., 2012. The 6 August 2010 Mount Meager rock slide-debris flow, Coast Mountains, British Columbia: characteristics, dynamics, and implications for hazard and risk assessment. *Natural Hazards and Earth System Sciences*, 12(5), pp.1277-1294.
33. Guzzetti, F., Mondini, A.C., Cardinali, M., Fiorucci, F., Santangelo, M. and Chang, K.T., 2012. Landslide inventory maps: New tools for an old problem. *Earth-Science Reviews*, 112(1), pp.42-66.
34. Helsel, D.R. and Hirsch, R.M., 2002. Trend analysis. *Statistical methods in water resources*, pp.323-355.
35. Hilker, N., Badoux, A. and Hegg, C., 2009. The Swiss flood and landslide damage database 1972-2007. *Natural Hazards and Earth System Sciences*, 9(3), p.913.
36. Holm, K., Bovis, M. and Jakob, M., 2004. The landslide response of alpine basins to post-Little Ice Age glacial thinning and retreat in southwestern British Columbia. *Geomorphology*, 57(3), pp.201-216.
37. Houghton, J., Jenkins, G. and Ephraums, J., 1990. IPCC First Assessment Report 1990, Scientific Assessment of Climate Change: Report of Working Group 1.
38. Huggel, C., Caplan-Auerbach, J., Gruber, S., Molnia, B. and Wessels, R., 2008, June. The 2005 Mt. Steller, Alaska, rock-ice avalanche: A large slope failure in cold

- permafrost. In *Proceedings of the Ninth International Conference on Permafrost* (Vol. 29, pp. 747-752).
39. Huggel, C., Salzmann, N., Allen, S., Caplan-Auerbach, J., Fischer, L., Haeberli, W., Larsen, C., Schneider, D. and Wessels, R., 2010. Recent and future warm extreme events and high-mountain slope stability. *Philosophical Transactions of the Royal Society of London A: Mathematical, Physical and Engineering Sciences*, 368(1919), pp.2435-2459.
 40. Huggel, C., Clague, J.J. and Korup, O., 2012. Is climate change responsible for changing landslide activity in high mountains?. *Earth Surface Processes and Landforms*, 37(1), pp.77-91.
 41. Hungr, O. and Evans, S.G., 2004. Entrainment of debris in rock avalanches: an analysis of a long run-out mechanism. *Geological Society of America Bulletin*, 116(9-10), pp.1240-1252.
 42. Jakob, M. and Lambert, S., 2009. Climate change effects on landslides along the southwest coast of British Columbia. *Geomorphology*, 107(3), pp.275-284.
 43. Jiskoot, H., 2011. Long-runout rockslide on glacier at Tsar Mountain, Canadian Rocky Mountains: potential triggers, seismic and glaciological implications. *Earth Surface Processes and Landforms*, 36(2), pp.203-216.
 44. Korup, O., Görüm, T. and Hayakawa, Y., 2012. Without power? Landslide inventories in the face of climate change. *Earth Surface Processes and Landforms*, 37(1), pp.92-99.
 45. Larsen, C.F., Motyka, R.J., Freymueller, J.T., Echelmeyer, K.A. and Ivins, E.R., 2005. Rapid viscoelastic uplift in southeast Alaska caused by post-Little Ice Age glacial retreat. *Earth and Planetary Science Letters*, 237(3), pp.548-560.
 46. Mann, H.B., 1945. Nonparametric tests against trend. *Econometrica: Journal of the Econometric Society*, pp.245-259.
 47. Matsuoka, N. and Murton, J., 2008. Frost weathering: recent advances and future directions. *Permafrost and Periglacial Processes*, 19(2), pp.195-210.
 48. McColl, S.T., 2012. Periglacial rock-slope stability. *Geomorphology*, 153, pp.1-16.
 49. McColl, S.T. and Davies, T.R., 2013. Large ice-contact slope movements: glacial buttressing, deformation and erosion. *Earth Surface Processes and Landforms*, 38(10), pp.1102-1115.
 50. McGrew Jr, J.C. and Monroe, C.B., 2009. *An introduction to statistical problem solving in geography*. Waveland Press.
 51. Melillo, Jerry M., Terese (T.C.) Richmond, and Gary W. Yohe, Eds., 2014: Climate Change Impacts in the United States: The Third National Climate Assessment. U.S. Global Change Research Program, 841 pp. doi:10.7930/J0Z31WJ2.
 52. Mokievsky-Zubok, O., 1977. Glacier-caused slide near Pylon Peak, British Columbia. *Canadian Journal of Earth Sciences*, 14(11), pp.2657-2662.
 53. Moore, R.D. and Demuth, M.N., 2001. Mass balance and streamflow variability at Place Glacier, Canada, in relation to recent climate fluctuations. *Hydrological Processes*, 15(18), pp.3473-3486.
 54. Moore, R.D., Fleming, S.W., Menounos, B., Wheate, R., Fountain, A., Stahl, K., Holm, K. and Jakob, M., 2009. Glacier change in western North America: influences on

- hydrology, geomorphic hazards and water quality. *Hydrological Processes*, 23(1), pp.42-61.
55. Nichols, T.C., 1980. Rebound, its nature and effect on engineering works. *Quarterly Journal of Engineering Geology and Hydrogeology*, 13(3), pp.133-152.
 56. Noetzli, J. and Gruber, S., 2009. Transient thermal effects in Alpine permafrost. *The Cryosphere*, 3(1), pp.85-99.
 57. Ommanney CSI., 2002. Glaciers of the Canadian Rockies J199-289. In *Satellite Image Atlas of Glaciers of the World: North America*. United States Geological Survey Professional paper 1386J-I, Williams RS Jr. Ferrigno JG (eds.) US Government Printing Office: Washington, DC.
 58. Pacific Climate Impacts Consortium, University of Victoria, and PRISM Climate Group, Oregon State University, (Jan. 2014). High Resolution Climatology. Downloaded from <<https://www.pacificclimate.org/data/high-resolution-prism-climatology>> on <March 14th, 2017>.
 59. Paul, F., Huggel, C., & Käab, A. (2004). Combining satellite multispectral image data and a digital elevation model for mapping of debris-covered glaciers. *Remote Sensing of Environment*, 89(4), 510–518.
 60. Petley, D., 2012. Global patterns of loss of life from landslides. *Geology*, 40(10), pp.927-930.
 61. Plafker, G., 1970. *Tectonics of the March 27, 1964, Alaska earthquake*. US Government Printing Office.
 62. Post, A.S., 1964. Effects on glaciers. *The great Alaska earthquake of, 3*, pp.266-308.
 63. Raper, S.C. and Braithwaite, R.J., 2009. Glacier volume response time and its links to climate and topography based on a conceptual model of glacier hypsometry. *The Cryosphere*, 3(2), pp.183-194.
 64. Schiefer, E., Menounos, B. and Wheate, R., 2007. Recent volume loss of British Columbian glaciers, Canada. *Geophysical Research Letters*, 34(16).
 65. Schiefer, E., Menounos, B. and Wheate, R., 2008. An inventory and morphometric analysis of British Columbia glaciers, Canada. *Journal of Glaciology*, 54(186), pp.551-560.
 66. Schneider, D., Huggel, C., Haeberli, W. and Kaitna, R., 2011. Unraveling driving factors for large rock–ice avalanche mobility. *Earth Surface Processes and Landforms*, 36(14), pp.1948-1966.
 67. Sen, P.K., 1968. Estimates of the regression coefficient based on Kendall's tau. *Journal of the American Statistical Association*, 63(324), pp.1379-1389.
 68. Solomon, S., Qin, D., Manning, M., Chen, Z., Marquis, M., Averyt, K.B., Tignor, M. and Miller, H.L., 2007. IPCC, 2007: summary for policymakers. *Climate change, 2007*, p.79.
 69. Sosio, R., Crosta, G.B., Chen, J.H. and Hungr, O., 2012. Modelling rock avalanche propagation onto glaciers. *Quaternary Science Reviews*, 47, pp.23-40.
 70. Stewart, I.S., Sauber, J. and Rose, J., 2000. Glacio-seismotectonics: ice sheets, crustal deformation and seismicity. *Quaternary Science Reviews*, 19(14), pp.1367-1389.
 71. Stocker, T.F., Qin, D., Plattner, G.K., Tignor, M., Allen, S.K., Boschung, J., Nauels, A., Xia, Y., Bex, B. and Midgley, B.M., 2013. IPCC, 2013: climate change 2013: the

- physical science basis. Contribution of working group I to the fifth assessment report of the intergovernmental panel on climate change.
72. Stoffel, M., Tiranti, D. and Huggel, C., 2014. Climate change impacts on mass movements—case studies from the European Alps. *Science of the Total Environment*, 493, pp.1255-1266.
 73. Streicker, J., 2016. Yukon Climate Change Indicators and Key Findings 2015. Northern Climate ExChange, Yukon Research Centre, Yukon College, 84 p.
 74. Suleimani, E., Nicolsky, D.J., Haeussler, P.J. and Hansen, R., 2011. Combined effects of tectonic and landslide-generated tsunami runup at Seward, Alaska during the Mw 9.2 1964 earthquake. *Pure and applied geophysics*, 168(6-7), pp.1053-1074.
 75. Uhlmann, M., Korup, O., Huggel, C., Fischer, L. and Kargel, J.S., 2013. Supra-glacial deposition and flux of catastrophic rock–slope failure debris, south-central Alaska. *Earth Surface Processes and Landforms*, 38(7), pp.675-682.
 76. Wood, N.J. and Peters, J., 2015. Variations in population vulnerability to tectonic and landslide-related tsunami hazards in Alaska. *Natural Hazards*, 75(2), pp.1811-1831.

Appendix A – Mann-Kendall Results

ID	STATION NAME	LONGITUDE	LATITUDE	ELEVATION (M)	START YEAR	END YEAR
0	Agassiz CDA	-121.76	49.24	15	1890	2006

MONTH	MEAN MAX TEMP TAU	MEAN MAX TEMP P	MEAN MIN TEMP TAU	MEAN MIN TEMP P	MEAN TEMP TAU	MEAN TEMP P	EXTR MAX TEMP TAU	EXTR MAX TEMP P	EXTR MIN TEMP TAU	EXTR MIN TEMP P	TOTAL RAIN TAU	TOTAL RAIN P	TOTAL SNOW TAU	TOTAL SNOW P	TOTAL PRECIP TAU	TOTAL PRECIP P
JAN	0.139	0.026	0.188	0.003	0.160	0.011	0.205	0.001	0.157	0.012	0.202	0.001	-0.055	0.381	0.160	0.010
FEB	0.201	0.001	0.272	<0.001	0.241	<0.001	0.165	0.009	0.196	0.002	0.091	0.147	-0.109	0.092	0.009	0.893
MAR	0.005	0.936	0.307	<0.001	0.128	0.044	-0.007	0.910	0.172	0.007	0.097	0.122	-0.082	0.215	0.073	0.245
APR	-0.113	0.076	0.414	<0.001	0.113	0.077	0.000	0.998	0.155	0.018	0.080	0.204	-0.034	0.648	0.080	0.204
MAY	-0.187	0.003	0.404	<0.001	0.084	0.189	-0.047	0.468	0.271	<0.001	-0.115	0.070	-0.098	0.207	-0.110	0.083
JUN	-0.196	0.002	0.499	<0.001	0.167	0.009	-0.108	0.093	0.376	<0.001	-0.055	0.386	na	na	-0.055	0.386
JUL	-0.177	0.005	0.523	<0.001	0.121	0.057	-0.101	0.115	0.405	<0.001	0.051	0.418	na	na	0.050	0.428
AUG	-0.158	0.013	0.525	<0.001	0.192	0.003	-0.099	0.122	0.378	<0.001	0.050	0.425	na	na	0.055	0.381
SEPT	-0.011	0.869	0.426	<0.001	0.281	<0.001	-0.018	0.776	0.428	<0.001	-0.115	0.067	na	na	-0.112	0.075
OCT	-0.173	0.006	0.345	<0.001	0.099	0.121	0.036	0.576	0.171	0.008	0.070	0.264	-0.024	0.761	0.066	0.298
NOV	-0.041	0.522	0.275	<0.001	0.111	0.081	-0.028	0.669	0.133	0.037	0.104	0.099	-0.098	0.147	0.095	0.133
DEC	0.033	0.605	0.198	0.002	0.114	0.070	0.133	0.037	0.032	0.615	0.077	0.215	0.008	0.905	0.074	0.236

ID	STATION NAME	LONGITUDE	LATITUDE	ELEVATION (M)	START YEAR	END YEAR
1	Anchorage	-150.0278	61.169	36.6	1954	2016

MONTH	MEAN MAX TEMP TAU	MEAN MAX TEMP P	MEAN MIN TEMP TAU	MEAN MIN TEMP P	MEAN TEMP TAU	MEAN TEMP P	EXTR MAX TEMP TAU	EXTR MAX TEMP P	EXTR MIN TEMP TAU	EXTR MIN TEMP P	PRCP TAU	PRCP P	SNOW TAU	SNOW P
JAN	0.141	0.104	0.224	0.010	0.183	0.035	0.110	0.218	0.247	0.005	-0.036	0.678	0.045	0.606
FEB	0.194	0.026	0.279	0.001	0.238	0.006	0.155	0.084	0.267	0.002	-0.072	0.410	-0.071	0.413
MAR	0.128	0.138	0.198	0.021	0.203	0.019	0.051	0.568	0.193	0.026	0.102	0.237	0.072	0.407
APR	0.218	0.012	0.236	0.006	0.236	0.006	0.195	0.026	0.060	0.493	-0.103	0.230	-0.120	0.167
MAY	0.215	0.013	0.245	0.005	0.237	0.006	0.190	0.031	0.217	0.016	-0.008	0.926	0.070	0.485
JUN	0.223	0.010	0.112	0.196	0.143	0.100	0.072	0.415	0.120	0.182	0.100	0.244	na	na
JUL	0.117	0.179	0.344	<0.001	0.226	0.009	-0.070	0.435	0.396	<0.001	-0.004	0.963	na	na
AUG	0.139	0.109	0.323	<0.001	0.258	0.003	0.091	0.305	0.344	<0.001	0.109	0.205	na	na
SEPT	0.124	0.155	0.291	0.001	0.247	0.004	0.004	0.972	0.137	0.124	0.166	0.054	0.066	0.514
OCT	0.142	0.100	0.229	0.008	0.179	0.039	0.067	0.452	0.226	0.009	0.045	0.606	-0.151	0.081
NOV	0.062	0.476	0.123	0.152	0.099	0.254	0.005	0.958	0.140	0.109	0.011	0.899	0.033	0.702
DEC	0.206	0.018	0.252	0.004	0.235	0.007	0.175	0.049	0.357	<0.001	0.048	0.585	0.108	0.213

ID	STATION NAME	LONGITUDE	LATITUDE	ELEVATION (M)	START YEAR	END YEAR
2	Atlin	-133.7	59.57	673.6	1967	2006

MONTH	MEAN MAX TEMP TAU	MEAN MAX TEMP P	MEAN MIN TEMP TAU	MEAN MIN TEMP P	MEAN TEMP TAU	MEAN TEMP P	EXTR MAX TEMP TAU	EXTR MAX TEMP P	EXTR MIN TEMP TAU	EXTR MIN TEMP P	TOTAL RAIN TAU	TOTAL RAIN P	TOTAL SNOW TAU	TOTAL SNOW P	TOTAL PRECIP TAU	TOTAL PRECIP P
JAN	0.276	0.012	0.322	0.003	0.302	0.006	0.089	0.430	0.275	0.013	0.103	0.408	0.127	0.247	0.129	0.238
FEB	0.101	0.363	0.206	0.059	0.171	0.118	0.071	0.528	0.266	0.016	-0.098	0.449	0.035	0.753	0.034	0.762
MAR	0.084	0.456	0.155	0.165	0.140	0.208	0.136	0.232	0.154	0.172	0.072	0.574	0.067	0.552	0.071	0.529
APR	0.326	0.003	0.272	0.014	0.347	0.002	0.361	0.001	0.091	0.424	0.165	0.152	0.005	0.972	-0.006	0.963
MAY	0.288	0.010	0.419	<0.001	0.371	0.001	0.223	0.047	0.177	0.124	0.040	0.727	-0.087	0.491	0.030	0.798
JUN	0.353	0.002	0.481	<0.001	0.419	<0.001	0.433	<0.001	0.469	<0.001	0.089	0.428	0.017	0.931	0.090	0.421
JUL	0.324	0.004	0.446	<0.001	0.409	<0.001	0.179	0.112	0.422	<0.001	0.096	0.389	na	na	0.096	0.389
AUG	0.223	0.045	0.387	0.001	0.329	0.003	0.147	0.197	0.072	0.534	-0.008	0.954	na	na	-0.008	0.954
SEP	0.190	0.090	0.250	0.025	0.240	0.031	0.033	0.778	0.101	0.378	0.164	0.139	-0.106	0.406	0.105	0.345
OCT	0.152	0.172	0.137	0.221	0.163	0.145	0.276	0.015	-0.085	0.455	0.023	0.843	-0.034	0.771	-0.058	0.608
NOV	0.042	0.717	0.107	0.339	0.077	0.492	-0.020	0.870	0.055	0.624	-0.079	0.497	0.098	0.382	0.041	0.718
DEC	0.272	0.014	0.284	0.011	0.286	0.010	0.205	0.070	0.230	0.040	0.170	0.159	0.257	0.020	0.264	0.017

ID	STATION NAME	LONGITUDE	LATITUDE	ELEVATION (M)	START YEAR	END YEAR
3	Barrow	-156.7815	71.2834	9.4	1944	2016

MO NTH	MEAN MAX TEMP TAU	MEAN MAX TEMP P	MEAN MIN TEMP TAU	MEAN MIN TEMP P	MEAN TEMP TAU	MEAN TEMP P	EXTR MAX TEMP TAU	EXTR MAX TEMP P	EXTR MIN TEMP TAU	EXTRMIN TEMP P	PRCP TAU	PRC P P	SNOW TAU	SNO W P
JAN	0.158	0.049	0.169	0.035	0.175	0.030	0.009	0.913	0.122	0.133	-0.067	0.404	0.180	0.025
FEB	0.288	<0.001	0.321	<0.001	0.310	<0.001	0.116	0.153	0.176	0.031	0.035	0.665	0.210	0.009
MAR	0.157	0.052	0.179	0.028	0.174	0.032	0.082	0.319	0.170	0.038	-0.069	0.402	0.103	0.203
APR	0.199	0.014	0.288	<0.001	0.239	0.003	0.050	0.542	0.235	0.004	-0.001	0.992	0.186	0.021
MAY	0.300	<0.001	0.371	<0.001	0.355	<0.001	0.268	0.001	0.156	0.055	0.197	0.014	0.205	0.011
JUN	0.436	<0.001	0.443	<0.001	0.453	<0.001	0.208	0.011	0.251	0.002	0.073	0.363	0.119	0.152
JUL	0.257	0.001	0.361	<0.001	0.297	<0.001	0.057	0.492	0.311	<0.001	0.060	0.460	-0.060	0.500
AUG	0.162	0.044	0.194	0.016	0.186	0.021	0.042	0.613	0.165	0.047	-0.034	0.675	0.047	0.572
SEPT	0.275	0.001	0.271	0.001	0.264	0.001	0.181	0.026	0.119	0.144	0.138	0.085	0.145	0.071
OCT	0.255	0.002	0.279	0.001	0.266	0.001	0.068	0.413	0.169	0.037	-0.096	0.234	0.213	0.008
NOV	0.178	0.027	0.188	0.019	0.180	0.025	0.098	0.231	0.084	0.303	0.105	0.192	0.340	<0.001
DEC	0.278	0.001	0.283	<0.001	0.282	<0.001	0.077	0.345	0.168	0.040	-0.038	0.644	0.349	<0.001

ID STATION LONGITUDE LATITUDE ELEVATION (M) START YEAR END YEAR
NAME

4 | **Bella Coola** | **-126.69** | **52.37** | **18.3** | **1895** | **2002**

MO NT H	MEAN MAX TEMP TAU	MEAN MAX TEMP P	MEAN MIN TEMP TAU	MEAN MIN TEMP P	MEAN TEMP TAU	MEAN TEMP P	EXTR MAX TEMP TAU	EXTR MAX TEMP P	EXTR MIN TEMP TAU	EXTR MIN TEMP P	TOTAL RAIN TAU	TOTAL RAIN P	TOTAL SNOW TAU	TOTAL SNOW P	TOTAL PRECIP TAU	TOTAL PRECIP P
JAN	0.169	0.015	0.152	0.029	0.160	0.022	0.237	0.001	0.173	0.013	0.199	0.004	-0.057	0.416	0.163	0.019
FEB	0.232	0.001	0.232	0.001	0.247	<0.001	0.177	0.010	0.267	<0.001	0.249	<0.001	-0.067	0.318	0.227	0.001
MAR	0.252	<0.001	0.248	<0.001	0.263	<0.001	0.079	0.254	0.141	0.043	0.158	0.017	-0.131	0.051	0.094	0.153
APR	0.136	0.044	0.278	<0.001	0.247	<0.001	0.024	0.723	0.176	0.011	0.232	<0.001	-0.081	0.288	0.225	0.001
MAY	-0.005	0.944	0.350	<0.001	0.163	0.016	-0.054	0.433	0.194	0.005	0.093	0.160	NA	NA	0.093	0.160
JUN	-0.036	0.593	0.381	<0.001	0.138	0.041	-0.071	0.297	0.264	<0.001	0.155	0.019	NA	NA	0.155	0.019
JUL	-0.045	0.504	0.419	<0.001	0.122	0.070	-0.099	0.146	0.231	0.001	0.102	0.120	NA	NA	0.102	0.120
AUG	-0.069	0.305	0.448	<0.001	0.134	0.049	-0.104	0.127	0.244	0.001	0.078	0.238	NA	NA	0.078	0.238
SEP	-0.016	0.810	0.309	<0.001	0.181	0.007	-0.132	0.052	0.152	0.027	0.075	0.261	NA	NA	0.075	0.261
OCT	-0.023	0.729	0.167	0.013	0.093	0.170	0.009	0.896	0.056	0.422	0.196	0.003	-0.080	0.306	0.197	0.003
NOV	0.048	0.478	0.031	0.648	0.050	0.467	-0.015	0.830	0.002	0.977	0.127	0.056	0.135	0.050	0.121	0.068
DEC	0.057	0.403	0.010	0.889	0.048	0.481	0.011	0.878	-0.017	0.807	0.111	0.095	0.189	0.005	0.167	0.012

ID STATION LONGITUDE LATITUDE ELEVATION (M) START YEAR END YEAR
 NAME

5 Boat Bluff -128.52 52.64 10.7 1975 2007

MO NT H	MEAN MAX TEMP TAU	MEAN MAX TEMP P	MEAN MIN TEMP TAU	MEAN MIN TEMP P	MEAN TEMP TAU	MEAN TEMP P	EXTR MAX TEMP TAU	EXTR MAX TEMP P	EXTR MIN TEMP TAU	EXTR MIN TEMP P	TOTAL RAIN TAU	TOTAL RAIN P	TOTAL SNOW TAU	TOTAL SNOW P	TOTAL PRECIP TAU	TOTAL PRECIP P
JAN	0.120	0.363	0.093	0.486	0.093	0.486	0.205	0.123	0.049	0.721	0.301	0.013	-0.089	0.508	0.246	0.044
FEB	0.098	0.454	0.097	0.454	0.107	0.414	0.016	0.918	0.232	0.074	-0.191	0.135	-0.059	0.665	-0.196	0.126
MAR	-0.055	0.681	-0.058	0.668	-0.065	0.630	-0.120	0.370	-0.135	0.315	0.044	0.748	0.021	0.886	0.067	0.617
APR	0.174	0.186	0.155	0.239	0.130	0.326	0.289	0.029	-0.034	0.813	0.067	0.617	-0.203	0.154	0.076	0.568
MAY	0.152	0.246	0.093	0.486	0.132	0.317	-0.072	0.592	0.045	0.747	-0.078	0.556	0.205	0.204	-0.078	0.556
JUN	0.076	0.568	0.205	0.120	0.125	0.344	0.207	0.116	0.129	0.346	-0.067	0.617	na	na	-0.067	0.617
JUL	-0.041	0.759	0.116	0.376	-0.011	0.946	0.066	0.621	0.212	0.112	0.123	0.341	na	na	0.123	0.341
AUG	-0.039	0.772	0.136	0.298	-0.011	0.946	0.002	1.000	0.279	0.034	0.153	0.234	na	na	0.153	0.234
SEP	-0.107	0.414	-0.072	0.585	-0.120	0.358	-0.227	0.082	0.018	0.905	-0.041	0.760	na	na	-0.041	0.760
OCT	0.104	0.424	-0.094	0.474	0.031	0.825	-0.064	0.633	-0.142	0.281	0.195	0.114	0.024	0.894	0.188	0.129
NOV	0.100	0.453	-0.037	0.789	0.021	0.886	0.085	0.538	0.019	0.900	0.156	0.209	0.158	0.248	0.148	0.233
DEC	0.313	0.017	0.188	0.153	0.249	0.058	0.299	0.024	0.144	0.276	0.175	0.158	0.060	0.656	0.246	0.047

ID	STATION NAME	LONGITUDE	LATITUDE	ELEVATION (M)	START YEAR	END YEAR
6	Chatham Point	-125.45	50.33	22.9	1959	2007

MONTH	MEAN MAX TEMP TAU	MEAN MAX TEMP P	MEAN MIN TEMP TAU	MEAN MIN TEMP P	MEAN TEMP TAU	MEAN TEMP P	EXTR MAX TEMP TAU	EXTR MAX TEMP P	EXTR MIN TEMP TAU	EXTR MIN TEMP P	TOTAL RAIN TAU	TOTAL RAIN P	TOTAL SNOW TAU	TOTAL SNOW P	TOTAL PRECIP TAU	TOTAL PRECIP P
JAN	0.264	0.008	0.271	0.007	0.269	0.007	0.215	0.032	0.150	0.133	0.181	0.068	-0.267	0.008	0.128	0.199
FEB	0.063	0.534	0.069	0.496	0.080	0.427	0.051	0.616	0.003	0.986	-0.037	0.711	-0.035	0.738	-0.030	0.769
MAR	0.202	0.046	0.276	0.006	0.249	0.014	0.060	0.557	0.202	0.046	0.194	0.053	-0.191	0.069	0.184	0.066
APR	0.230	0.023	0.251	0.014	0.266	0.009	0.171	0.089	0.047	0.649	0.239	0.017	-0.261	0.027	0.202	0.044
MAY	0.093	0.359	0.316	0.002	0.208	0.041	0.066	0.516	0.211	0.039	0.134	0.182	na	na	0.134	0.182
JUN	0.085	0.403	0.270	0.008	0.164	0.107	0.077	0.450	0.098	0.340	0.088	0.384	na	na	0.088	0.384
JUL	-0.086	0.393	0.280	0.006	0.037	0.717	-0.104	0.300	0.134	0.191	0.026	0.796	na	na	0.026	0.796
AUG	0.067	0.506	0.259	0.010	0.148	0.140	-0.043	0.673	0.170	0.095	-0.094	0.343	na	na	-0.094	0.343
SEP	0.131	0.195	0.268	0.008	0.192	0.056	-0.037	0.717	0.264	0.009	-0.123	0.214	na	na	-0.123	0.214
OCT	-0.055	0.586	0.125	0.214	0.026	0.802	-0.056	0.581	-0.079	0.432	-0.009	0.938	0.060	0.623	-0.009	0.938
NOV	0.092	0.360	0.151	0.133	0.122	0.224	0.058	0.569	0.103	0.304	0.225	0.023	-0.076	0.479	0.233	0.019
DEC	0.073	0.469	0.116	0.248	0.103	0.304	0.009	0.936	0.096	0.338	0.117	0.241	-0.159	0.113	0.039	0.698
ALL	0.018	0.508	0.051	0.068	0.032	0.254	0.012	0.663	0.032	0.246	0.048	0.086	-0.070	0.025	0.035	0.207

ID STATION LONGITUDE LATITUDE ELEVATION (M) START YEAR END YEAR
 NAME

7 Cordova -145.45 60.49 9.4 1909 2016

MO NT H	MEAN MAX TEMP TAU	MEAN MAX TEMP P	MEAN MIN TEMP TAU	MEAN MIN TEMP P	MEAN TEMP TAU	MEAN TEMP P	EXTR MAX TEMP TAU	EXTR MAX TEMP P	EXTR MIN TEMP TAU	EXTRMI N TEMP P	TOTAL RAIN TAU	TOTAL RAIN P	GREATEST PRECIP TAU	GREATEST PRECIP P	TOTAL SNOW TAU	TOTAL SNOW P
JAN	0.082	0.230	-0.040	0.553	0.012	0.863	0.211	0.002	-0.161	0.019	-0.098	0.148	-0.135	0.046	-0.256	<0.001
FEB	0.038	0.579	-0.077	0.256	-0.030	0.658	0.160	0.021	-0.094	0.166	-0.133	0.048	-0.169	0.012	-0.230	0.001
MAR	-0.007	0.920	-0.103	0.129	-0.071	0.295	0.060	0.393	-0.063	0.361	-0.183	0.007	-0.193	0.004	-0.215	0.002
APR	0.122	0.073	-0.075	0.272	0.041	0.547	0.205	0.003	-0.096	0.164	-0.237	<0.001	-0.193	0.004	-0.094	0.171
MAY	0.203	0.003	-0.059	0.390	0.109	0.109	0.319	<0.001	-0.258	<0.001	-0.205	0.002	-0.229	0.001	0.056	0.460
JUN	0.057	0.403	-0.110	0.108	-0.013	0.855	0.168	0.015	-0.229	0.001	-0.026	0.696	-0.093	0.170	0.010	0.897
JUL	0.058	0.391	-0.140	0.038	-0.056	0.407	0.087	0.200	-0.333	<0.001	-0.123	0.064	-0.184	0.006	0.007	0.925
AUG	0.121	0.074	-0.205	0.002	-0.024	0.728	0.222	0.001	-0.353	<0.001	-0.138	0.039	-0.165	0.014	0.053	0.490
SEP	-0.008	0.914	-0.249	<0.001	-0.138	0.042	0.028	0.693	-0.363	<0.001	-0.127	0.057	-0.192	0.004	0.054	0.483
OCT	0.002	0.984	-0.234	0.001	-0.138	0.041	0.030	0.670	-0.275	<0.001	-0.281	<0.001	-0.211	0.002	-0.080	0.249
NOV	-0.102	0.130	-0.218	0.001	-0.171	0.011	0.008	0.914	-0.244	<0.001	-0.224	0.001	-0.255	<0.001	0.017	0.801
DEC	0.050	0.463	-0.061	0.367	-0.018	0.792	0.105	0.133	-0.154	0.023	-0.126	0.061	-0.142	0.035	-0.193	0.004

ID STATION LONGITUDE LATITUDE ELEVATION (M) START YEAR END YEAR
 NAME

8 | **Egg Island** | **-127.84** | **51.25** | **14** | **1966** | **2007**

MO NT H	MEAN MAX TEMP TAU	MEAN MAX TEMP P	MEAN MIN TEMP TAU	MEAN MIN TEMP P	MEAN TEMP TAU	MEAN TEMP P	EXTR MAX TEMP TAU	EXTR MAX TEMP P	EXTR MIN TEMP TAU	EXTR MIN TEMP P	TOTAL RAIN TAU	TOTAL RAIN P	TOTAL SNOW TAU	TOTAL SNOW P	TOTAL PRECIP TAU	TOTAL PRECIP P
JAN	0.274	0.011	0.312	0.004	0.302	0.005	0.312	0.004	0.199	0.067	0.052	0.633	-0.298	0.007	-0.006	0.965
FEB	0.040	0.720	0.040	0.720	0.043	0.696	-0.029	0.795	-0.002	0.991	-0.052	0.633	-0.050	0.663	-0.069	0.530
MAR	0.196	0.077	0.190	0.085	0.171	0.121	0.128	0.247	0.234	0.034	0.160	0.144	0.057	0.637	0.107	0.328
APR	0.444	<0.001	0.356	0.001	0.434	<0.001	0.313	0.005	0.326	0.003	0.078	0.479	-0.202	0.109	0.061	0.582
MAY	0.356	0.001	0.344	0.002	0.349	0.002	0.005	0.973	0.180	0.105	-0.046	0.678	0.188	0.163	-0.046	0.678
JUN	0.456	<0.001	0.310	0.005	0.405	<0.001	0.211	0.057	0.095	0.398	0.048	0.670	na	na	0.048	0.670
JUL	0.405	<0.001	0.311	0.005	0.395	<0.001	0.216	0.050	0.462	<0.001	0.031	0.787	na	na	0.031	0.787
AUG	0.249	0.027	0.225	0.046	0.229	0.043	0.183	0.102	0.108	0.338	0.059	0.600	na	na	0.059	0.600
SEP	0.096	0.403	0.136	0.235	0.126	0.270	0.150	0.191	0.107	0.350	-0.188	0.095	na	na	-0.188	0.095
OCT	0.089	0.424	0.165	0.137	0.121	0.279	-0.061	0.589	0.019	0.875	0.044	0.694	0.114	0.397	0.044	0.694
NOV	0.001	1.000	0.068	0.544	0.035	0.761	-0.014	0.910	0.141	0.204	0.195	0.074	-0.017	0.902	0.193	0.078
DEC	0.195	0.072	0.238	0.028	0.227	0.036	0.228	0.036	0.209	0.055	0.040	0.721	-0.168	0.130	0.014	0.905
ALL	0.056	0.064	0.059	0.053	0.057	0.059	0.056	0.065	0.052	0.088	0.029	0.336	-0.026	0.451	0.014	0.638

ID	STATION NAME	LONGITUDE	LATITUDE	ELEVATION (M)	START YEAR	END YEAR
9	Germansen Landing	-124.7	55.79	766	1952	2006

MONTH	MEAN MAX TEMP TAU	MEAN MAX TEMP P	MEAN MIN TEMP TAU	MEAN MIN TEMP P	MEAN TEMP TAU	MEAN TEMP P	EXTR MAX TEMP TAU	EXTR MAX TEMP P	EXTR MIN TEMP TAU	EXTRMIN TEMP P	TOTAL RAIN TAU	TOTAL RAIN P	TOTAL SNOW TAU	TOTAL SNOW P	TOTAL PRECIP TAU	TOTAL PRECIP P
JAN	0.237	0.010	0.256	0.006	0.248	0.007	0.099	0.292	0.153	0.099	0.212	0.037	-0.076	0.412	-0.050	0.591
FEB	0.065	0.484	0.115	0.213	0.090	0.333	-0.112	0.229	0.134	0.149	-0.066	0.500	-0.068	0.467	-0.068	0.467
MAR	0.125	0.181	0.231	0.014	0.189	0.043	0.023	0.816	0.157	0.092	0.188	0.046	0.012	0.908	0.052	0.581
APR	0.327	0.000	0.237	0.012	0.316	0.001	0.208	0.027	0.181	0.054	0.083	0.376	-0.256	0.006	-0.103	0.270
MAY	0.043	0.652	0.247	0.009	0.092	0.327	0.007	0.948	0.173	0.071	0.259	0.005	0.077	0.450	0.309	0.001
JUN	0.229	0.014	0.320	0.001	0.284	0.002	0.177	0.061	0.172	0.073	0.138	0.141	0.042	0.729	0.104	0.267
JUL	0.061	0.518	0.245	0.009	0.145	0.122	0.082	0.387	0.227	0.017	0.079	0.400	na	na	0.079	0.400
AUG	0.138	0.140	0.059	0.537	0.120	0.204	0.120	0.203	0.034	0.721	-0.118	0.206	na	na	-0.045	0.637
SEP	-0.001	1.000	0.169	0.070	0.052	0.581	-0.076	0.416	0.055	0.561	0.101	0.276	0.053	0.613	0.117	0.206
OCT	0.026	0.783	0.113	0.226	0.068	0.470	-0.124	0.184	0.084	0.365	0.204	0.027	0.038	0.682	0.116	0.211
NOV	0.010	0.921	0.074	0.424	0.061	0.511	-0.103	0.269	0.091	0.329	0.047	0.619	-0.074	0.424	-0.008	0.938
DEC	0.136	0.141	0.178	0.054	0.156	0.092	-0.074	0.428	0.191	0.039	-0.081	0.419	-0.064	0.493	-0.079	0.392

ID	STATION NAME	LONGITUDE	LATITUDE	ELEVATION (M)	START YEAR	END YEAR
10	Graham Inlet	-134.18	59.6	659.9	1974	2007

MONTH	MEAN MAX TEMP TAU	MEAN MAX TEMP P	MEAN MIN TEMP TAU	MEAN MIN TEMP P	MEAN TEMP TAU	MEAN TEMP P	EXTR MAX TEMP TAU	EXTR MAX TEMP P	EXTR MIN TEMP TAU	EXTR MIN TEMP P	TOTAL RAIN TAU	TOTAL RAIN P	TOTAL SNOW TAU	TOTAL SNOW P	TOTAL PRECIP TAU	TOTAL PRECIP P
JAN	0.105	0.467	0.151	0.290	0.133	0.354	-0.041	0.797	0.143	0.345	0.040	0.848	-0.062	0.691	-0.062	0.691
FEB	0.174	0.211	0.200	0.150	0.212	0.128	-0.003	1.000	0.231	0.110	-0.043	0.817	-0.160	0.261	-0.136	0.343
MAR	-0.093	0.486	0.051	0.708	0.009	0.957	-0.003	1.000	0.127	0.348	0.056	0.765	-0.079	0.561	-0.074	0.586
APR	0.120	0.347	0.160	0.205	0.142	0.263	0.202	0.114	0.061	0.638	-0.047	0.737	-0.096	0.486	-0.168	0.209
MAY	0.263	0.034	0.268	0.031	0.256	0.039	0.074	0.565	0.138	0.281	0.061	0.631	-0.095	0.507	0.061	0.631
JUN	0.358	0.004	0.375	0.003	0.396	0.001	0.306	0.015	0.398	0.002	0.089	0.476	-0.031	0.875	0.087	0.486
JUL	0.274	0.027	0.331	0.007	0.343	0.006	0.103	0.418	0.384	0.003	0.145	0.250	na	na	0.145	0.250
AUG	0.129	0.292	0.275	0.024	0.276	0.024	0.011	0.941	0.311	0.013	0.010	0.948	na	na	0.010	0.948
SEP	-0.192	0.119	0.264	0.030	0.090	0.467	-0.142	0.252	0.170	0.178	0.253	0.037	-0.153	0.287	0.213	0.080
OCT	-0.011	0.941	0.093	0.449	0.029	0.824	0.098	0.431	-0.060	0.634	-0.125	0.306	0.092	0.458	-0.075	0.543
NOV	-0.051	0.722	0.077	0.573	-0.021	0.890	-0.138	0.341	0.003	1.000	-0.304	0.044	0.032	0.828	-0.122	0.374
DEC	0.253	0.074	0.234	0.098	0.269	0.058	0.176	0.232	0.195	0.183	0.248	0.139	-0.053	0.724	-0.046	0.758
ALL	0.034	0.337	0.054	0.122	0.046	0.191	0.020	0.566	0.036	0.308	0.013	0.717	-0.038	0.316	-0.005	0.890

ID STATION LONGITUDE LATITUDE ELEVATION (M) START YEAR END YEAR
 NAME

11 | Grand Forks -118.47 49.03 531.9 1941 2006

MO NT H	MEAN MAX TEMP TAU	MEAN MAX TEMP P	MEAN MIN TEMP TAU	MEAN MIN TEMP P	MEAN TEMP TAU	MEAN TEMP P	EXTR MAX TEMP TAU	EXTR MAX TEMP P	EXTR MIN TEMP TAU	EXTR MIN TEMP P	TOTAL RAIN TAU	TOTAL RAIN P	TOTAL SNOW TAU	TOTAL SNOW P	TOTAL PRECIP TAU	TOTAL PRECIP P
JAN	0.126	0.137	0.292	0.001	0.219	0.009	-0.083	0.329	0.143	0.089	0.111	0.193	0.050	0.552	0.125	0.137
FEB	0.054	0.523	0.246	0.004	0.175	0.038	-0.114	0.181	0.129	0.128	0.060	0.478	-0.137	0.102	-0.029	0.737
MAR	0.233	0.006	0.373	0.000	0.323	0.000	0.110	0.199	0.308	0.000	0.136	0.107	0.040	0.648	0.176	0.037
APR	-0.034	0.690	0.252	0.003	0.085	0.319	-0.042	0.630	0.202	0.019	0.353	0.000	-0.045	0.649	0.335	0.000
MAY	-0.025	0.769	0.257	0.003	0.073	0.394	0.046	0.595	0.280	0.001	0.209	0.013	0.121	0.248	0.209	0.013
JUN	0.025	0.769	0.282	0.001	0.108	0.209	0.127	0.137	0.250	0.004	0.030	0.727	na	na	0.030	0.727
JUL	-0.106	0.213	0.372	0.000	0.056	0.510	-0.090	0.297	0.366	0.000	0.199	0.018	na	na	0.199	0.018
AUG	0.063	0.458	0.312	0.000	0.199	0.019	0.020	0.820	0.239	0.006	-0.024	0.782	na	na	-0.024	0.782
SEP	-0.026	0.761	0.193	0.024	0.068	0.428	-0.067	0.435	0.173	0.045	0.018	0.838	na	na	0.018	0.838
OCT	-0.040	0.638	0.044	0.606	-0.011	0.899	-0.027	0.756	-0.088	0.307	-0.017	0.846	-0.032	0.751	-0.017	0.842
NOV	-0.018	0.833	0.094	0.273	0.057	0.506	-0.097	0.256	0.031	0.723	0.036	0.670	0.187	0.028	0.125	0.141
DEC	-0.088	0.303	0.101	0.234	0.030	0.723	-0.210	0.014	0.079	0.352	-0.002	0.987	0.058	0.496	0.076	0.370

ID	STATION NAME	LONGITUDE	LATITUDE	ELEVATION (M)	START YEAR	END YEAR
12	Kitimat Townsite	-128.63	54.05	98	1954	2007

MONTH	MEAN MAX TEMP TAU	MEAN MAX TEMP P	MEAN MIN TEMP TAU	MEAN MIN TEMP P	MEAN TEMP TAU	MEAN TEMP P	EXTR MAX TEMP TAU	EXTR MAX TEMP P	EXTR MIN TEMP TAU	EXTR MIN TEMP P	TOTAL RAIN TAU	TOTAL RAIN P	TOTAL SNOW TAU	TOTAL SNOW P	TOTAL PRECIP TAU	TOTAL PRECIP P
JAN	0.206	0.030	0.212	0.026	0.207	0.032	0.126	0.215	0.134	0.172	0.276	0.006	-0.252	0.012	0.001	1.000
FEB	0.152	0.112	0.150	0.113	0.137	0.151	0.116	0.238	0.147	0.126	-0.106	0.269	-0.247	0.012	-0.197	0.045
MAR	0.121	0.212	0.257	0.007	0.192	0.048	-0.050	0.621	0.179	0.064	0.142	0.140	-0.234	0.015	0.051	0.603
APR	0.237	0.015	0.348	0.000	0.299	0.002	0.145	0.152	0.272	0.006	0.048	0.628	-0.136	0.189	0.040	0.688
MAY	0.088	0.367	0.275	0.005	0.168	0.086	-0.013	0.900	0.226	0.024	0.068	0.493	0.224	0.054	0.066	0.503
JUN	0.199	0.039	0.303	0.002	0.279	0.004	0.238	0.015	0.309	0.002	0.072	0.453	na	na	0.072	0.453
JUL	0.097	0.311	0.184	0.055	0.132	0.169	0.008	0.937	0.180	0.068	0.088	0.360	na	na	0.088	0.360
AUG	0.130	0.174	0.132	0.174	0.161	0.097	0.088	0.365	0.105	0.291	-0.002	0.994	na	na	-0.002	0.994
SEP	-0.056	0.560	0.054	0.575	0.002	0.988	-0.122	0.208	-0.046	0.639	-0.014	0.893	na	na	-0.014	0.893
OCT	0.134	0.162	0.148	0.123	0.160	0.097	-0.001	1.000	0.038	0.706	-0.119	0.225	-0.064	0.557	-0.124	0.207
NOV	0.054	0.580	0.098	0.307	0.062	0.522	-0.138	0.161	0.075	0.443	0.066	0.503	-0.042	0.673	0.021	0.834
DEC	0.096	0.320	0.140	0.143	0.116	0.230	0.058	0.568	0.104	0.286	0.085	0.398	-0.178	0.069	-0.069	0.494
ALL	0.031	0.252	0.057	0.034	0.044	0.098	0.007	0.800	0.043	0.112	0.053	0.050	-0.034	0.246	0.003	0.926

ID	STATION NAME	LONGITUDE	LATITUDE	ELEVATION (M)	START YEAR	END YEAR
13	Malibu Jervis Inlet	-123.85	50.17	18	1974	2006

MONTH	MEAN MAX TEMP TAU	MEAN MAX TEMP P	MEAN MIN TEMP TAU	MEAN MIN TEMP P	MEAN TEMP TAU	MEAN TEMP P	EXTR MAX TEMP TAU	EXTR MAX TEMP P	EXTR MIN TEMP TAU	EXTR MIN TEMP P	TOTAL RAIN TAU	TOTAL RAIN P	TOTAL SNOW TAU	TOTAL SNOW P	TOTAL PRECIP TAU	TOTAL PRECIP P
JAN	0.261	0.040	0.258	0.045	0.262	0.043	0.164	0.204	0.009	0.959	0.359	0.004	-0.152	0.230	0.302	0.016
FEB	0.213	0.088	0.034	0.795	0.133	0.298	0.194	0.126	0.191	0.141	-0.212	0.085	-0.142	0.268	-0.265	0.031
MAR	0.054	0.683	0.182	0.158	0.107	0.414	0.044	0.745	-0.002	1.000	0.114	0.377	0.107	0.459	0.133	0.300
APR	0.105	0.416	0.189	0.139	0.173	0.172	0.129	0.313	0.143	0.273	0.230	0.067	-0.239	0.104	0.230	0.067
MAY	0.238	0.060	0.239	0.061	0.234	0.064	0.236	0.066	-0.146	0.265	0.057	0.662	na	na	0.057	0.662
JUN	0.188	0.135	0.178	0.162	0.137	0.284	0.219	0.085	0.200	0.124	-0.020	0.884	na	na	-0.020	0.884
JUL	0.191	0.139	0.187	0.148	0.199	0.122	0.260	0.047	0.258	0.051	0.058	0.659	na	na	0.058	0.659
AUG	0.171	0.185	0.122	0.349	0.161	0.214	0.067	0.619	0.179	0.187	-0.140	0.277	na	na	-0.140	0.277
SEP	0.143	0.251	0.048	0.710	0.091	0.475	0.096	0.446	0.097	0.453	-0.063	0.627	na	na	-0.063	0.627
OCT	0.038	0.768	0.070	0.591	0.064	0.626	0.015	0.913	-0.067	0.613	0.004	0.988	-0.060	0.706	0.004	0.988
NOV	0.163	0.192	0.074	0.570	0.098	0.445	0.057	0.661	0.098	0.453	0.044	0.733	0.072	0.599	0.044	0.733
DEC	0.188	0.132	0.071	0.581	0.112	0.381	0.086	0.503	0.080	0.537	0.057	0.653	-0.057	0.653	0.038	0.768
ALL	0.039	0.254	0.033	0.336	0.040	0.251	0.038	0.269	0.028	0.419	0.033	0.328	-0.011	0.770	0.025	0.464

ID	STATION NAME	LONGITUDE	LATITUDE	ELEVATION (M)	START YEAR	END YEAR
14	McCarthy	-142.996	61.418	381	1984	2016

MONTH	MEAN MAX TEMP TAU	MEAN MAX TEMP P	MEAN MIN TEMP TAU	MEAN MIN TEMP P	MEAN TEMP TAU	MEAN TEMP P	EXTR MAX TEMP TAU	EXTR MAX TEMP P	EXTR MIN TEMP TAU	EXTR MIN TEMP P	TOTAL RAIN TAU	TOTAL RAIN P	GREATEST PRECIP TAU	GREATEST PRECIP P	TOTAL SNOW TAU	TOTAL SNOW P
JAN	-0.161	0.261	-0.086	0.552	-0.108	0.453	-0.192	0.184	0.148	0.300	-0.231	0.103	-0.171	0.233	-0.105	0.467
FEB	0.235	0.091	0.160	0.251	0.174	0.211	-0.041	0.785	0.344	0.014	-0.217	0.118	-0.095	0.504	-0.365	0.008
MAR	-0.027	0.846	-0.121	0.338	-0.083	0.516	0.000	1.000	0.053	0.685	-0.247	0.052	-0.228	0.075	-0.181	0.157
APR	0.103	0.417	0.090	0.485	0.090	0.485	0.079	0.546	0.047	0.720	-0.004	0.987	-0.010	0.948	0.051	0.704
MAY	0.268	0.033	0.273	0.031	0.297	0.019	0.379	0.003	0.131	0.323	0.079	0.538	0.045	0.733	0.231	0.105
JUN	0.204	0.113	0.538	0.000	0.443	0.001	0.170	0.198	0.319	0.018	-0.181	0.158	-0.163	0.208	na	na
JUL	0.016	0.910	0.398	0.002	0.234	0.066	0.166	0.206	0.204	0.119	0.042	0.746	-0.051	0.697	na	na
AUG	0.041	0.759	0.476	0.000	0.285	0.027	0.231	0.078	0.478	0.000	0.041	0.760	-0.100	0.444	na	na
SEPT	-0.063	0.642	0.248	0.058	0.197	0.134	0.026	0.857	0.259	0.051	0.110	0.402	0.109	0.412	0.169	0.245
OCT	0.054	0.113	0.068	0.046	0.060	0.077	0.057	0.098	0.091	0.008	-0.032	0.339	-0.030	0.385	-0.041	0.248
NOV	0.021	0.890	0.029	0.843	0.037	0.797	0.106	0.451	0.187	0.172	-0.032	0.828	0.048	0.737	-0.032	0.828
DEC	-0.254	0.066	-0.205	0.139	-0.214	0.123	-0.232	0.098	0.101	0.478	-0.354	0.010	-0.263	0.058	-0.105	0.453
SUM	0.083	0.517	0.170	0.178	0.120	0.347	0.139	0.293	0.334	0.008	-0.210	0.095	-0.197	0.119	-0.250	0.046
MAR Y	0.054	0.113	0.068	0.046	0.060	0.077	0.057	0.098	0.091	0.008	-0.032	0.339	-0.030	0.385	-0.041	0.248

ID STATION LONGITUDE LATITUDE ELEVATION (M) START YEAR END YEAR
 NAME

15 | StewartA | -129.99 | 55.94 | 7.3 | 1975 | 2007

MO NT H	MEAN MAX TEMP TAU	MEAN MAX TEMP P	MEAN MIN TEMP TAU	MEAN MIN TEMP P	MEAN TEMP TAU	MEAN TEMP P	EXTR MAX TEMP TAU	EXTR MAX TEMP P	EXTR MIN TEMP TAU	EXTR MIN TEMP P	TOTAL RAIN TAU	TOTAL RAIN P	TOTAL SNOW TAU	TOTAL SNOW P	TOTAL PRECIP TAU	TOTAL PRECIP P
JAN	0.023	0.865	0.040	0.757	0.025	0.852	0.096	0.447	-0.017	0.901	0.326	0.008	0.011	0.938	0.138	0.265
FEB	0.067	0.598	0.008	0.963	0.038	0.768	-0.002	1.000	0.032	0.804	-0.125	0.314	0.009	0.951	-0.174	0.159
MAR	0.002	1.000	-0.055	0.673	-0.041	0.758	0.176	0.163	-0.123	0.330	0.194	0.123	0.010	0.948	0.190	0.132
APR	0.254	0.044	0.039	0.770	0.181	0.153	0.208	0.098	0.000	1.000	0.121	0.339	-0.006	0.974	0.077	0.549
MAY	0.170	0.178	0.144	0.256	0.187	0.140	0.112	0.381	-0.055	0.673	-0.097	0.446	0.169	0.279	-0.097	0.446
JUN	0.249	0.048	0.233	0.066	0.238	0.060	0.309	0.014	0.194	0.127	-0.133	0.292	na	na	-0.133	0.292
JUL	-0.026	0.846	0.298	0.020	0.083	0.516	-0.126	0.322	0.229	0.071	0.184	0.144	na	na	0.184	0.144
AUG	0.047	0.721	0.171	0.182	0.090	0.485	-0.122	0.338	-0.125	0.330	0.270	0.031	-0.153	0.330	0.270	0.031
SEP	-0.112	0.380	0.162	0.205	0.053	0.685	-0.232	0.067	0.069	0.592	0.194	0.123	na	na	0.194	0.123
OCT	-0.031	0.825	-0.152	0.240	-0.076	0.563	0.039	0.772	-0.221	0.088	-0.114	0.377	0.179	0.184	-0.093	0.475
NOV	0.037	0.782	0.059	0.649	0.045	0.733	-0.049	0.709	-0.030	0.820	-0.004	0.987	0.113	0.372	-0.018	0.897
DEC	0.248	0.049	0.196	0.119	0.218	0.083	0.181	0.153	0.222	0.077	0.135	0.284	-0.109	0.390	-0.006	0.974
ALL	0.021	0.543	0.020	0.560	0.019	0.588	0.017	0.624	0.003	0.936	0.075	0.029	0.019	0.598	0.049	0.156

ID	STATION NAME	LONGITUDE	LATITUDE	ELEVATION (M)	START YEAR	END YEAR
16	Tatlayoko Lake	-124.41	51.67	870	1930	2005

MONTH	MEAN MAX TEMP TAU	MEAN MAX TEMP P	MEAN MIN TEMP TAU	MEAN MIN TEMP P	MEAN TEMP TAU	MEAN TEMP P	EXTR MAX TEMP TAU	EXTR MAX TEMP P	EXTR MIN TEMP TAU	EXTR MIN TEMP P	TOTAL RAIN TAU	TOTAL RAIN P	TOTAL SNOW TAU	TOTAL SNOW P	TOTAL PRECIP TAU	TOTAL PRECIP P
JAN	0.034	0.670	0.045	0.577	0.045	0.577	0.030	0.711	0.025	0.759	0.022	0.786	-0.028	0.730	0.014	0.858
FEB	0.119	0.135	0.052	0.513	0.094	0.236	0.038	0.644	0.130	0.101	-0.022	0.790	-0.101	0.201	-0.130	0.098
MAR	0.139	0.080	0.091	0.256	0.136	0.088	0.137	0.087	0.056	0.484	0.070	0.384	-0.003	0.974	-0.002	0.985
APR	0.037	0.651	-0.165	0.041	-0.038	0.637	0.061	0.454	-0.086	0.293	0.033	0.684	-0.075	0.347	0.005	0.953
MAY	-0.097	0.233	-0.063	0.442	-0.117	0.153	-0.055	0.501	-0.070	0.395	0.114	0.152	0.080	0.368	0.128	0.107
JUN	-0.038	0.644	-0.114	0.162	-0.058	0.481	-0.024	0.777	-0.099	0.230	-0.004	0.960	-0.141	0.145	-0.005	0.953
JUL	-0.025	0.762	0.024	0.772	-0.003	0.974	-0.138	0.089	0.082	0.316	0.110	0.162	-0.015	0.891	0.110	0.163
AUG	-0.062	0.437	-0.049	0.539	-0.095	0.236	-0.091	0.259	-0.117	0.152	0.086	0.271	na	na	0.086	0.271
SEP	-0.056	0.484	-0.132	0.099	-0.108	0.177	-0.161	0.045	-0.104	0.199	-0.097	0.215	0.047	0.622	-0.093	0.233
OCT	-0.074	0.360	-0.210	0.009	-0.192	0.017	0.020	0.812	-0.092	0.258	0.067	0.392	0.039	0.645	0.050	0.524
NOV	-0.099	0.218	-0.058	0.469	-0.079	0.325	-0.159	0.050	-0.059	0.466	-0.006	0.946	0.103	0.193	0.017	0.833
DEC	-0.087	0.277	-0.079	0.327	-0.090	0.259	-0.122	0.131	-0.051	0.525	-0.128	0.105	-0.043	0.590	-0.109	0.164
ALL	-0.004	0.842	-0.014	0.526	-0.009	0.695	-0.015	0.515	-0.010	0.663	0.014	0.536	0.004	0.854	0.012	0.575

ID STATION LONGITUDE LATITUDE ELEVATION (M) START YEAR END YEAR
 NAME

17 Terrace A -128.58 54.47 217.3 1953 2013

MO NT H	MEAN MAX TEMP TAU	MEAN MAX TEMP P	MEAN MIN TEMP TAU	MEAN MIN TEMP P	MEAN TEMP TAU	MEAN TEMP P	EXTR MAX TEMP TAU	EXTR MAX TEMP P	EXTR MIN TEMP TAU	EXTRMI N TEMP P	TOTAL RAIN TAU	TOTAL RAIN P	TOTAL SNOW TAU	TOTAL SNOW P	TOTAL PRECIP TAU	TOTAL PRECIP P
JAN	0.186	0.043	0.199	0.030	0.202	0.028	0.148	0.110	0.166	0.071	0.255	0.005	-0.061	0.502	0.103	0.257
FEB	0.098	0.286	0.074	0.424	0.083	0.371	0.098	0.291	0.116	0.205	-0.016	0.867	-0.133	0.142	-0.090	0.324
MAR	0.046	0.620	0.113	0.223	0.058	0.531	-0.064	0.487	0.061	0.508	0.192	0.034	-0.081	0.376	0.129	0.155
APR	0.063	0.495	0.114	0.220	0.077	0.408	-0.014	0.885	0.010	0.918	0.080	0.377	-0.069	0.448	0.029	0.754
MAY	0.013	0.890	0.179	0.053	0.092	0.321	-0.049	0.596	0.161	0.083	0.202	0.026	0.075	0.478	0.198	0.029
JUN	0.064	0.485	0.217	0.017	0.155	0.091	0.199	0.029	0.203	0.026	0.116	0.198	na	na	0.116	0.198
JUL	-0.032	0.732	0.213	0.020	0.045	0.629	-0.013	0.888	0.224	0.014	0.033	0.719	na	na	0.033	0.719
AUG	0.118	0.197	0.174	0.057	0.145	0.112	0.119	0.195	0.245	0.008	-0.003	0.975	na	na	-0.003	0.975
SEP	0.004	0.969	0.184	0.044	0.081	0.373	-0.089	0.330	-0.004	0.968	0.059	0.511	-0.065	0.564	0.059	0.511
OCT	-0.004	0.969	-0.023	0.804	-0.008	0.932	0.059	0.524	0.084	0.361	-0.138	0.121	0.068	0.478	-0.144	0.107
NOV	0.074	0.421	0.110	0.227	0.093	0.308	-0.083	0.361	0.131	0.149	-0.025	0.784	0.094	0.298	0.023	0.804
DEC	0.052	0.568	0.083	0.365	0.074	0.421	-0.065	0.481	0.098	0.283	-0.002	0.990	-0.054	0.552	-0.079	0.381
ALL	0.012	0.638	0.028	0.275	0.018	0.477	0.002	0.943	0.032	0.212	0.058	0.020	-0.003	0.923	0.022	0.374

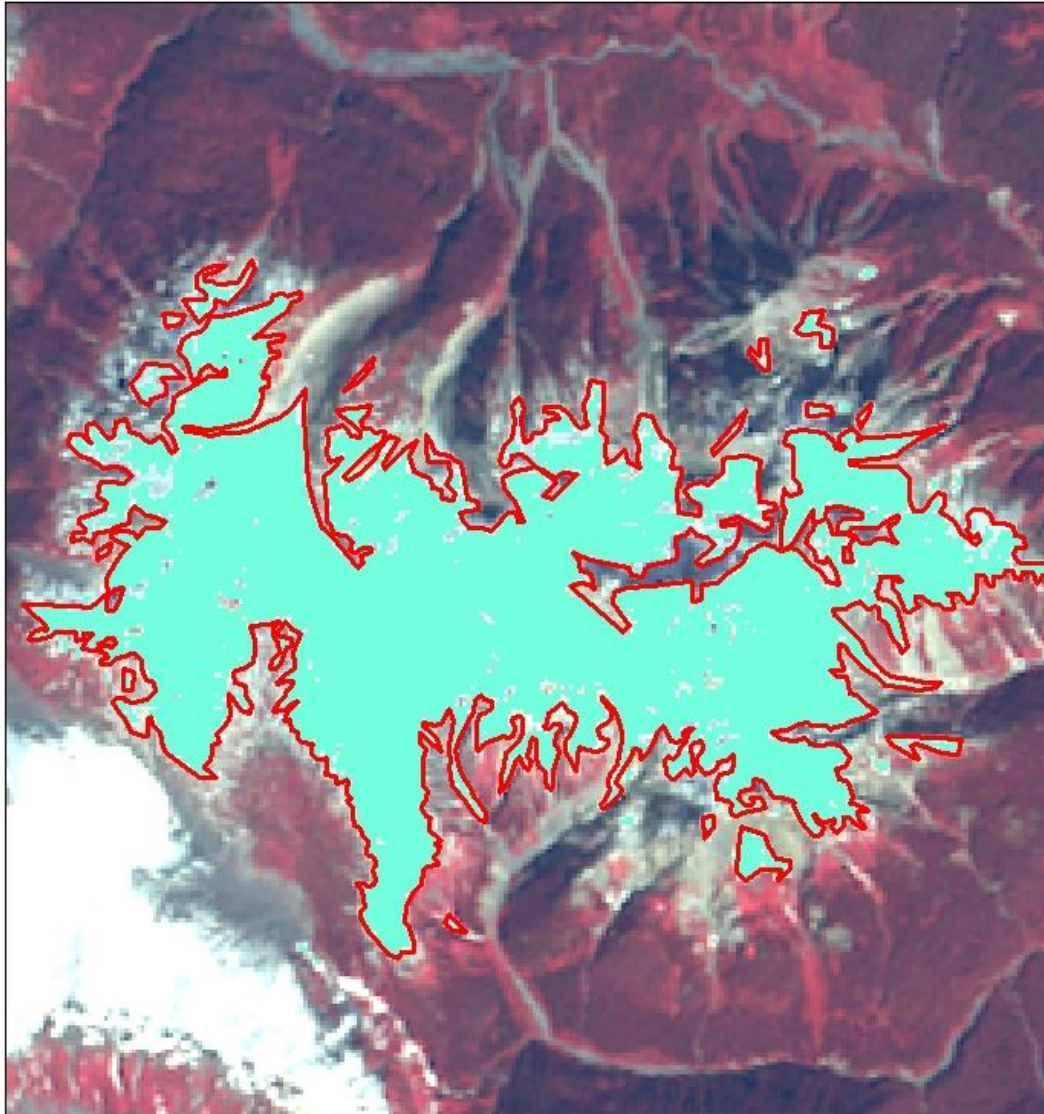
ID STATION LONGITUDE LATITUDE ELEVATION (M) START YEAR END YEAR
 NAME


18 Yakutat -139.671 59.512 10 1917 2016

MON TH	MEAN MAX TEMP TAU	MEAN MAX TEMP P	MEAN MIN TEMP TAU	MEAN MIN TEMP P	MEAN TEMP TAU	MEAN TEMP P	EXTR MAX TEMP TAU	EXTR MAX TEMP P	EXTR MIN TEMP TAU	EXTR MIN TEMP P	TOTAL RAIN TAU	TOTAL RAIN P	GREATEST PRECIP TAU	GREATEST PRECIP P	TOTAL SNOW TAU	TOTAL SNOW P
JAN	0.026	0.714	-0.027	0.697	-0.004	0.962	0.121	0.097	-0.181	0.010	0.092	0.186	0.024	0.728	0.057	0.412
FEB	0.093	0.186	-0.056	0.425	0.010	0.893	0.161	0.026	-0.100	0.156	0.120	0.085	0.070	0.324	0.023	0.749
MAR	0.131	0.064	-0.099	0.160	-0.022	0.756	0.156	0.031	-0.139	0.050	0.020	0.784	-0.025	0.724	0.101	0.151
APR	0.155	0.028	-0.109	12372.000	0.057	0.425	0.231	0.001	-0.125	0.082	0.004	0.953	0.076	0.283	0.064	0.370
MAY	0.196	0.005	0.054	0.448	0.188	0.008	0.237	0.001	0.016	0.833	0.031	0.659	-0.019	0.796	-0.064	0.430
JUN	0.084	0.235	0.105	0.137	0.098	0.165	0.063	0.374	-0.095	0.191	0.121	0.083	0.086	0.217	-0.390	<0.001
JUL	0.183	0.009	0.194	0.006	0.250	<0.001	0.120	0.094	-0.055	0.453	-0.044	0.533	-0.015	0.829	-0.367	<0.001
AUG	0.199	0.005	0.001	0.995	0.198	0.005	0.243	0.001	-0.122	0.094	0.102	0.153	0.164	0.021	-0.368	<0.001
SEPT	0.063	0.379	-0.043	0.550	0.015	0.837	0.140	0.052	-0.175	0.015	0.241	0.001	0.110	0.118	-0.257	0.002
OCT	0.023	0.219	-0.026	0.177	0.010	0.599	0.052	0.007	-0.051	0.008	0.049	0.010	0.045	0.020	-0.014	0.496
NOV	-0.120	0.090	-0.189	0.007	-0.170	0.016	-0.081	0.268	-0.236	0.001	-0.061	0.389	-0.135	0.055	0.185	0.009
DEC	0.056	0.433	-0.045	0.528	-0.002	0.979	0.041	0.574	-0.134	0.058	0.076	0.278	0.128	0.068	0.113	0.107
SUM MAR Y	0.023	0.219	-0.026	0.177	0.010	0.599	0.052	0.007	-0.051	0.008	0.049	0.010	0.045	0.020	-0.014	0.496
ALL	0.023	0.219	-0.026	0.177	0.010	0.599	0.052	0.007	-0.051	0.008	0.049	0.010	0.045	0.020	-0.014	0.496

**Appendix B – Comparison of Manually Digitized and
Automatically Classified Glacier Extents, Mount Meager**

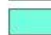
Comparison of Unsupervised Classification and Manual Digitization of Glacial Area
Mt. Meager, British Columbia, Canada (September 13th, 1974)



 Manual Digitizing

Unsupervised Iso Cluster Classification

 Not Glacier (Hollow Symbol)

 Glacier

Landsat 1 MSS

 Band 6

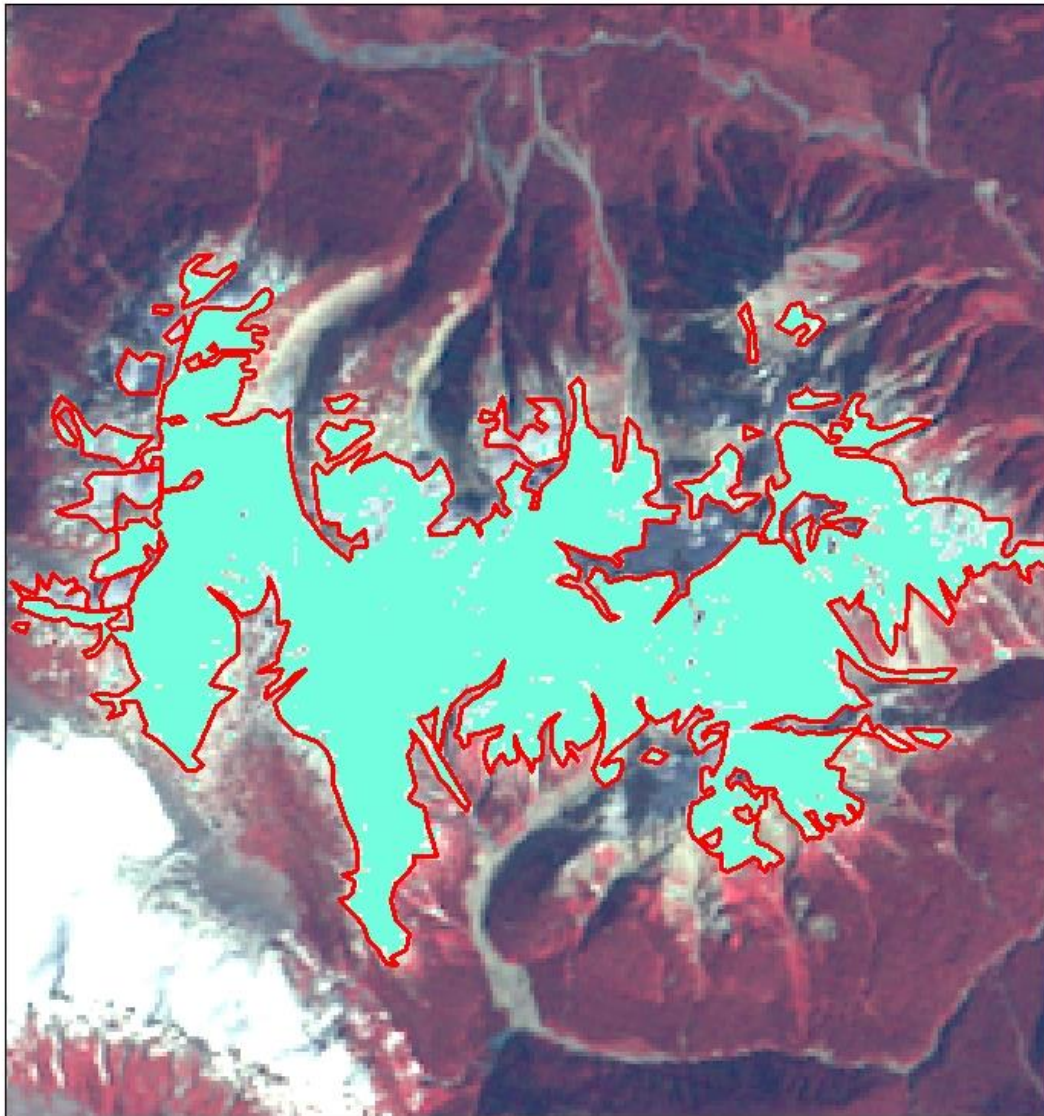
 Band 5


 Band 4

0 1.25 2.5 5 Kilometers

Author: Madison Reid
Date Created: November 20th, 2015
Projection: WGS 84 UTM Zone 10N
Data Sources: United States Geological Survey (1974)

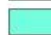
Comparison of Unsupervised Classification and Manual Digitization of Glacial Area
Mt. Meager, British Columbia, Canada (September 20th, 1976)



 Manual Digitizing

Unsupervised Iso Cluster Classification

 Not Glacier (Hollow Symbol)

 Glacier

Landsat 1 MSS

 Band 6

 Band 5

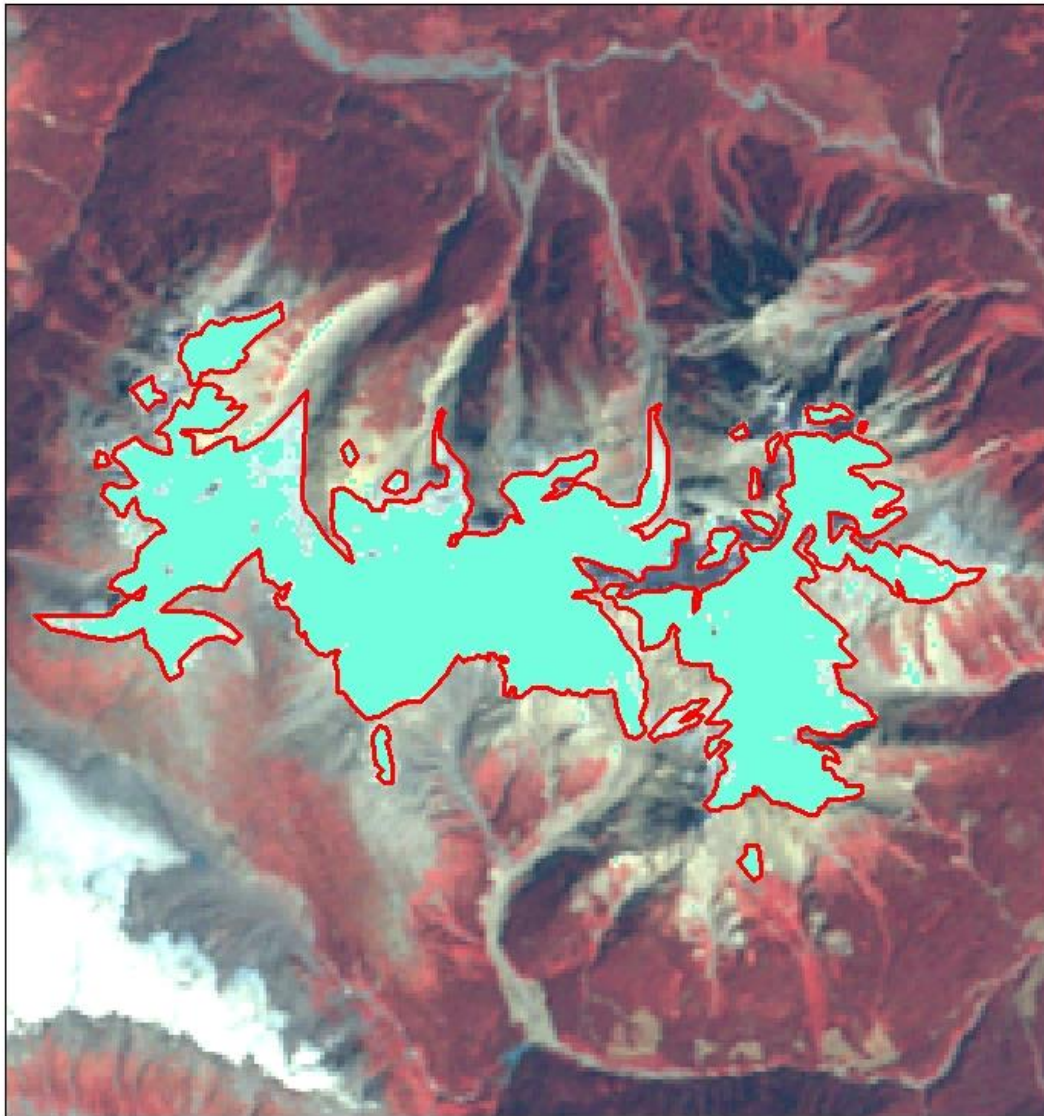
 Band 4


0 1.25 2.5 5 Kilometers



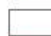
Author: Madison Reid
Date Created: November 20th, 2015
Projection: WGS 84 UTM Zone 10N
Data Sources: United States Geological Survey (1976)

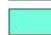
Comparison of Unsupervised Classification and Manual Digitization of Glacial Area
Mt. Meager, British Columbia, Canada (September 14th, 1979)



 Manual Digitizing

Unsupervised Iso Cluster Classification

 Not Glacier (Hollow Symbol)

 Glacier

Landsat 2 MSS

 Band 6

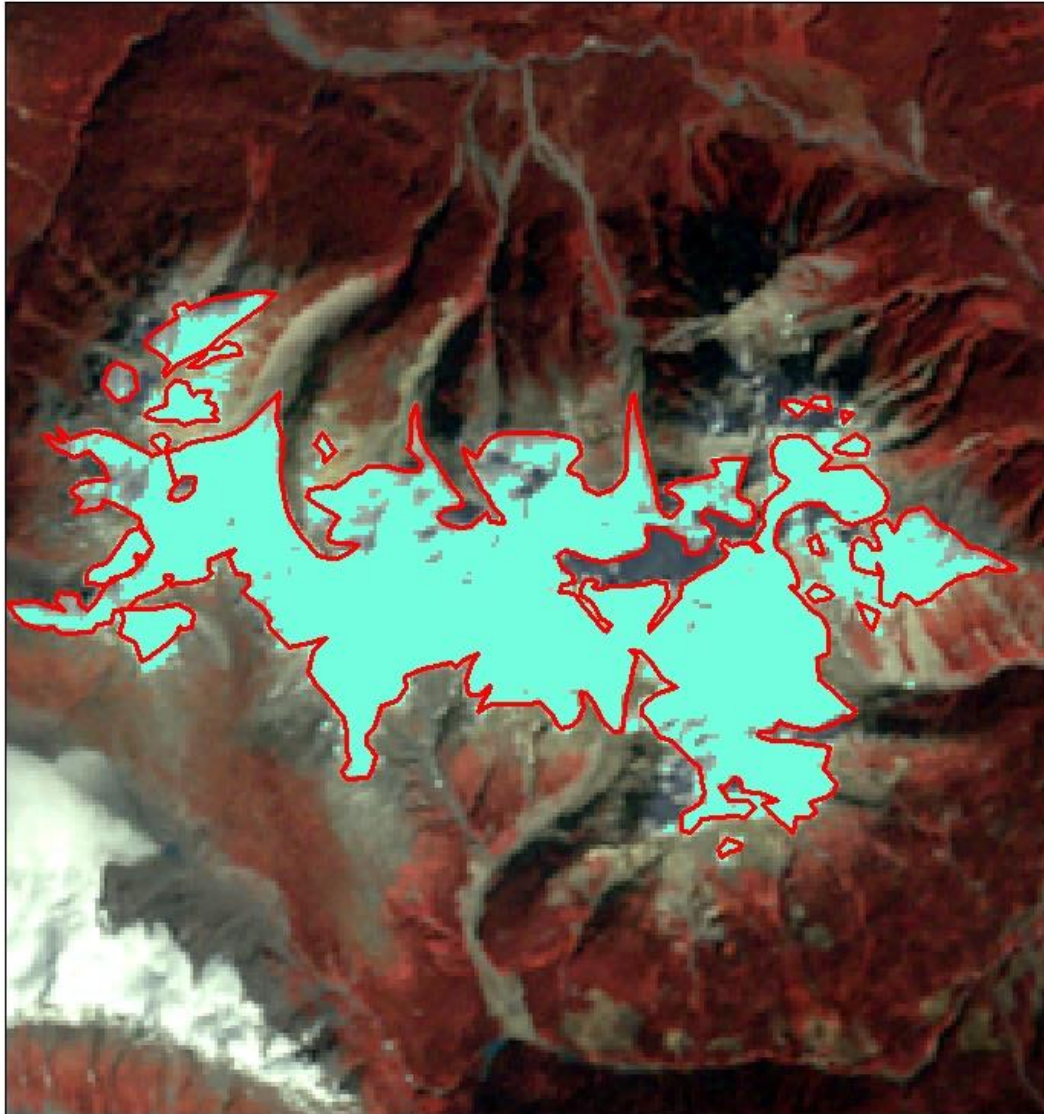
 Band 5


 Band 4

0 1.25 2.5 5 Kilometers

Author: Madison Reid
Date Created: November 20th, 2015
Projection: WGS 84 UTM Zone 10N
Data Sources: United States Geological Survey (1979)


Comparison of Unsupervised Classification and Manual Digitization of Glacial Area
Mt. Meager, British Columbia, Canada (September 25th, 1980)



 Manual Digitizing

Unsupervised Iso Cluster Classification

 Not Glacier (Hollow Symbol)

 Glacier

Landsat 2 MSS

 Band 6

 Band 5

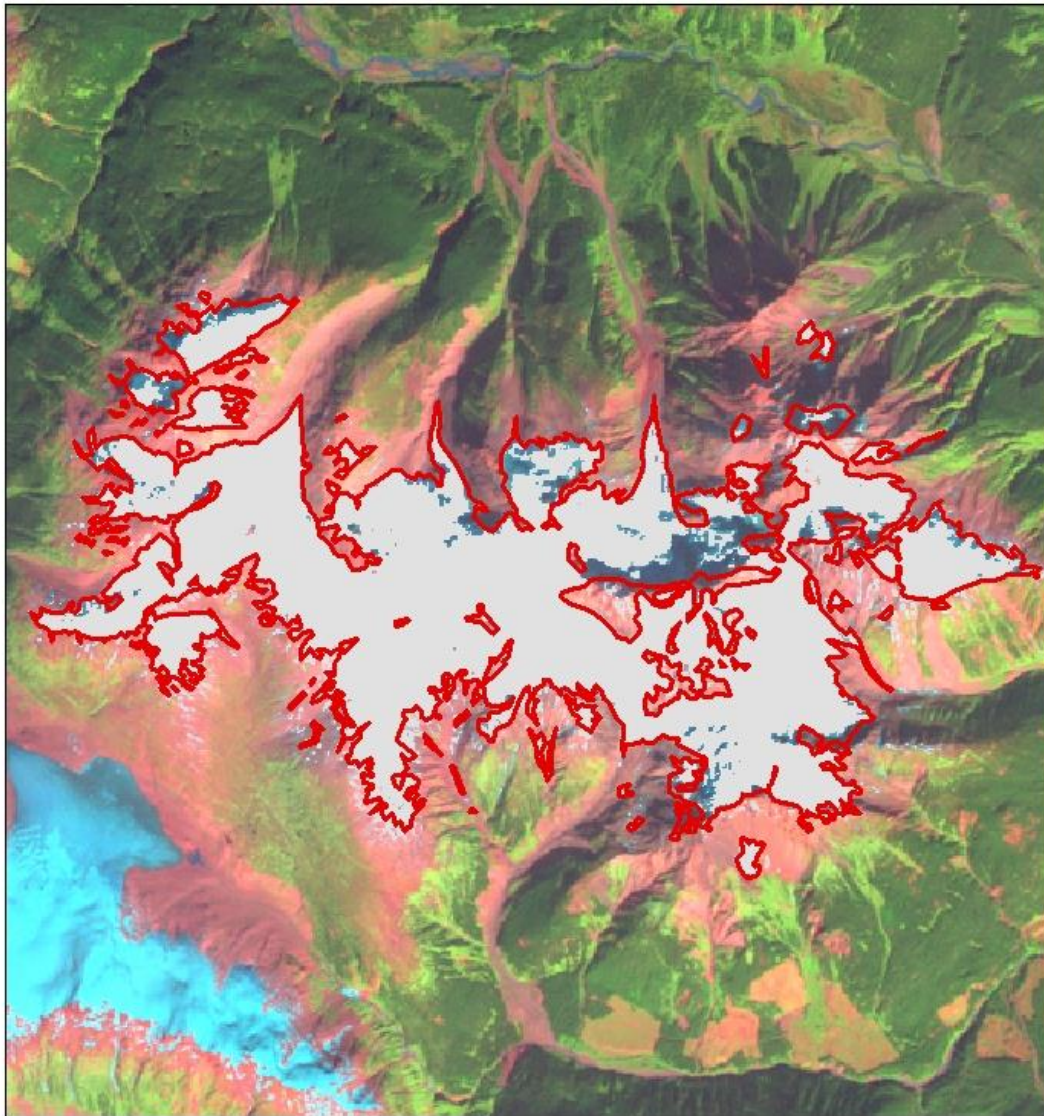
 Band 4


0 1.25 2.5 5 Kilometers




Author: Madison Reid
Date Created: November 20th, 2015
Projection: WGS 84 UTM Zone 10N
Data Sources: United States Geological Survey (1980)

Comparison of Unsupervised Classification and Manual Digitization of Glacial Area Mt. Meager, British Columbia, Canada (September 19th, 1984)



 Manual Digitizing

Unsupervised Iso Cluster Classification

 Not Glacier (Hollow Symbol)

 Glacier

Landsat 5 TM

 Band 7

 Band 4

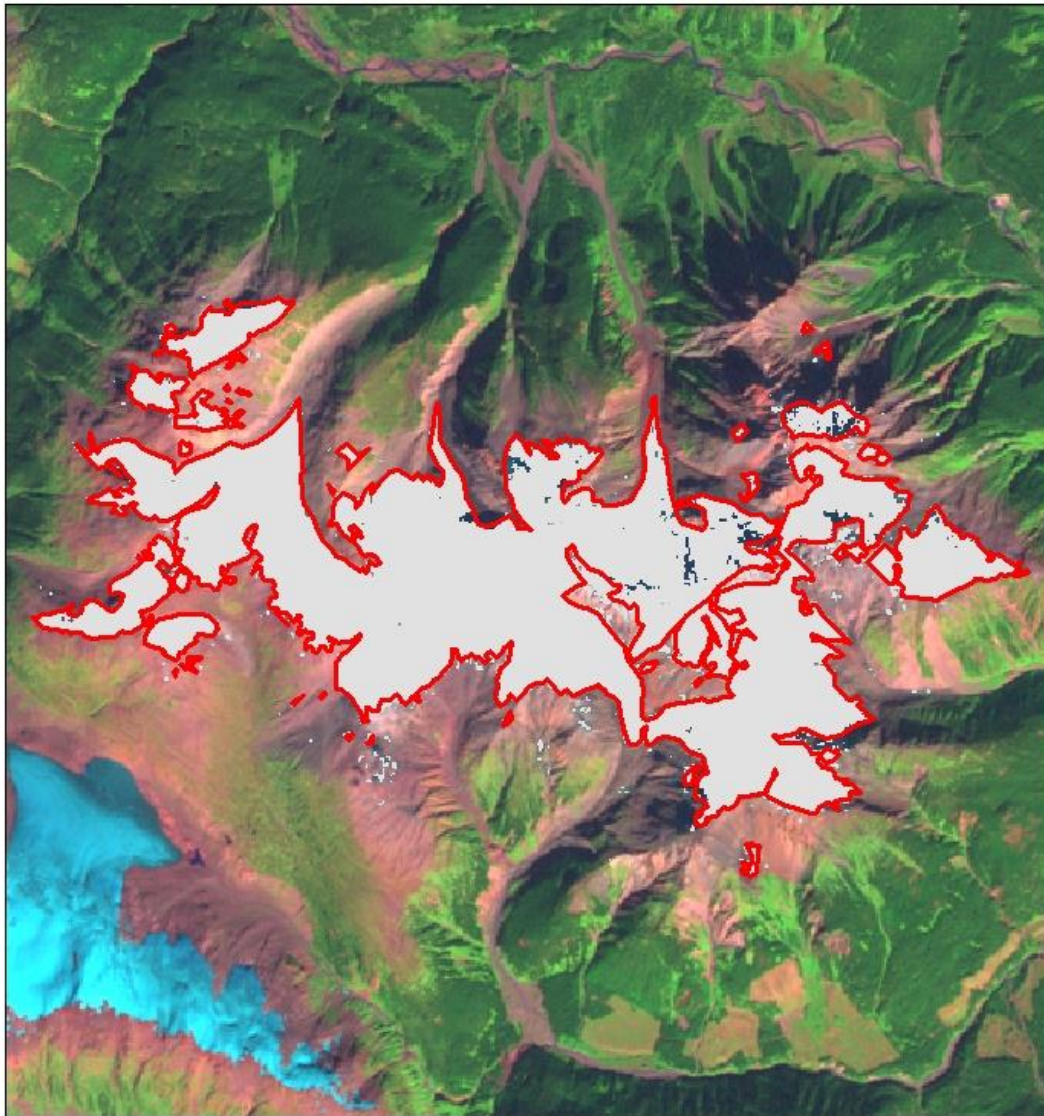
 Band 2


0 1.25 2.5 5 Kilometers



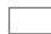
Author: Madison Reid
Date Created: November 20th, 2015
Projection: WGS 84 UTM Zone 10N
Data Sources: United States Geological Survey (1984)

Comparison of Unsupervised Classification and Manual Digitization of Glacial Area
Mt. Meager, British Columbia, Canada (September 22nd, 1985)



 Manual Digitizing

Unsupervised Iso Cluster Classification

 Not Glacier (Hollow Symbol)

 Glacier

Landsat 5 TM

 Band 7

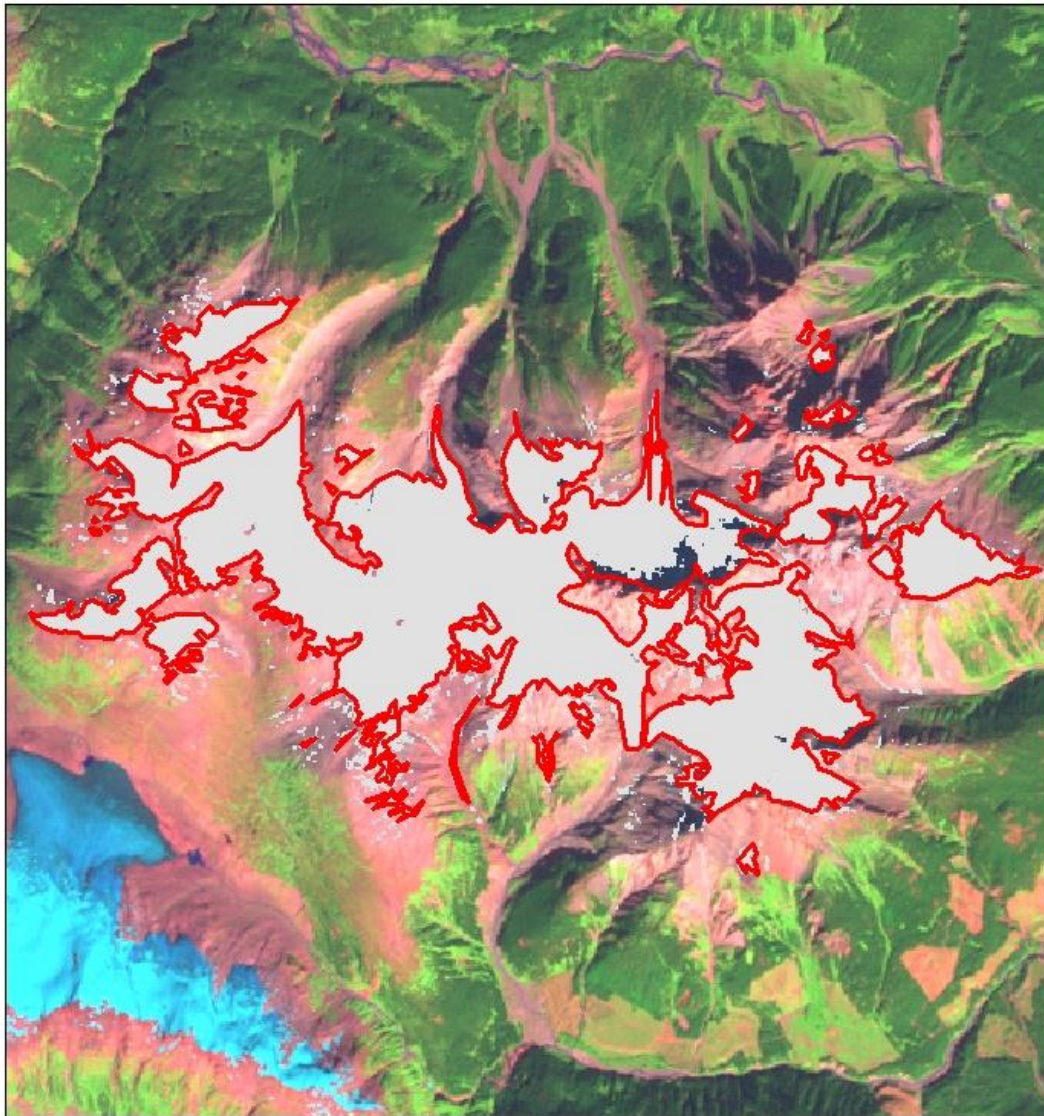
 Band 4


 Band 2

0 1.25 2.5 5 Kilometers

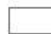
Author: Madison Reid
Date Created: November 20th, 2015
Projection: WGS 84 UTM Zone 10N
Data Sources: United States Geological Survey (1985)

Comparison of Unsupervised Classification and Manual Digitization of Glacial Area Mt. Meager, British Columbia, Canada (September 14th, 1988)



 Manual Digitizing

Unsupervised Iso Cluster Classification

 No Glacier (Hollow Symbol)

 Glacier

Landsat 5 TM

 Band 7

 Band 4

 Band 2

0 1.25 2.5 5 Kilometers



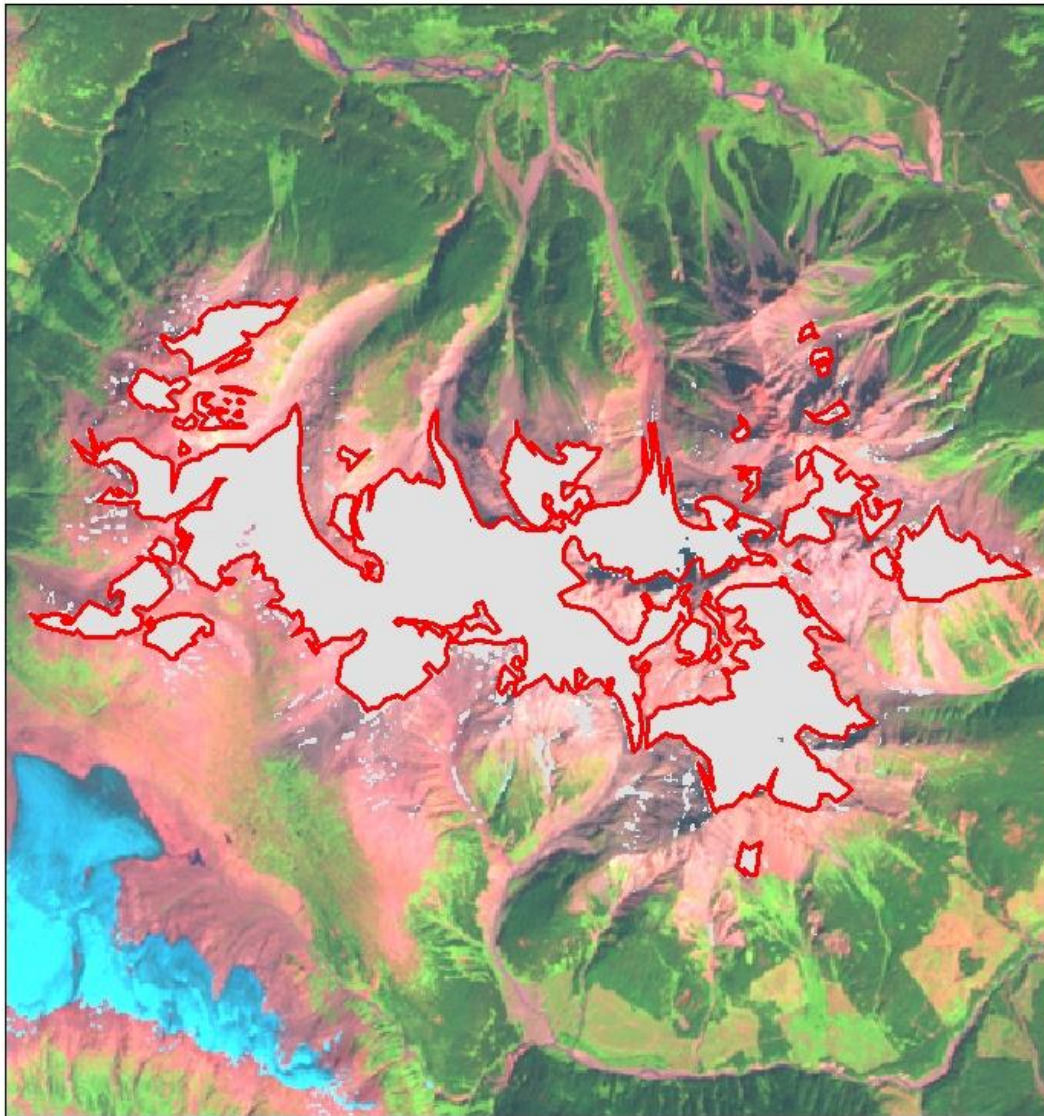
Author: Madison Reid


Date Created: November 20th, 2015

Projection: WGS 84 UTM Zone 10N

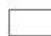
Data Sources: United States Geological Survey (1988)

Comparison of Unsupervised Classification and Manual Digitization of Glacial Area Mt. Meager, British Columbia, Canada (August 24th, 1992)



 Manual Digitizing

Unsupervised Iso Cluster Classification

 Not Glacier (Hollow Symbol)

 Glacier

Landsat 5 TM

 Band 7

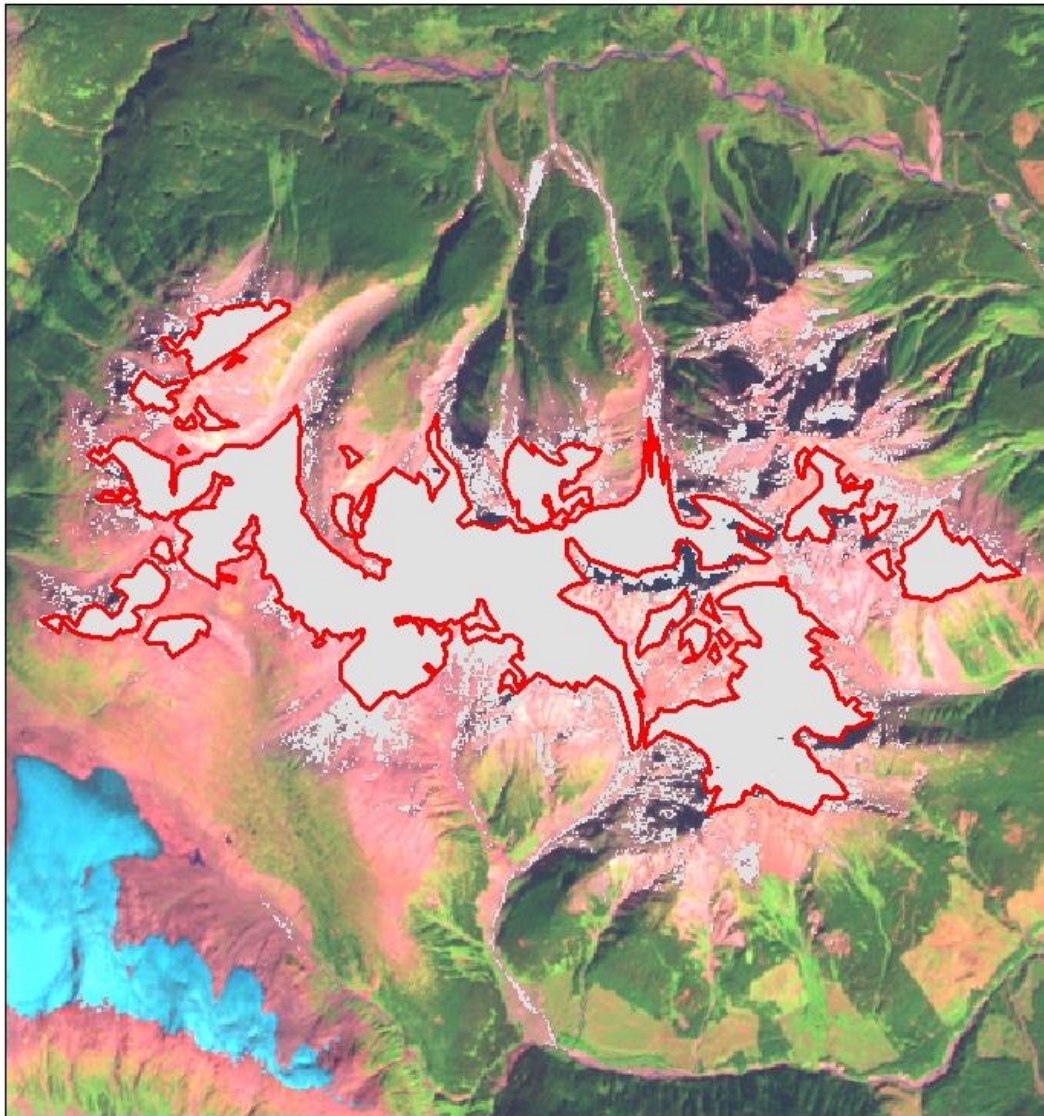
 Band 4


 Band 2

0 1.25 2.5 5 Kilometers

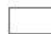
Author: Madison Reid
Date Created: November 20th, 2015
Projection: WGS 84 UTM Zone 10N
Data Sources: United States Geological Survey (1992)

Comparison of Unsupervised Classification and Manual Digitization of Glacial Area Mt. Meager, British Columbia, Canada (September 12th, 1993)



 Manual Digitizing

Unsupervised Iso Cluster Classification

 Not Glacier (Hollow Symbol)

 Glacier

Landsat 5 TM

 Band 7

 Band 4

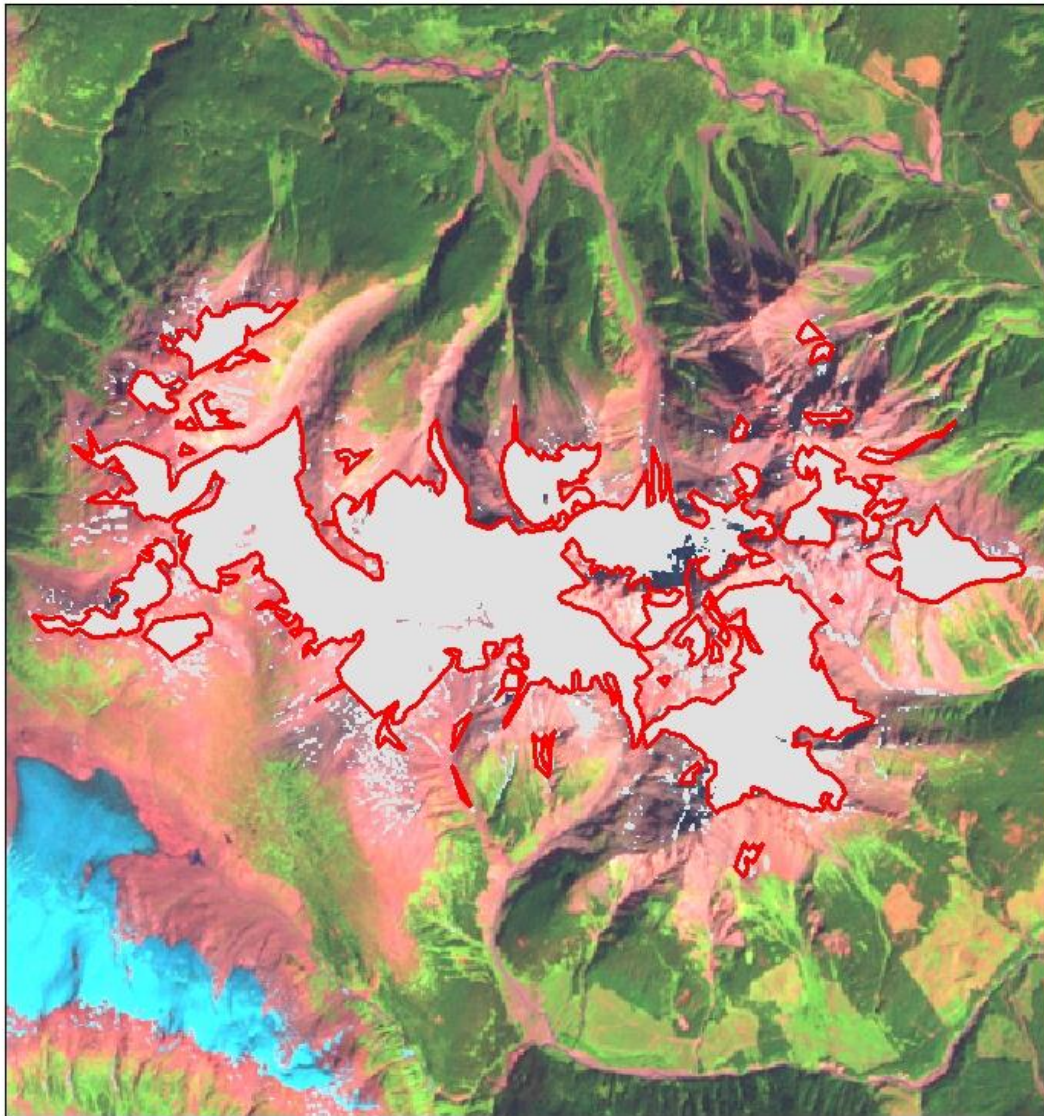
 Band 2


0 1.25 2.5 5 Kilometers



Author: Madison Reid
Date Created: November 20th, 2015
Projection: WGS 84 UTM Zone 10N
Data Sources: United States Geological Survey (1993)

Comparison of Unsupervised Classification and Manual Digitization of Glacial Area Mt. Meager, British Columbia, Canada (September 2nd, 1995)



 Manual Digitizing

Unsupervised Iso Cluster Classification

 Not Glacier (Hollow Symbol)

 Glacier

Landsat 5 TM

 Band 7

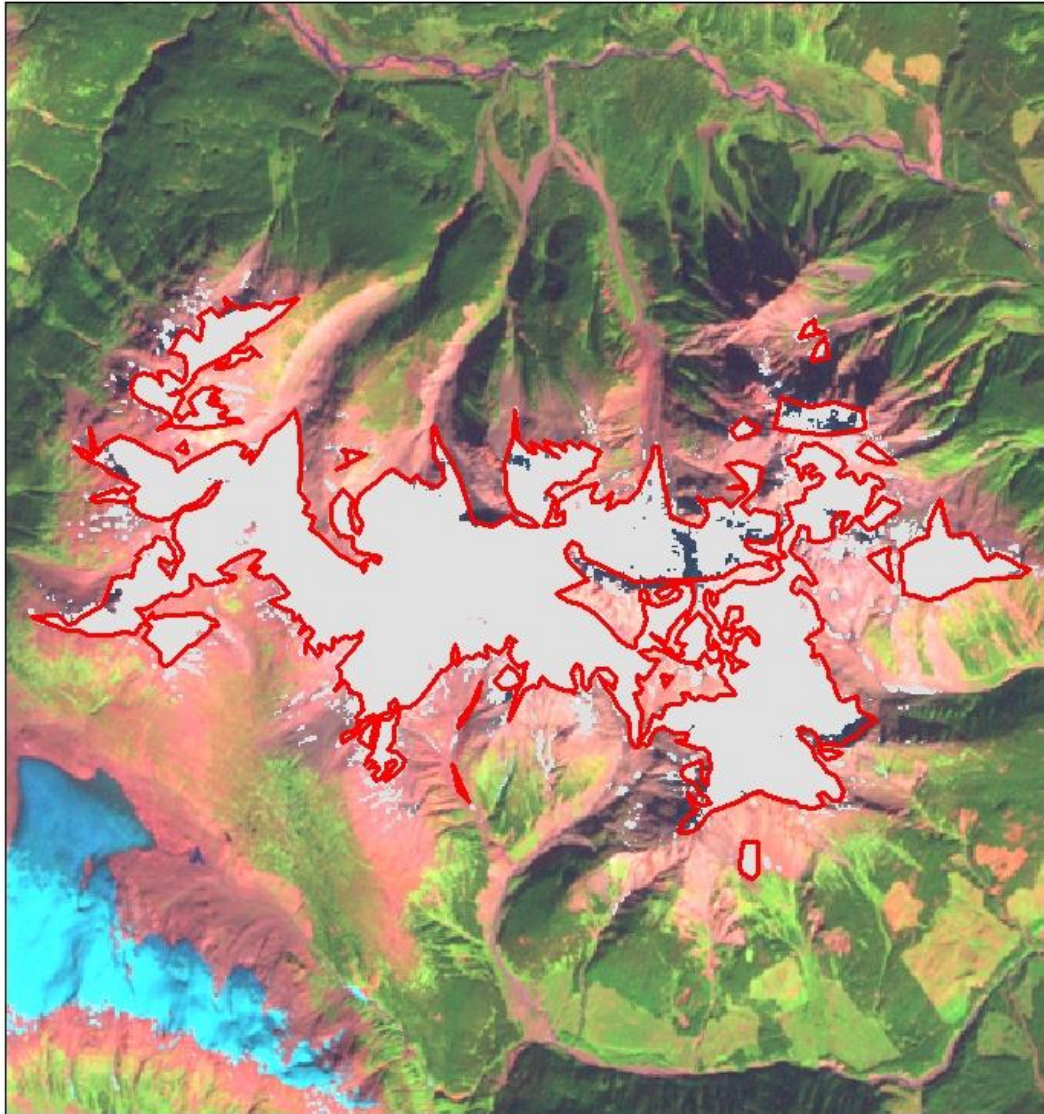
 Band 4


 Band 2

0 1.25 2.5 5 Kilometers

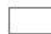
Author: Madison Reid
Date Created: November 20th, 2015
Projection: WGS 84 UTM Zone 10N
Data Sources: United States Geological Survey (1995)

Comparison of Unsupervised Classification and Manual Digitization of Glacial Area Mt. Meager, British Columbia, Canada (September 23rd, 1997)



 Manual Digitizing

Unsupervised Iso Cluster Classification


 Not Glacier (Hollow Symbol)

 Glacier

Landsat 5 TM

 Band 7

 Band 4

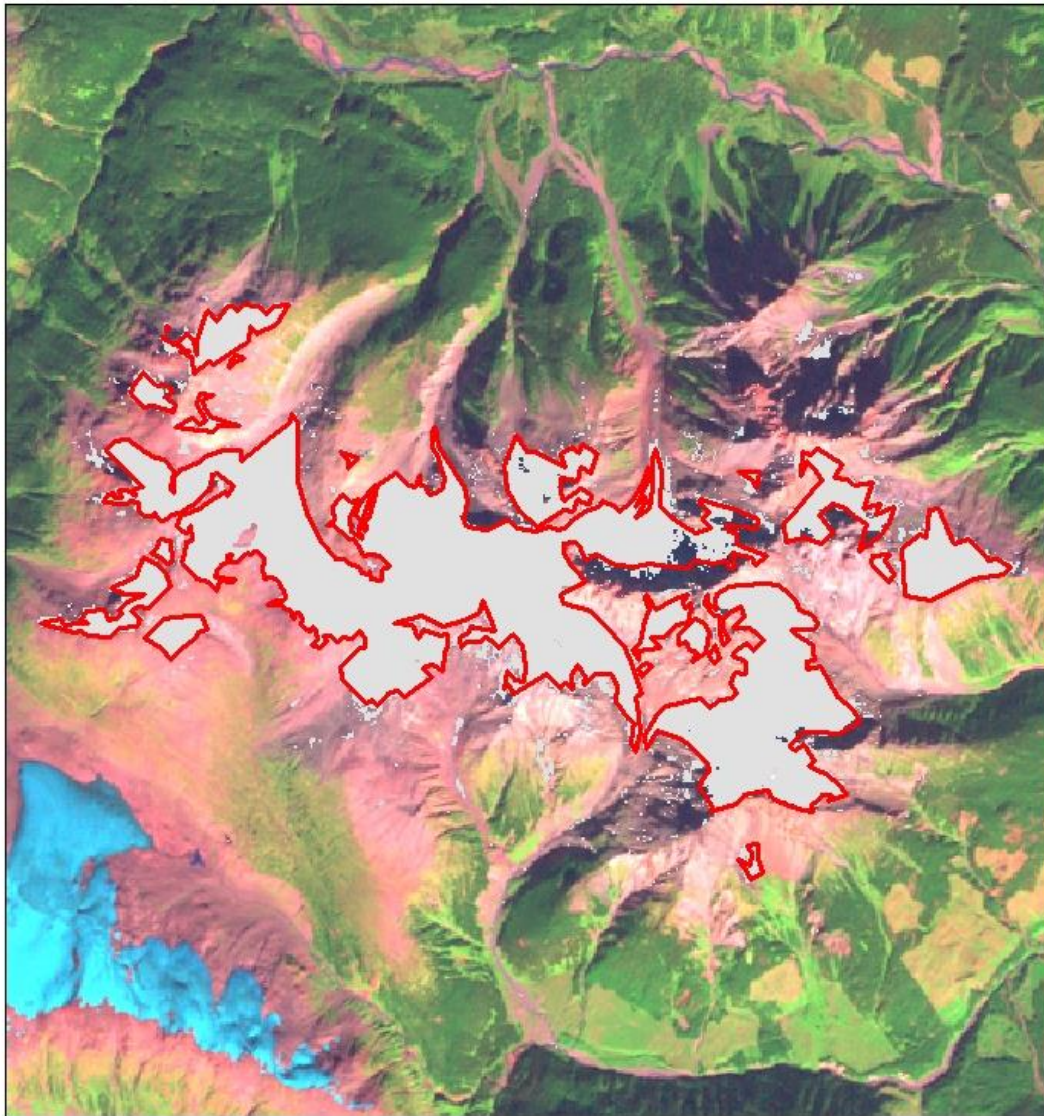
 Band 2


0 1.25 2.5 5 Kilometers



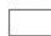
Author: Madison Reid
Date Created: November 20th, 2015
Projection: WGS 84 UTM Zone 10N
Data Sources: United States Geological Survey (1997)

Comparison of Unsupervised Classification and Manual Digitization of Glacial Area Mt. Meager, British Columbia, Canada (September 26th, 1998)



 Manual Digitizing

Unsupervised Iso Cluster Classification

 Not Glacier (Hollow Symbol)

 Glacier

Landsat 5 TM

 Band 7

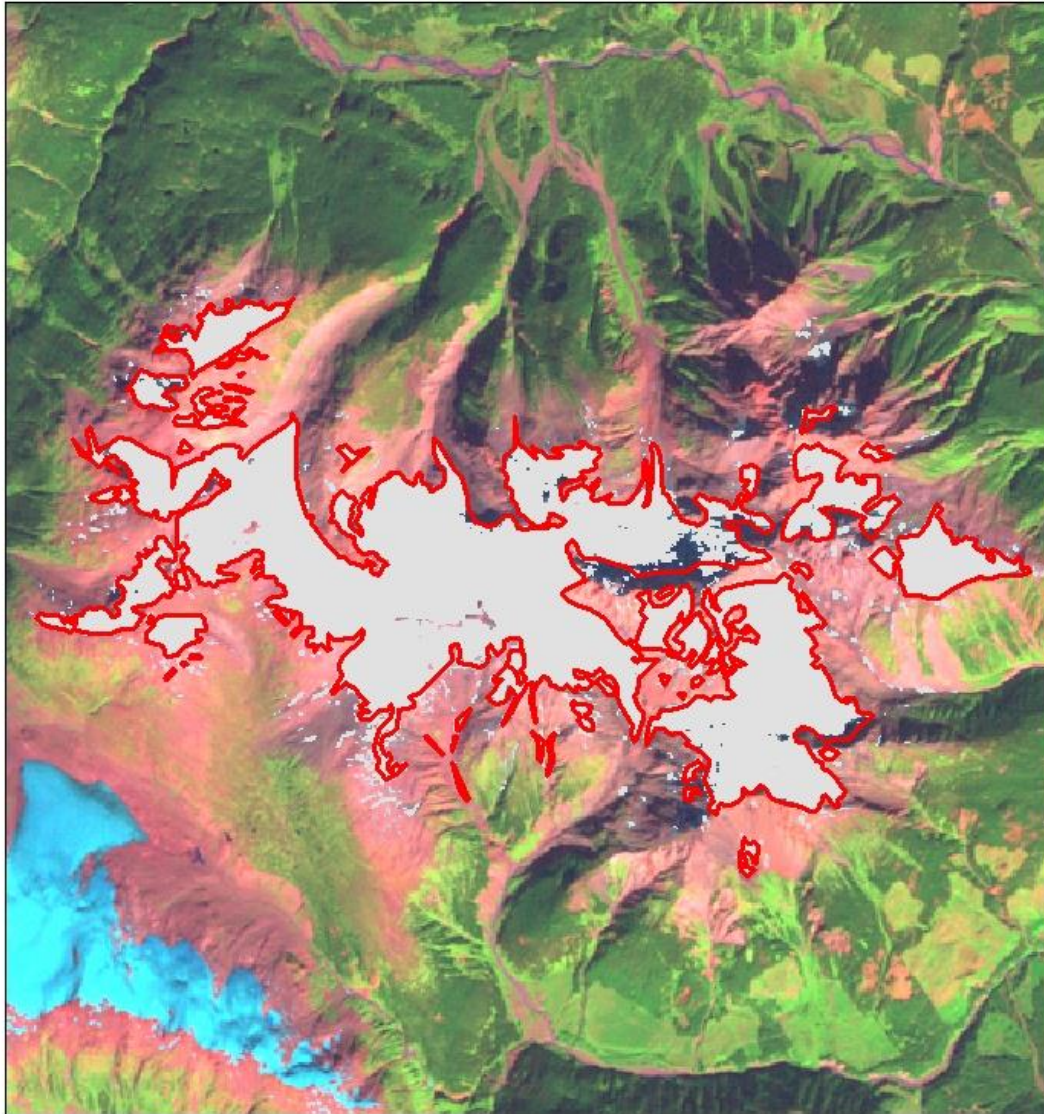
 Band 4


 Band 2

0 1.25 2.5 5 Kilometers

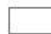
Author: Madison Reid
Date Created: November 20th, 2015
Projection: WGS 84 UTM Zone 10N
Data Sources: United States Geological Survey (1998)

Comparison of Unsupervised Classification and Manual Digitization of Glacial Area Mt. Meager, British Columbia, Canada (September 21st, 2002)



 Manual Digitizing

Unsupervised Iso Cluster Classification

 Not Glacier (Hollow Symbol)

 Glacier

Landsat 5 TM

 Band 7

 Band 4

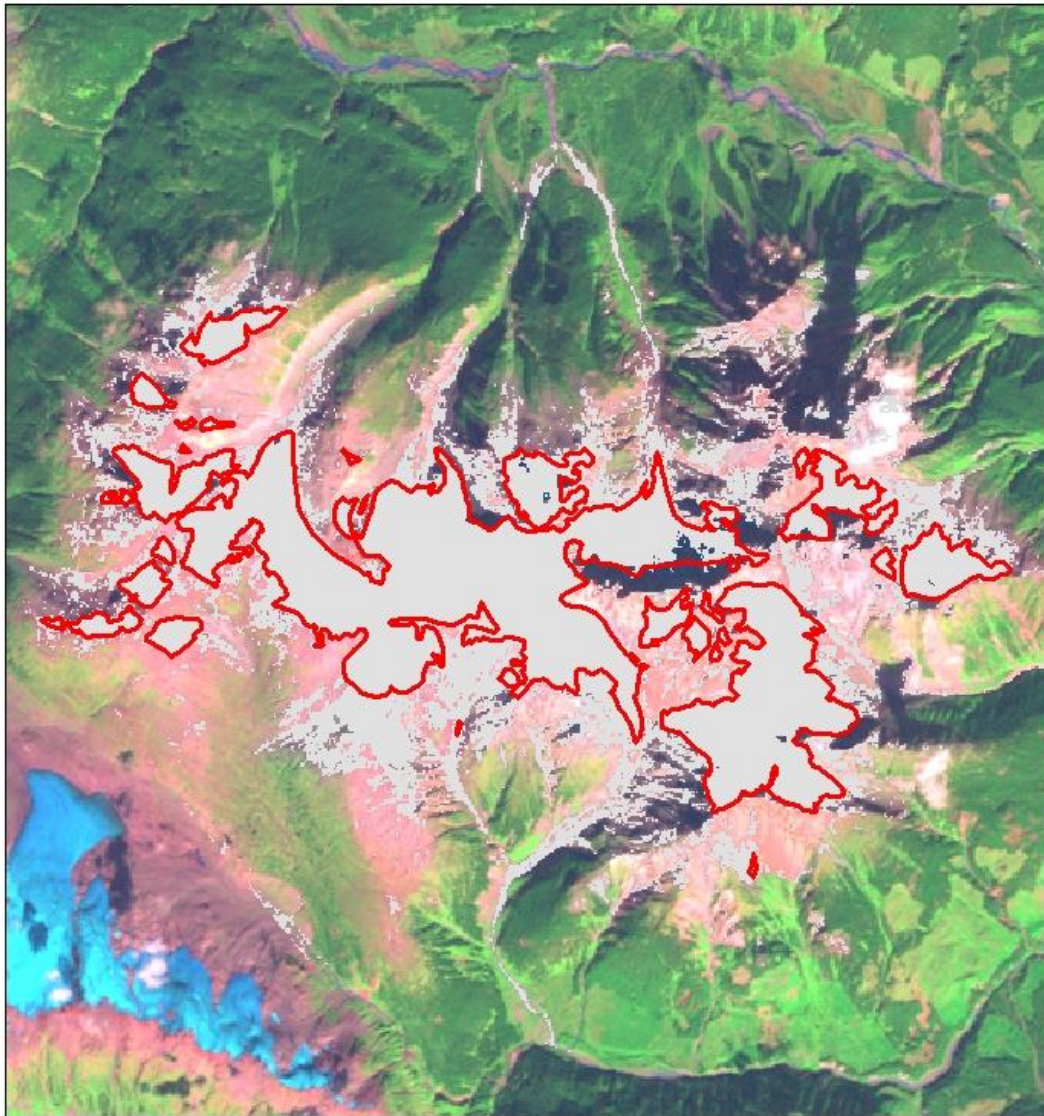
 Band 2


0 1.25 2.5 5 Kilometers



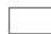
Author: Madison Reid
Date Created: November 20th, 2015
Projection: WGS 84 UTM Zone 10N
Data Sources: United States Geological Survey (2002)

Comparison of Unsupervised Classification and Manual Digitization of Glacial Area Mt. Meager, British Columbia, Canada (September 24th, 2009)



 Manual Digitizing

Unsupervised Iso Cluster Classification

 Not Glacier (Hollow Symbol)

 Glacier

Landsat 5 TM

 Band 7

 Band 4

 Band 2

0 1.25 2.5 5 Kilometers



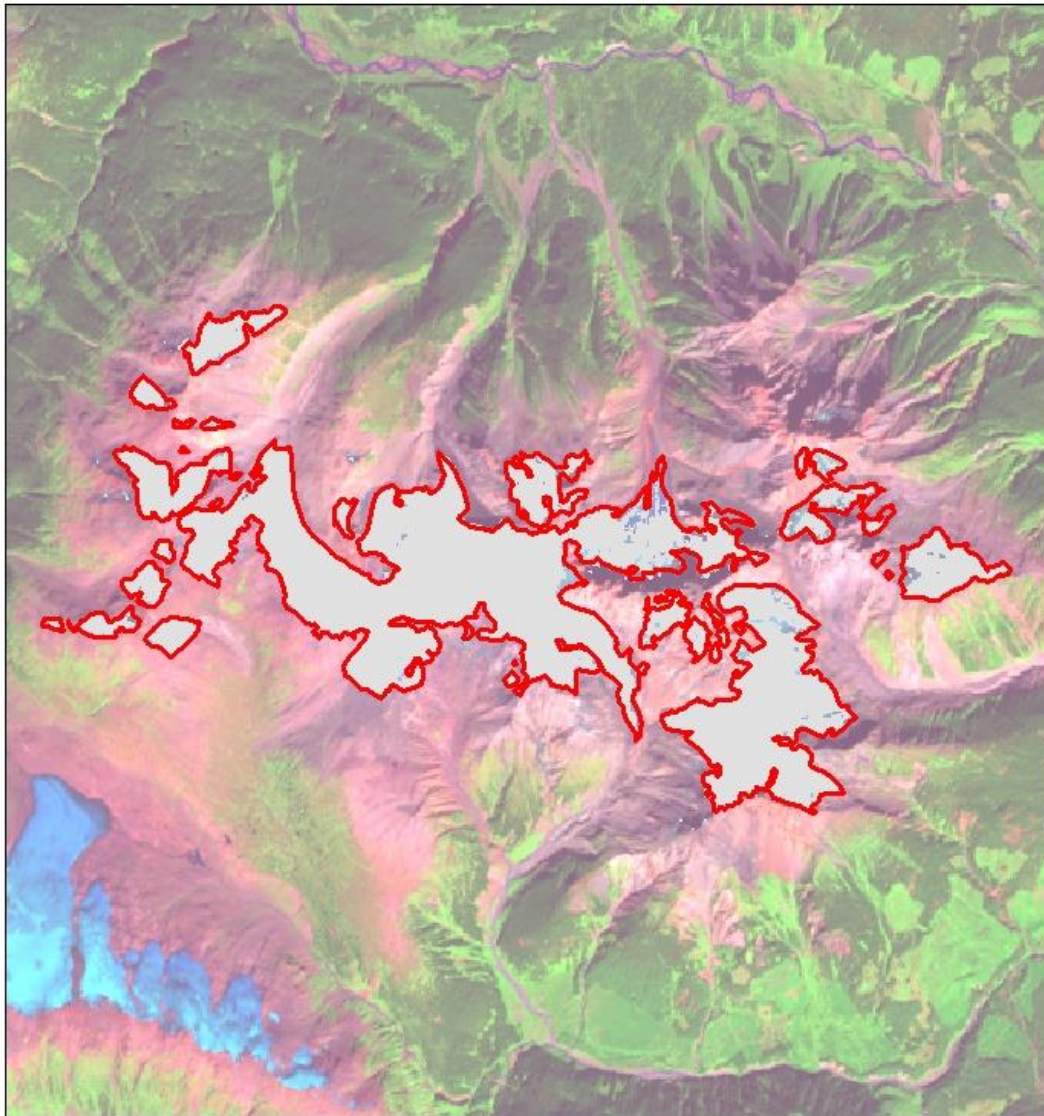
Author: Madison Reid


Date Created: November 20th, 2015

Projection: WGS 84 UTM Zone 10N

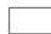
Data Sources: United States Geological Survey (2009)

Comparison of Unsupervised Classification and Manual Digitization of Glacial Area Mt. Meager, British Columbia, Canada (September 6th, 2014)



 Manual Digitizing

Unsupervised Iso Cluster Classification

 Not Glacier (Hollow Symbol)

 Glacier

Landsat 8 OLI

 Band 7

 Band 5

 Band 3

0 1.25 2.5 5 Kilometers

Author: Madison Reid
Date Created: November 20th, 2015
Projection: WGS 84 UTM Zone 10N
Data Sources: United States Geological Survey (2014)